ELECTRICAL COMMUNICATION

Technical Journal of the
International Telephone and Telegraph Corporation
and Associate Companies

TACAN

Radio Bearing and Distance System
for Aerial Navigation

Volume 33 **MARCH, 1956** **Number 1**

ELECTRICAL COMMUNICATION

Technical Journal of the
International Telephone and Telegraph Corporation
and Associate Companies

Published Quarterly by the
INTERNATIONAL TELEPHONE AND TELEGRAPH CORPORATION
67 BROAD STREET, NEW YORK 4, NEW YORK, U.S.A.

Sosthenes Behn, Chairman William H. Harrison, President
Geoffrey A. Ogilvie, Vice President and Secretary

Subscription, $2.00 per year; single copies, 50 cents

Volume 33 MARCH, 1956 Number 1

CONTENTS

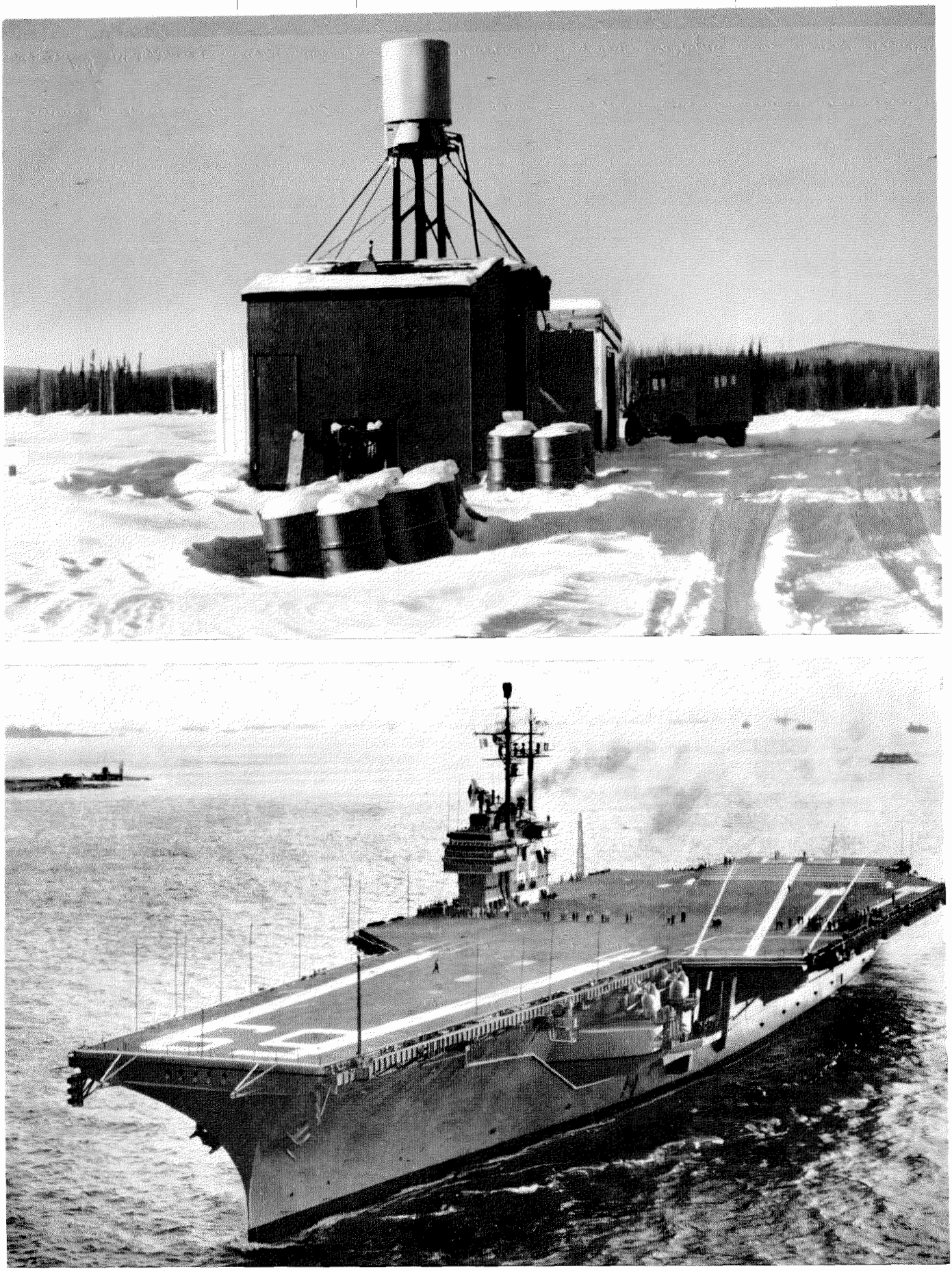

Tacan has been tested under widely different environments. Above is an Air Force installation in Alaska and below it is the *USS Forrestal* with a tacan antenna at the top of its main mast.

Tacan Symposium Issue

ELECTRONIC SYSTEMS have been developed to provide the fast response, accuracy, and direct-reading features that distinguish modern navigation from the centuries-old methods that were adequate for navigation on the surface of the earth. This issue of *Electrical Communication* is devoted exclusively to a recently declassified system of navigation called tacan, a contraction of "tactical aerial navigation."

Tacan is a system that provides both bearing and distance information on direct-reading instruments in an airplane within 200 nautical miles of a selected ground station. With the equipment developed during the past decade, 126 clear radio channels are available for the ground stations within the band from 960 to 1215 megacycles per second. Additional facilities may be added to the basic bearing and distance functions that have received the major attention of the designers up to now.

A development of such wide scope is not the work of one man or of one group of men. Many groups have influenced the development of tacan. Coordination of interests and objectives has resulted in the adoption of tacan by the United States Air Force and the Navy; tacan is now under consideration for adoption as the common system for civil as well as military users. The common use by both military and civil aircraft of an effective integrated system of navigation cannot help but increase the safety, economy, and reliability of these services.

Military security restrictions have severely limited the release of information on tacan during its long and intensive development and trial stages. In view of the widespread interest in the system, its possible future importance for civil as well as military aviation, and the general applicability of the technical advances in the art that arose out of its development, the International Telephone and Telegraph system has felt that a definite need would be served by an authoritative release of information on tacan at the earliest time permitted by the declassification of the system, and to the fullest extent permitted by certain security restrictions that are still in force.

Accordingly, the aim in preparation of this "Tacan Symposium" issue of *Electrical Communication* has been to provide a consolidated and comprehensive presentation of all major aspects of tacan. After an introductory historical review of the tacan development program, the reader will find a description of the general principles of the system, followed by a series of detailed papers on tacan equipment and operation. Finally, there are three papers devoted specifically to a fuller exposition of the three basic concepts underlying the design of tacan, namely the coordinated-system concept, clear-frequency channelling under full crystal control, and multilobe-bearing-system operation.

The Editor

Development of Tacan at Federal Telecommunication Laboratories

By PETER C. SANDRETTO

Federal Telecommunication Laboratories, a division of International Telephone and Telegraph Corporation; Nutley, New Jersey

UNDER DEVELOPMENT for nearly a decade, tacan is the end result of the needs, opinions, plans, inventions, and hopes of a great many workers in military and civilian aviation and electronics. Ordinarily, such a project would have been disclosed in the technical press in a series of progress reports that would identify the contributors to the various phases of the development. Circumstances did not permit such a presentation and it is desirable therefore that attention be directed now to those organizations and individuals who contributed importantly to the program. The view of the subject presented here is from Federal Telecommunication Laboratories, which had the priviledge of doing the engineering, fabricating of models, and testing that culminated in this recently declassified system of navigation. No apology is made for the high redundancy of names of individuals and organizations in the report; they are its reason for being.

Federal Telecommunication Laboratories' postwar work in the air-navigation–traffic-control field began with a study by three men; E. M. Deloraine, technical director of International Telephone and Telegraph Corporation, H. Busignies, executive vice president of Federal Telecommunication Laboratories, and P. R. Adams, director of the electronic systems laboratory. In 1945, these men addressed themselves to the study of the air-navigation–traffic-control situation. This general problem is not simple for it involves such things as governmental regulations, construction of airport systems, and other related noncommunication considerations. However, it is not difficult to outline in general terms the requirements of the electronic and radio portions of the problem. Briefly, they are as follows.

A. Means whereby the pilot can know his position in three dimensions so he can navigate to his destination.

B. Means whereby a ground authority, capable of regulating the flow of air traffic, can know the position of *all* aircraft.

C. Means whereby the ground authority can forecast the future positions of *all* aircraft.

D. Means whereby the central authority can issue approvals to pilots of aircraft to proceed or to hold.

The air-navigation–traffic-control system in the United States grew as the product of necessity and without being planned.

It began in about 1919 with the installation of 4-course radio ranges for furnishing guidance to aircraft along definite routes. Later, other navigational aids were added such as markers (both low and high frequency) to indicate points along the airways. Still later, low-approach equipment was added. When a controlling agency was established on the ground, it was equipped with slips of paper to designate aircraft, and hand computations were used to determine their future positions. Reliance was placed on communications from the aircraft to learn of their positions. Communications were furnished largely through the high-frequency equipment owned and operated by the airlines. Teleprinter communications were added between the various control centers.

In looking over the system, it was quite obvious that it was slow and not very efficient. A multiplicity of radio equipments, each requiring separate transmission frequencies, were employed to perform the job; a situation that was abhorrent to those who had been long engaged in the design of systems to meet commercial communication requirements. Commercial systems must necessarily be very economical in the employment of frequencies and equipment must be designed so that they perform at minimum cost. As a result of the study, these men conceived a *coordinated system* (later called

navar) in which the navigational information was furnished to the pilot through a polar-coordinate system.

A polar-coordinate system is one in which a position in two dimensions is given as a direction and a distance from a single point. This is a natural system of coordinates, since man is born with a knowledge of right and left and he learns about distance when he learns to walk. Knowing the difficulty that had been experienced with the 4-course radio ranges in this country, it was very evident that the improved navigational system must be free from site effects. Therefore, the bearing system employed a very *narrow lobe* of energy to avoid these distortions. Insisting that a cleared radio channel be employed for as many functions as possible, it was decided that this could best be done at about 1000 megacycles per second, and extensive work was begun to furnish distance information in this frequency band. This work resulted in some circuit techniques that later were employed in the tacan equipment. Development of *crystal control* at this frequency was undertaken so that reliable rigidly established channels would be available. The navar system had many other features, such as surveillance radar, transpondor beacon, command link, and low approach.

Following the origin of this concept, it was necessary to set up a program to develop equipment to prove the practicability of such a system. As will be seen in Figure 1, the International Telephone and Telegraph Corporation initiated such a program about the middle of 1945. Its support has continued throughout the ensuing decade.

Now going from the situation as it existed in 1945 at Federal Telecommunication Laboratories, it is interesting to see what was happening at what is now the Wright Air Development Center. The communications and navigations laboratory there was conducting a study that produced a very thick volume, which was made generally available to interested persons in the United States in February 1946. Some of the personnel involved in the study were Captain C. R. Bryan as chairman of the navigation advisory group and Captain L. J. Perper as its secretary. There were two groups under the chairman: V. I. Weihe served as chairman of the long-distance subgroup and H. Davis served as its secretary. N. Braverman served as chairman of the short-distance group with F. B. Brady as its secretary. G. H. Arnstein was the editor of the group. Some of the more-senior officers who participated were Colonel S. A. Mundell, Colonel N. L. Winter, and Lieutenant-Colonel M. L. Haselton.

This group also came to the conclusion that for short-range navigational purposes, a polar-coordinate system was most desirable. This polar-coordinate system was to be formed by an omnidirectional radio range with distance-measuring equipment operating in the 1000-megacycle band. Wright Air Development Center had given a contract to one of the prominent electronic companies for the development of crystal-controlled distance-measuring equipment having channel widths of 6 megacycles. The system was to have a "clock-like" type of indicator and an accuracy of 0.2 nautical mile (0.37 kilometer) plus 1 percent of the distance reading. With this system, 21 channels would be provided. In the latter part of 1945 (or early in 1946), a second contract was placed with another manufacturer for a system not using crystal control. In this latter system, the required number of operating channels were to be obtained through a pulse-multiplex technique. The radio-frequency channels themselves had a width of about 20 megacycles.

After examining the work that Federal Telecommunication Laboratories had done on its own volition, the Air Force in April of 1946 entered into contract *W28-099-ac-108* with that organization for the *AN/APN-34* airborne interrogator and the *AN/GPN-4* ground beacon.

In October of 1946, early models of the crystal-controlled distance-measuring equipment operating on one channel were demonstrated by Federal Telecommunication Laboratories to a large number of personnel at Indianapolis. This was the occasion of the International Civil Aviation Organization (ICAO) meeting. There was also demonstrated at that time a combined distance-and-bearing system. The 1000-megacycle distance-measuring system was combined with bearing indications supplied by a narrow-lobe system operating at 3000 megacycles. Actually, the 1000-megacycle system acted as part of the bearing facility. A small crystal receiver picked up the 3000-megacycle narrow

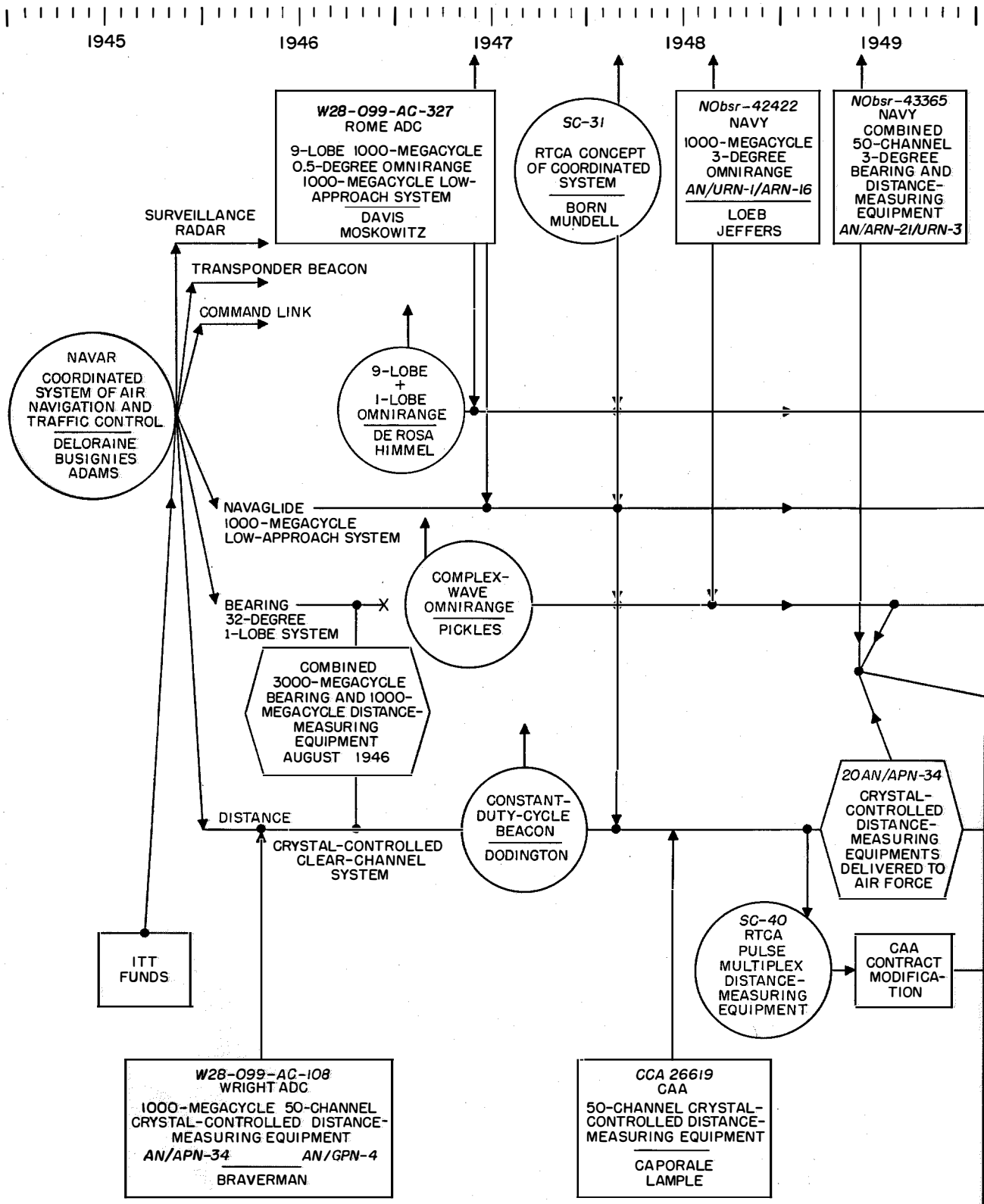

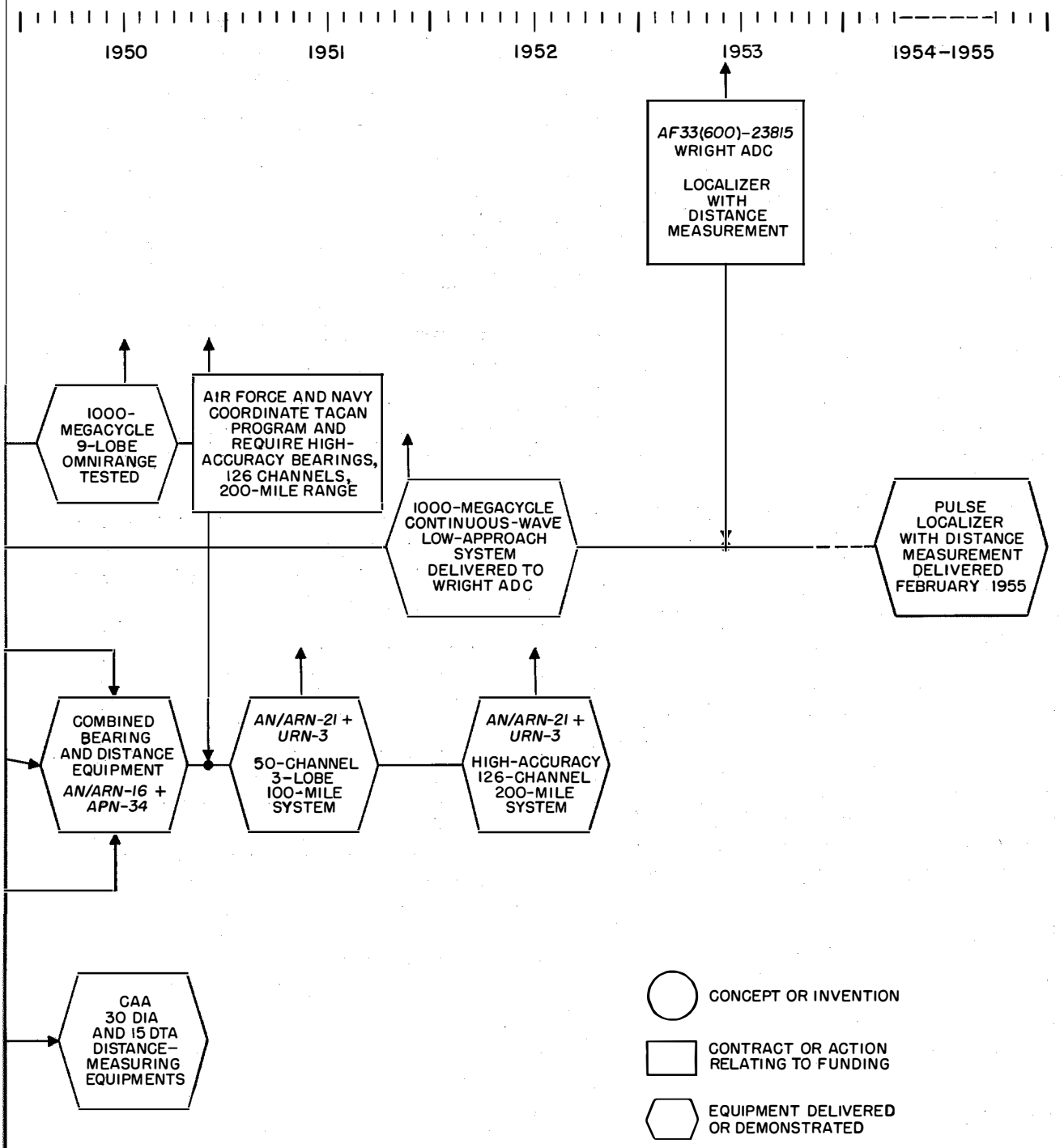

Figure 1—Graphic presentation of development of tacan. Abbreviations: *ADC* = Air Development Center, *CAA* = Civil Aeronautics Administration, *ITT* = International Telephone and Telegraph Corporation, and *RTCA* = Radio Technical Commission for Aeronautics.

lobe and direction was derived by comparing the phase of its output with a reference signal from a receiver operating on the 1000-megacycle distance-measurement channel.

Early in 1947, L. A. deRosa and L. Himmel of the Laboratories proposed an omnidirectional radio range operating at 1000 megacycles that would be capable of furnishing bearing with an accuracy of 0.5 degree. This conception consisted in fact of two omniranges, one having a single lobe and the other having 9 lobes. The system was to make distance-measuring use of the receiver being developed for Wright Field. A contract was awarded to Federal Telecommunication Laboratories for this development in June 1947 by the Air Force's Watson Laboratory, now the Rome Air Development Center. H. Davis, the technical director of the Rome Air Development Center, played a prominent part in this decision. It will be remembered that he also played an important role in the Air Force's navigation advisory group that had met the previous year. At the same time that an award was made for the high-precision omnirange, the contract also contained provisions for work on a 1000-megacycle instrument low-approach system.

Also early in 1947, Sidney Pickles, then of Federal Telecommunication Laboratories, disclosed to the patent department a system similar to the deRosa–Himmel concept; however, a simplification had been accomplished by replacing the two waves with a single complex wave. This wave consisted of a fundamental with a prominent third harmonic.

The work in the development of the 1000-megacycle crystal-controlled distance-measuring equipment had been assigned to S. H. Dodington, director of the radio navigation laboratory of Federal Telecommunication Laboratories, and, in the autumn of 1947, he came forth with one of the most ingenious concepts required for the tacan system. This was the concept of a constant-duty-cycle beacon; that is, a beacon that always sends out the same number of pulses regardless of the number of interrogations. In his memorandum describing this development, Dodington mentioned that a reflector could be rotated about the beacon antenna normally used to give distance measurement only and that it would then also give direction.

In the summer of 1947, the Radio Technical Commission for Aeronautics organized its committee *SC-31*. The second phase, under the chairmanship of Captain A. S. Born, was to determine the requirements of the equipment for the most-desirable air-navigation–traffic-control system. The report of this committee was issued in February 1948. The navigation subcommittee was under the chairmanship of Colonel S. A. Mundell, who, it may be remembered, had participated in the Air Force's air navigation advisory group in 1945. Committee *SC-31* recommended the development of a coordinated system that is specified in its report as follows.

"b. The Navigation Equipment (Equipment No. 2 of Figure No. 1) is a transmitter–receiver having multiple channels. This equipment, with associated ground equipment:

"(1) Provides distance and bearing information for navigation. These data, when used in conjunction with a computer, will allow the pilot to fly any desired course.

"(2) Provides precise slope, localizer, and distance information for instrument approaches.

"(3) Provides information for airport surface navigation to enable the pilot to taxi his aircraft.

"(4) Provides air–ground aural communication of a reliable and static-free type.

"(5) Provides a situation display in pictorial form which enables the pilot to monitor traffic conditions in his vicinity or receive other pertinent data such as holding areas, airlane locations, and weather maps from the ground.

"(6) Provides suitable output to allow the aircraft to be automatically flown, either en route or during final approach and landing."

The target navigation system is further described in the subparagraph on page 34 of the *SC-31* report, which states, "the airborne navigation equipment and its directly associated ground elements are wholly contained in the 960–1215-megacycle band."

The airborne navigational equipment for the ultimate system is further described on pages 55 and 68, and the accuracy is given as ±0.6 degree in bearing and ±0.2 nautical mile (0.37

kilometer) or 1 percent of distance, whichever is greater.

Though the equipment proposed by *SC-31* for the ultimate or target system is very dissimilar to the navar system, it constitutes a coordinated system with essentially the same elements that had been described by Deloraine, Busignies, and Adams. Committee *SC-31* had brought together the thinking of the Air Force and the Navy as well as the civil industry. Through *SC-31*, each group learned of the thinking that had gone on in the other groups.

It was about the time of the *SC-31* meeting that the Navy was looking for a system to replace its *YE/YG* beacon. The *YE/YG* beacon had provided very satisfactory service during the war, but it presented bearings aurally; that is, the pilot determined his position by listening to a signal. It was found that this device was ineffective with jet operation. The Navy considered the Civil Aeronautics Administration very-high-frequency omnidirectional radio range and mounted one on the aircraft carrier *USS Mississippi*. It was found that errors of the order of 15 degrees were produced by the superstructure and that the large installation required was impractical for shipboard. The Navy, therefore decided that an omnirange built along the complex-wave principle would be suitable for fulfilling its requirements. A contract was therefore issued to Federal Telecommunication Laboratories in June of 1948 that called for an airborne equipment known as the *AN/ARN-16* and a shipboard equipment known as *AN/URN-1*. This equipment was to constitute a 20-channel 3-degree system. It was to provide *only* direction and not distance. The naval personnel having engineering cognizance of this work were J. Loeb of the Bureau of Ships and N. L. Jeffers of the Bureau of Aeronautics.

In 1951, the Bureau of Aeronautics' interest came under the cognizance of G. Harding, who worked under the direction of A. B. Winnick. Loeb, who at one time was employed by the Civil Aeronautics Administration and has many years of experience in air navigation, continued to direct the efforts of the Bureau of Ships. His able activities on the project won for him the highest civilian award of the Navy in 1951. Certainly, if anyone can claim the cognomen of "Father of the Modern Tacan," it is Loeb.

Committee *SC-31* had said that distance-measuring equipment should be associated with each very-high-frequency omnidirectional radio range, and early in 1948 P. Caporale and C. Lample of the Civil Aeronautics Administration acquainted themselves with the Wright Air Development Center crystal-controlled distance-measuring equipment. As a result of their efforts, requests for bids were placed. In August of 1948, an award was made to Federal Telecommunication Laboratories for a quantity of ground and airborne distance-measuring equipments that would be crystal-controlled and made essentially to the same specifications as those being constructed for the Air Force.

Committee *SC-40* of the Radio Technical Commission for Aeronautics had been formed in early December of 1947 for the purpose of studying the two channelling techniques under development for distance-measuring equipment. One of these was the clear-channel crystal-control technique and the other the pulse multiplex system. This committee made its report in December of 1948. The recommendation consisted of a compromise in that both crystal-control *and* pulse multiplex techniques were included.

In the autumn of 1948, the Navy, which had continued to study its problem on navigation, came to the conclusion that jet aircraft require a knowledge of distance as well as direction to operate satisfactorily. Accordingly, specifications were prepared for distance-measuring equipment that closely paralleled that being developed for the Air Force. It is interesting to note, therefore, that early in 1949 the thinking of the Civil Aeronautics Administration, the Air Force, and the Navy on distance measurement was identical. In the spring of 1949, however, the Civil Aeronautics Administration felt itself bound by the *SC-40* report with its compromise solution and, therefore, modified *its* contract with Federal Telecommunication Laboratories to call for a system conforming to the *SC-40* principles. These historical facts are interesting in light of the later accusations appearing in the public press that the military had not held to agreements in *SC-31* and had developed a "competing" system.

Twenty *AN/APN-34* crystal-controlled distance-measuring equipments were delivered to

the Air Force in mid 1949; a year later, one of these was attached to a Navy *AN/ARN-16* and demonstrated that the combination successfully produced both bearing and distance.

In mid 1950, the 1000-megacycle, 9-lobe system of the Air Force was also tested and showed beyond a doubt its capabilities of providing accuracies of better than 0.5 degree. In about October or November of 1950, the Air Force examined the Navy contract for a combined distance-and-bearing system. It decided that it was necessary to have one common system between the two services but asked that the Navy modify its specification to include the specific concepts that the Air Force had been developing through the work of the Wright and the Rome Air Development Centers. It was requested that the requirements for the *ARN-21* now be for 126 rather than 50 channels. It was requested that the accuracy within 3 degrees be increased to 0.75 degree and that the range be changed from 100 to 200 nautical miles (185 to 370 kilometers).

In the spring of 1951, Federal Telecommunication Laboratories delivered to the destroyer *USS Krause* the first *AN/URN-3* and to the naval air station at Atlantic City some *AN/ARN-21* airborne equipments, which provided the 50 channels that had characterized the original Air Force distance-measuring equipment. Bearing was provided by a 3-lobe system. The equipment was tested very successfully and was ready for production had it not been for the added requirements of the Air Force. These added requirements meant, however, that virtually the entire development had to be done over.

It will be remembered that one of the early goals in the development of crystal-control at 1000 megacycles was a 6-megacycle channel. The new Air Force requirements now meant that the radio frequency had to occupy a channel width of only 1 megacycle. This was an unheard-of requirement and became the greatest problem in the development of the ultimate tacan system. This hurdle was overcome after a tremendous effort and resulted in a demonstration model in February of 1952. The demonstration model, however, did not operate successfully throughout the band but equipment that did so was demonstrated in September of 1952.

It is interesting to note the history of the low-approach system. A 1000-megacycle low-approach system was delivered to Wright Air Development Center in about November of 1951. This was a continuous-wave system, however, and did not include distance as one of the services. A contract for modifying this equipment to provide distance was issued in March 1953. In February 1955, a satisfactory localizer that simultaneously produced distance measurement and provided great freedom from site effects was delivered to the Air Force.

This history shows that many factors have gone into the tacan development. Suitable ideas became equipments through the application of supporting funds. The ideas represent the best that the industry has been able to offer. They were selected by technical and operational groups in both military and civil organizations. It must be noted that in each case whenever one of the groups in *any* of the organizations showed a superior concept, it was accepted and incorporated in the final plans. The only deviation was the decision to accept the compromise solution of *SC-40* of the Radio Technical Commission for Aeronautics. Complete harmony would not have been abrogated had it not been for this single action. The tacan system as now produced does not fully meet all of the requirements of *SC-31* for the ultimate coordinated system. It is earnestly hoped that this development will be continued in accordance with the concepts of the far-thinking planners of *SC-31*.

Principles of Tacan

By ROBERT I. COLIN and SVEN H. DODINGTON

Federal Telecommunication Laboratories,
a division of International Telephone and Telegraph Corporation;
Nutley, New Jersey

TACAN is a radio aerial navigational system of the polar-coordinate type illustrated in Figure 1. That is, there is a *bearing* facility that provides on the aircraft a meter indication of its direction in degrees of bearing from the ground beacon selected by the pilot. Also, there is a *distance* facility that provides on the aircraft a meter indication in nautical miles of its distance from the ground beacon. Knowing bearing and distance from a specific geographic point, the pilot can fix his position on a chart.

The bearing function is of a general type known as an omnidirectional radio range, commonly called an omnirange or "ODR," in distinction to other directional radio navigational systems such as 4-course ranges, radio compasses, and direction finders. The distance-measuring equipment, commonly called "DME," is of the general type of radio aid that furnishes meter indications of distance. Tacan is a code word for "tactical air navigational system." The military nomenclature for the airborne equipment is *AN/ARN-21* and for the ground or shipborne apparatus is *AN/URN-3.*

1. System Features

An omnidirectional radio range requires a transmitter in association with a special directional antenna on the ground and a multichannel receiver on the aircraft. A distance-measuring system requires: a receiver–transmitter combination (transpondor) with a nondirectional antenna on the ground and a multichannel transmitter–receiver combination or interrogator on the aircraft. The ground equipments or stations are frequently referred to as beacons.

The radio elements of tacan are indicated in Figure 2. The entire system operates in the 1000-megacycle-per-second band. One multichannel airborne receiver–transmitter, operating with pulses, provides both distance and bearing functions. That is, the same radio signals transmitted over a selected channel convey both distance and bearing information. Actually, both a coarse and a fine indication are combined to produce highly accurate bearing measurements. Only one airborne antenna and channel selector are required.

Tacan has 126 two-way operating channels of 1-megacycle spacing. For air-to-ground transmission (required only for the distance function), there are 126 frequencies within the band 1025 to 1150 megacycles. For ground-to-air transmission (serving both bearing and distance functions), there are 63 channels between 962 and 1024 megacycles and a like number from 1151 to 1213 megacycles. The channels are clear frequencies established solely on the basis

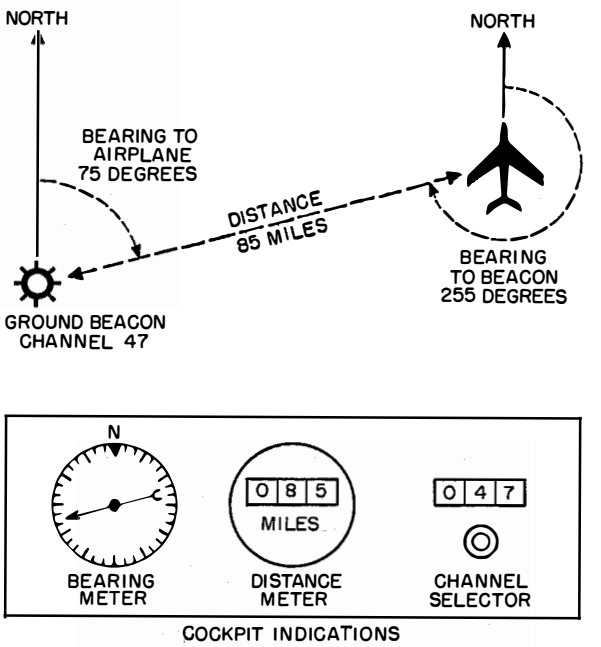

Figure 1—A polar-coordinate system of navigation provides bearing and distance information from a known reference point. The bearing information is shown in degrees from north and the distance is displayed directly in miles from the reference point as is shown by the cockpit indicators.

of radio-frequency selectivity; they do not depend on pulse coding. Pulse coding, that is, the transmission of characteristic pulse groups with some prearranged spacing between component pulses of the group, is used to increase the average radiated power or the signal-to-noise ratio, to discriminate against pulse interference, and also for multiplexing the bearing function on the distance-measuring channels.

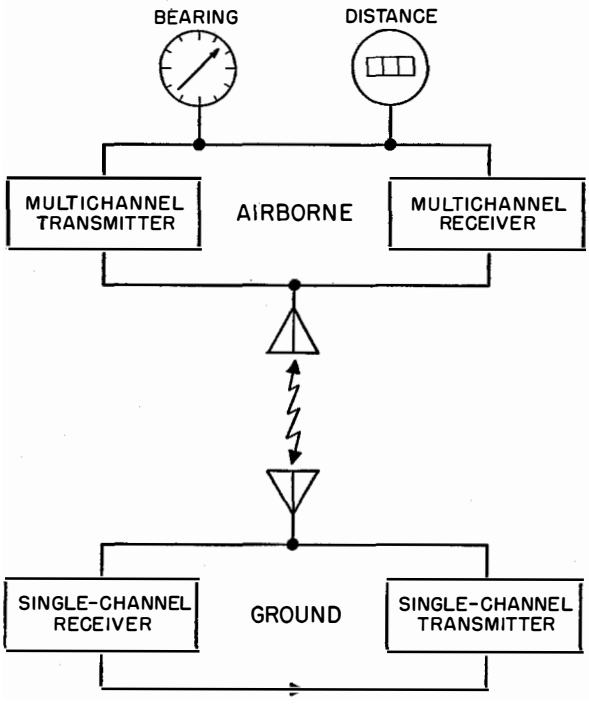

Figure 2—Radio elements of tacan system. By selecting the proper channel, the aircraft operates with the desired ground beacon. There are 126 channels available.

It is possible to multiplex on the tacan channels, additional navigational functions such as localizer, glide slope, marker, air-traffic-control transpondor (radar safety beacon), et cetera. Some of these functions have already been demonstrated experimentally over airborne equipment. When the additional functions are so multiplexed, no further airborne radio equipment is required. It is only necessary to add relatively small adapters and indicators.

The saving in radio spectrum and in weight and size of airborne equipment with tacan would be even more pronounced if all the present navigational functions shown in Table 1 were added to it by multiplexing.

TABLE 1
PRESENT NAVIGATIONAL SERVICES

Service	Present Frequency Band in Megacycles
Omnidirectional Range	112—118
Distance Measurement, Civil	963—986 1188—1210
Traffic-Control Transponder	1039—1090
Low-Approach System	
Localizer	108—112
Glide Slope	328—335
Marker	75

In tacan operation, there is no possibility through either a manual error or malfunctioning of an automatic channel-pairing mechanism to receive bearing from one ground station and distance from another ground station because the two services are provided by one radio set operating on one channel. This situation is quite analogous to modern television service, where one radio channel conveys signals for both picture and sound.

2. Distance Measurement

2.1 Operating Principles

Distance-measuring equipment is an outgrowth of radar ranging techniques, whereby distance is determined by measuring the time of round-trip travel of radio pulse signals between the two points. In navigational distance measurements, however, instead of using cathode-ray tubes as indicators, easy-to-read numbers are displayed on the distance meter. Also, instead of depending on natural reflections or echoes for the return trip of the pulses, a radio transpondor or beacon is used to transmit reply pulses. These responses are stronger than echoes and the radio channel over which they are transmitted positively identifies the source and hence the geographic location of the "echoing" point.

Referring to Figure 3, the airborne transmitter repeatedly sends out very narrow and very widely spaced interrogation pulses. These are picked up by the ground-beacon receiver, whose output triggers the associated transmitter into

sending out reply pulses on a different channel. These replies are picked up by the airborne receiver. Timing circuits automatically measure the interval between interrogation and reply pulses and convert this time into electrical signals that operate the distance meter.

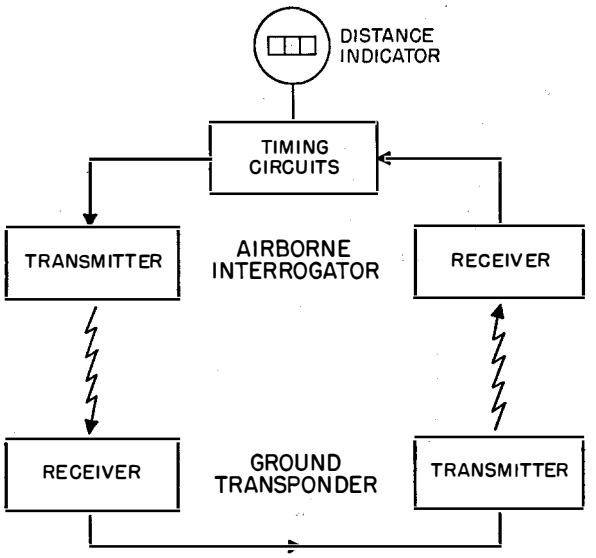

Figure 3—Principles of navigational distance measurement. Interrogation pulses from the airborne transmitter cause the ground receiver to trigger its transmitter to send reply pulses on a different channel to the airborne receiver. The timing circuits actuate the distance meter on the basis of the elapsed time for the round trip.

A given ground beacon may be interrogated simultaneously by a number of aircraft that are in the vicinity and have selected its channel for guidance. The ground beacon will reply to all interrogations and each airplane will receive all the replies being transmitted. To permit interference-free operation under these normal conditions, it is arranged that the interrogation pulses of each airplane occur at a rate that is intentionally permitted to "jitter," or vary within certain limits in an irregular or random manner. The jitter effect is obtained essentially by permitting a nonstabilized multivibrator circuit to exercise partial control over the interrogation rate. To sort out from among all the pulses received on an airplane those that are replies to its own interrogation pulses, use is made of a stroboscopic search process that is entirely automatic in operation.

The strobe locates the reply pulses by finding the one fixed or very slowly changing time delay, *always measured from its own previous interrogation pulse*, at which a reply pulse is repeatedly received. Because the interrogation pulses from other aircraft are nonsynchronous or random with respect to those from a given airplane, reply pulses corresponding to such foreign interrogation pulses will not be received regularly at any fixed time delay on the given airplane.

The strobe searches automatically each time the airborne radio set is tuned to a new ground-beacon channel or if there is some *major* interruption in the radio signals. The strobe scans progressively over various time-delay intervals by means of a sliding range gate or time slot. It quickly tests each time-slot position for the number of successive reply pulses received within a certain uniform checking period. If no replies or only sporadic replies are received, the strobe advances the range gate to test a slightly longer time-delay interval, and so on. When, at some particular time-delay interval, safe evidence of recurrent replies is detected by a counting process, the strobe has completed its search and stops, since this condition is fulfilled only by reception of the desired reply pulses. Those pulses are the only ones that are always received in synchronism with the randomly jittered interrogation pulses.

The complete search process covering the entire range of time delays may require up to a maximum of 20 seconds. Thereafter, the strobe locks to the proper reply pulses and converts to a tracking operation. Then the delay setting of the range gate automatically and continuously follows any normal variations in the time delay of the proper reply pulses. Such variations will occur if the distance between the airplane and the beacon is actually changing as a result of its flight path, and are necessarily very slow because of the relation between interrogation rates and airplane speeds.

While the strobe is in the search condition, the interval between successive interrogation pulses is about 1/150 second. Consider an airplane traveling radially at 1000 nautical miles (1853 kilometers) per hour. The change in round-trip travel time from one interrogation to the next would be about 0.023 microsecond.

If, for example, about 10 successive pulses must be received at a constant delay to confirm that they were the proper replies, during the interval of about 1/15 second required to check this response, the total change in round-trip travel time would be only about 0.23 microsecond. As the width of the pulses is about 3.2 microseconds, it is clear that during a search operation the round-trip travel time of the pulses is for all practical purposes a fixed quantity. Even in track operation, when the interval between successive interrogation pulses is about 1/24 second, the change in round-trip travel time from one interrogation to the next is quite small, about 0.14 microsecond, for the fairly extreme case of an airplane traveling radially at 1000 nautical miles (1853 kilometers) per hour. Hence, in practice, the tracking circuits are confronted with only quite-small incremental changes in delay due to airplane travel.

When the strobe is locked to the proper reply pulses, the time-delay setting of the range gate is a proportionate measure of the distance of the airplane from the ground beacon (approximately 12 microseconds round-trip travel time per nautical mile, or 7 microseconds per kilometer). The mechanical position of the device that varies the time delay of the range gate is used to control electrically the position of the numerical indicators on the distance meter.

A crystal-controlled 4044-cycle-per-second oscillator is used as a "yardstick" or time reference. For this frequency, the period $1/f = 242$ microseconds, which is the round-trip travel time to an object 20 nautical miles (37 kilometers) away. In essence, the time interval between interrogation and reply (the time-delay setting of the range gate) is measured in terms of the corresponding number of cycles and fractions of a cycle of the 4044-cycle reference wave. The principle is similar to that used in precision radar indicators; a crystal-controlled oscillator generates range markers that serve to measure microsecond intervals for the accurate determination of distance. In tacan, the time delay between the transmitted interrogation pulse and the opening of the range gate is controlled by a voltage divider and a phase shifter. These control devices set the delay equal to known numbers of cycles and fractions of a cycle of the reference wave. To establish an accurate and convenient zero reference for the delay measurement, each interrogation pulse is actually triggered by one of the 4044-cycle oscillations, the particular one being determined in a limited random manner by the 24- or 150-pulse-per-second rate of the nonstabilized multivibrator circuit. This method is very stable and accurate and also lends itself to making the distance data available in the form of a shaft rotation for control of automatic pilots, computers, et cetera.

The time-measuring circuits have a memory provision, so that if reply signals fail to be received for approximately 10 seconds, the preexisting distance indication will be maintained without the search operation being restarted.

The ground beacon periodically transmits a station-identification signal in international Morse code. These signals are transmitted automatically about every 75 seconds and temporarily replace all reply pulses that would normally occur at that time. The memory feature prevents this substitution from interrupting the airborne distance indications. The ground beacon produces the identification signal by automatically keying a 2700-cycle tuning-fork-controlled oscillator circuit. On the aircraft, the identification signal is received audibly in telegraphic code.

By strobe principles, which are common to all types of distance-measuring equipment, many (more than 100) aircraft may simultaneously and without mutual interference obtain distance service from one ground beacon. Pulse interrogation rates from each aircraft are of the order of 24 per second during tracking operation; they are temporarily higher, approximately 150 per second, during the search process. The over-all average rate is considered to be about 30 per second on the basis that the average airplane within range will be tracking 95 percent of the time and searching 5 percent of the time. The pulses are of the order of 3.2 microseconds wide and the duty cycle, or percentage of time during which radio-frequency energy is being transmitted, is very low. The average interval between successive interrogation pulses from an airplane is approximately 33 000 microseconds; the average interval between successive reply pulses to 100 airplanes is approximately 370 microseconds. It is evident that even with 100 aircraft receiving service from a beacon,

the radio channels are unoccupied during the very long spaces between successive pulses. These spaces are available in tacan for transmitting information for other navigational functions.

Actually the pulse signals are always twin pulses, with a prearranged spacing between the two components. The receivers, both ground and airborne, are followed by discriminators or twin-pulse decoders that pass only pulse pairs of the prescribed spacing. Isolated single pulses or pulse pairs with some other spacing will not pass the decoder. This technique increases the average power radiated and makes the system less susceptible to errors or interference caused by false signals. False signals might be produced by radars, ignition systems, and other extraneous sources of radio-frequency energy but only rarely will they have the right spacing to pass twin-pulse decoders. The original formation and the decoding of twin pulses may be accomplished by use of delay circuits or lines, coincidence circuits, and similar techniques.

The twin-pulse technique is used only for the purposes mentioned above and not for establishing operating channels by using differently spaced twins to define a number of channels on each radio frequency. The spacing between the components of the twin pulses is fixed at 12 microseconds for both airborne and ground equipment. Hence the ground and air equipments employ twin-pulse encoders and decoders of fixed setting. In this paper, all pulse signals (distance, identification, filler, or bearing) should be understood to refer to the basic twin pulses of 12-microsecond spacing.

2.2 Channel Assignments

The assignment of a clear radio-frequency channel to each beacon prevents it from being blocked or overloaded by interrogation pulses intended for other beacons in the same geographical area. A beacon receiver will receive only those interrogation pulses intended for it, since all others are transmitted on different radio channels.

All transmission frequencies are under direct crystal control, as is usual for standard high-quality military and commercial equipment. Hence, adjacent-channel rejection depends solely on the effective selectivity of the system without being compromised by frequency drifts.

In assigning frequencies to clear-channel crystal-controlled navigational stations, the same rules are followed as for established services such as aural and television broadcasting, mobile, and point-to-point. That is, the *identical* frequency is not assigned to two ground stations that are within likely interference range of each other. For tacan, this distance would be of the order of 400 miles (740 kilometers), dependent somewhat on aircraft altitude owing to line-of-sight considerations. Beyond that conventional restriction, any frequency, adjacent or far-removed, may be assigned with complete safety to any tacan station, close by or distant.

Actually, however, tacan has an important advantage over most other systems in the matter of cochannel interference. Because it uses low-duty-cycle pulse transmissions, the signals from two stations on the same radio channel will *interleave*, but not *add*. Thus, only the stronger will effect the receiver, the weaker being almost totally rejected. The net result is that the airborne equipment will display the correct *distance* and *bearing* to the nearer of the two stations. In continuous-wave systems, on the other hand, even a relatively weak interfering signal, while not taking complete control, may introduce large errors in bearing. This simplifies greatly the channel-allocation problem and should make the present 126 channels adequate for a long time to come.

2.3 Constant-Duty-Cycle Operation

In principle, the transmitter of a distance-measuring ground beacon need send out pulses only in reply to such interrogations as are actually received from aircraft. For each such aircraft, it would send out approximately 30 pulses per second. The total output of the beacon transmitter might then vary from zero to around 3000 pulses per second, depending on the existing traffic.

However, one of the major problems with all transpondors or beacons is to maintain their receiver sensitivity at the maximum level without having the associated transmitter continually triggered by noise. A very satisfactory solution is to operate the beacon on the constant-duty-

cycle principle. In this method of operation, the beacon receiver is provided with an automatic-gain-control system that maintains the number of pulses out of the receiver at an almost constant value; in this case of about 2700 pulses per second.

Thus, if few interrogations are being received, the gain of the receiver automatically increases, adding noise-generated "filler" pulses until the requisite total number is obtained. If several more aircraft come within range, the receiver gain drops slightly and the noise-generated filler pulses are replaced by replies to interrogations. If more than 100 aircraft interrogate, replies are made only to the strongest 100 pulses. The relation between gain and number of pulses is such that only a 3-decibel change in sensitivity occurs between the reception from 1 aircraft and from 100 aircraft.

An added advantage of this type of operation is the constant current drain on all transmitter circuits. This permits simpler power-supply design, minimizes drifts of tuned circuits, and allows a more predictable component life and maintenance cycle.

Stated differently, both the ground and the airborne equipments are forced to operate as if 100 aircraft were present all the time. The equipments are designed for this load and no adverse effects due to variations in actual traffic conditions can occur.

Since the beacon transmits at a constant rate of 2700 pulses per second even if 100 aircraft are interrogating, it would appear that in heavy traffic the aircraft may not receive 100-percent replies. It is assumed that among all the aircraft interrogating a beacon at a given time, 95 percent will be in track and 5 percent will be in search. The interrogation rate for 100 aircraft would be 24 pulses per second for each of 95 aircraft plus 150 pulses per second for each of 5 aircraft or a total of 3030 interrogations per second. If 2700 replies per second are returned to the 3030 interrogations per second, the ratio of replies to interrogations is 90 percent. However, the airborne strobe system is designed to operate safely with a reply ratio at least as low as 70 percent, that is 21 replies per second compared to 30 interrogations, or 2100 replies per second for 100 aircraft. Hence, an actual reply rate of 2700 replies per second to the interrogations transmitted under specified maximum traffic conditions represents a safe margin of operation.

Constant-duty-cycle operation has a still further advantage. With the beacon always putting out some 2700 pulses per second, from one source or another, there is provided a medium over which another navigational function can operate. As far as distance information is concerned, it is only the timing of the pulses that matters. Variations in strength of the pulses produced by pulse-amplitude modulation may be used to convey additional information. The tacan bearing function described in the next section applies this principle.

3. Bearing Indication

3.1 General Features

The radio apparatus over which tacan operates is essentially a 1000-megacycle distance-measuring equipment.

The impetus for the development of tacan came from a requirement of the Navy for a bearing system that could be installed on carriers to furnish homing-beacon service to carrier-based aircraft. Previous omnidirectional ranges, including very-high-frequency designs, were impracticable for such installations because of the size of their ground-beacon antennas and their siting requirements. To meet this need and as a first step in the development of tacan, an "omnirange only" predecessor was built and demonstrated (*AN/URN-1* and *AN/ARN-16*).

The Air Force also recognized the advantage of a bearing equipment that could be mounted on a truck or trailer for ready installation at field sites. Additionally desired were greater bearing accuracy and more freedom from siting restrictions even for permanent installations. Finally, both services recognized the feasibility and the utility of multiplexing distance and bearing services so that one small beacon with one airborne equipment could provide complete polar-coordinate navigational service from fixed or transportable installations on land or from ships.

The heart of any omnidirectional range is the ground-beacon antenna system. It must produce a specified directional radiation pattern that

somehow must be rotated or switched around a vertical axis. The physical dimensions of an antenna depends on its operating radio frequency or wavelength, and there is a 10-to-1 reduction in wavelength in going from the very-high-frequency band in which present omnidirectional ranges operate to the 1000-megacycle region used for tacan. Advantage is taken of this factor to increase the tacan-antenna size considerably *in terms of wavelength* for superior performance while still maintaining reasonably small physical dimensions.

The tacan ground antenna is fully enclosed in a cylindrically shaped protective cover that is approximately $3\frac{1}{2}$ feet (1.1 meters) in diameter with a total height including antenna proper and motor drive of about 6 feet (1.8 meters). No counterpoise is required and the antenna may be installed on a tower or on the mast of a ship.

3.2 Antenna and Coarse-Bearing System

Figure 4 illustrates the arrangement of the tacan ground-beacon antenna. Only the central element, shown as a vertical rod, is driven by radio-frequency energy from the transmitter. This is stationary and has no directivity in the horizontal plane. Actually, it is a vertical stack of discone radiators having a diameter of about 3 inches (7.6 centimeters).

Around the central element is an inner cylinder of insulating material (fiber glass) with a diameter of about 5 inches (12.7 centimeters). This cylinder carries a vertical conductive wire that is completely insulated from everything else. The wire acts as a parasitic antenna or reflector since it intercepts and reradiates some of the energy radiated towards it by the central element. Its distance from the central element is such that it distorts the normal circular radiation pattern into a cardioid as shown in Figure 5A. The entire cardioid pattern turns 15 times per second with the rotation of the inner cylinder.

As a result of the rotation of the cardioid pattern, the signal received at any given direction from the beacon goes through corresponding cyclic variations in strength as a function of time; identical to what an airborne receiver would experience if it were flown around a stationary cardioid pattern at 15 orbits per second. Figure 5B is obtained by replotting the polar-coordinate pattern in rectangular coordinates with time replacing direction angle as the variable of interest. The vertical axis represents signal strength and the horizontal axis represents time. A cardioid thus transformed into rectangular coordinates is simply a sine wave. For this discussion, the unvarying (direct-current) component may be neglected. Since the cardioid is a single-lobed pattern, it takes one full turn of the antenna or 1/15 second for the received signal to go through one complete cycle of variation. In short, the airplane receives a 15-cycle-per-second modulation that may be demodulated into a sine-wave signal by radio detection methods.

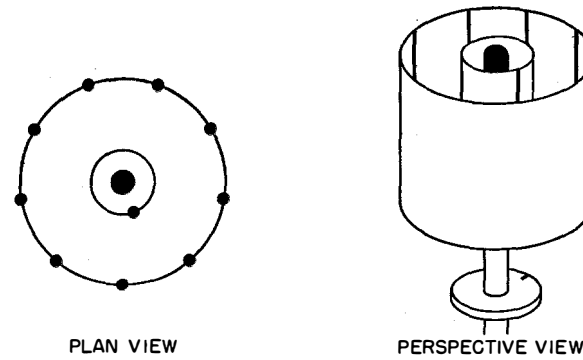

Figure 4—Ground-beacon antenna. Only the central element, which is fixed in position, is energized by the transmitter. The parasitic elements are embedded in two fiber-glass cylinders that rotate at 15 revolutions per second. A reference-pulse disk is mounted on the drive shaft below the antenna.

For bearing indication, it is the electrical phase of the audio signal that is important. Referring to the polar plot of Figure 5A, it is clear that if at a given instant of time the maximum of the lobe points due north, then this maximum will not aim due east until some time later (1/60 second, to be exact). This is a way of saying that along progressively clockwise directions around the beacon, the electrical phase of the received 15-cycle-per-second audio modulation is progressively retarded in comparison with the phase received due north. In the particular case of the cardioid, a single-lobed pattern, there is a one-to-one correspondence;

that is, for each degree of geographical bearing change, there is a one-degree change in electrical phase of the 15-cycle-per-second audio signal. It is only necessary to use the electrical phase of the received signal to position the pointer of a bearing indicator.

For phase measurements, it is necessary to have a fixed reference of the same frequency that is received at all directions around the beacon with identical phase. As a convenient standard, the phase of the reference wave might be adjusted so that its maximum occurs at the same instant of time that the maximum of the rotating cardioid lobe aims north. In this case, the airborne electrical phase difference measurement would numerically represent the airplane's geographic bearing, which is conventionally measured clockwise from north. Actually, any other standard adjustment for the reference wave might be adopted; the airborne phase-measuring circuits would simply be zero-calibrated accordingly.

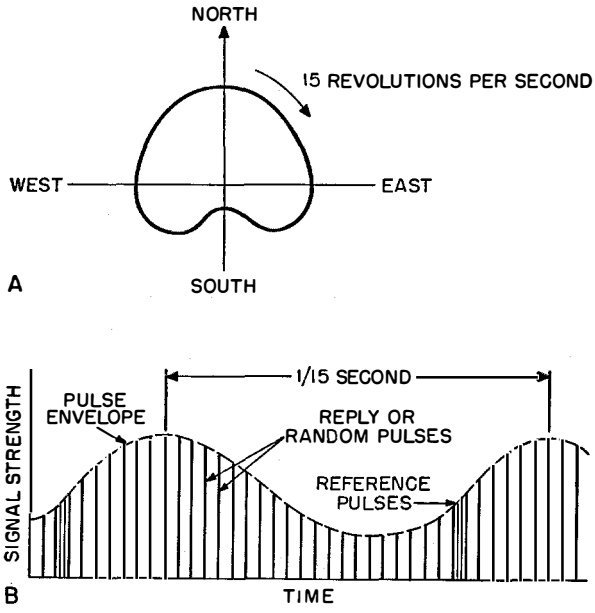

Figure 5—The circular radiation pattern of the central element of the antenna is distorted into the cardioid pattern at *A* by the parasitic element carried by the inner cylinder. At *B*, the polar-coordinate pattern has been replotted in rectangular coordinates producing a sine wave. The vertical lines represent reply or random pulses and the group of pulses much closer together are the reference signals for phase measurement.

3.3 Pulse Operation of Bearing System

The source of radio-frequency energy supplied to the central element of the antenna is the transmitter. Under constant-duty-cycle type of operation, some 2700 pulses per second are produced at all times. Some of these may be distance-measurement reply pulses, others are random filler pulses. All transmitter pulses are of absolutely equal amplitude. Their radiated strength, however, is controlled by the shape of the directional pattern of the antenna. Considering only the effect of the inner cylinder, this shape is a cardioid as plotted in Figure 5A.

The result is that the airplane receives an amplitude-modulated series of discrete pulses as represented by the spaced vertical lines in Figure 5B. The envelope of the amplitude of these pulses is indicated by the dashed line. This envelope is a sine wave of 15 cycles. The phase of this envelope gives bearing information, just as in the case of a continuous-wave system, but this envelope is extracted by a peak-riding type of detector, that is, one whose output follows the tops of the pulses.

With an average pulse rate of 2700 per second, during a 1/15-second modulation period there are some 180 pulses (actually twin pulses). This is a sufficient number so that the output of the peak-riding detector is a faithful reproduction of the sine wave corresponding to the rotating cardioid pattern of the antenna. The depth of modulation is intentionally kept well below 100 percent (somewhere between 12 to 30 percent) to avoid complete nulls in the envelope. This is done to insure that at no time and in no direction are pulses for distance-measurement or other purposes seriously weakened in strength.

A suitable reference signal is required for phase measurement. For this purpose, pulse signals transmitted at some fixed phase and at the correct frequency (15 cycles) serve as well as a complete wave. These signals are actually sent out each instant that the maximum of the rotating cardioid pattern aims due east (for a reason to be explained later). These 15-cycle or coarse-reference signals are distinguished from the distance-measuring signals by their coding. The distance replies or filler pulses are 12-microsecond twins that occur irregularly about 2700 times per second; hence the interval between

these signals is somewhere in the vicinity of 370 microseconds, with some variation in this figure. The 15-cycle reference signal, on the other hand, is a precisely regular group consisting of 12 pulses, each a 12-microsecond twin, spaced exactly 30 microseconds apart. This reference signal is illustrated in Figure 5B by a group of extra-close pulses and is for the case of an airplane due south of the beacon. For an airplane at a different bearing, the time of arrival of these pulses, relative to the maximum of the 15-cycle pulse envelope, would be different from that shown in the figure.

The reference signal is initiated on the ground in the following manner. An aluminum disk attached to the drive shaft of the rotating cylinder of Figure 4B has a thin iron slug mounted at its periphery in line with the direction of the maximum of the carioid-pattern lobe. A stationary pick-up coil mounted close to the periphery of the disk is due east of the center-line of the antenna. Hence, once each turn of the antenna cylinder, at the desired standard instant, a signal is inductively generated in the pick-up coil to trigger the distance-measuring transmitter into sending out the specially coded coarse-reference signal. On the airplane, this coded signal is separated from the distance-measuring pulses by a special pulse-group decoder and is then used as the timing reference for the measurement of the phase of the pulse envelope wave.

The phase measurement uses a calibrated rotary phase shifter. The audio-frequency modulation wave is applied to the phase shifter, and the output from the shifter is "searched" or moved about in phase until some preselected index point on the wave is found to coincide in time with the reception of the reference signal. Coincidence is investigated by having a narrow time slot or gate formed by the index point on the sine wave, and determining whether the reference signal is received during this time-slot interval. The bearing search may require up to a maximum of 20 seconds to complete, depending on the actual bearing at the time. Thereupon the bearing circuits go into track operation.[1] That is, the phase shifter locks to the reference signal and continuously and automatically follows any normal variations in its time of reception with respect to the phase of the bearing-signal envelope. Such normal variations will occur if the bearing is actually changing as a result of the flight path. All the time that the circuits are locked to the reference signal during the tracking operation, the angular position of the rotary phase shifter is a direct measure of the bearing of the airplane with respect to the ground beacon. The angular position of the phase shifter under proper zero calibration is used to position the pointer of the bearing meter. This method of operation is stable, accurate, and lends itself to making the bearing data available in the form of a shaft rotation for control of automatic pilots, computers, et cetera.

The bearing-search process starts automatically each time the airborne radio set is initially tuned to a new ground-beacon channel or if there is some *major* interruption in the radio signals. The bearing-measuring circuits also have a memory provision. If for some reason bearing signals are lost for a short time up to around three seconds, the pre-existing bearing indication will be maintained without the search operation being restarted.

It should be borne in mind that *all pulses* transmitted from the ground beacon, whether intended primarily for distance-measuring reply, filler, station identification, or phase-reference purposes contribute to forming the amplitude-modulated pulse envelope or bearing-phase signal. Hence, changing the particular character of the ground-beacon transmissions from time to time in normal system operation does not interrupt or otherwise disturb the bearing-phase signal. Also, the radiation of the vital reference signals is arranged to take precedence over any distance-measuring replies, filler pulses, or identity code pulses that might otherwise occur.

The preselected index point actually used for phase measurement is not the *maximum* of the sine wave, which is a rather-broad region, but the more sharply defined point at which the varying portion of the wave *crosses* what would be the *zero axis* in going from its minimum to its maximum value. This index point is 1/4 cycle ahead of the maximum and on the cardioid

[1] Although the terms search and track are used in discussing the operation of the bearing-measuring circuits, there is no stroboscopic discrimination process involved, such as is necessary in the case of distance measurement.

pattern it corresponds to a radial index line that is 90 degrees clockwise ahead of the maximum. When in the course of the rotation of the cardioid pattern this imaginary index line sweeps past south, the maximum of the cardioid will be momentarily aiming due east. As has been previously stated, the transmission of the 15-cycle reference signal has been standardized to occur at that precise moment.

By adhering to the above conventions, zero phase difference, that is, time coincidence of the reference signal and the index point on the envelope wave, will be received by an airplane that is *due south* of the beacon as is illustrated in Figure 5B. The reason for this type of calibration is as follows. Although any omnirange beacon fundamentally establishes bearing of the *airplane from the beacon* (conventionally measured clockwise from north), pilots prefer directional indications from their own point of view, that is, bearing of the *beacon from the airplane* (also expressed clockwise from north). The two numerical quantities concerned are opposite or reciprocal bearings exactly 180 degrees apart (Figure 1 illustrates the geometrical relation). Hence, when an airplane is actually 180 degrees or due south from the beacon, zero phase difference is measured by the airborne circuits, and the bearing-meter pointer will properly indicate 0 degrees or due north to the beacon. For the situation illustrated in Figure 1, if the airplane is 75 degrees from the beacon, the airborne circuits will measure 255 degrees phase difference and the bearing meter pointer will properly indicate 255 degrees (75 + 180) to the beacon.

The bearing meter illustrated in Figure 1 presents the basic data produced by any omnirange, that is, an *absolute* bearing or direction angle that is zero-referenced from some *fixed geographical direction*, generally north (either true or magnetic north, as desired). In line with the type of directional indications that pilots find more directly useful and to which they are accustomed, the tacan bearing circuits additionally provide outputs that operate either or both of the standard cockpit indicators, the *ID-249* and the *ID-250*.

On the *ID-250* meter, or "radio-magnetic indicator," the zero reference is the *fore-and-aft axis of the airplane*, the top of the fixed meter case or lubber line representing the nose of the airplane. To produce this type of indication, the radio–magnetic indicator automatically combines tacan bearing information with magnetic-compass information to actuate the pointer of the instrument. As a result, the angular position of the pointer from the lubber line on the fixed meter case represents bearing from the airplane to the beacon measured, not from north, but from the nose of the airplane. If the meter were to be placed in a horizontal position, the pointer would always physically point toward the beacon, regardless of the heading of the airplane. This *relative* bearing type of presentation is particularly graphic and convenient for purposes of homing, or keeping the nose of the airplane aimed directly toward the tacan omnirange beacon.

On the *ID-249* or "course-selector-cross-pointer meter" the center of the fixed meter dial can be made to represent *any selected omnirange radial* as the zero reference for the directional indications. This type of presentation is particularly convenient for keeping the airplane on a given radial track. The pilot sets for a desired tacan radial track by rotating a knob until the selected omnirange bearing figure appears on a numerical indicator. Thereafter any deviations of the airplane from the selected radial track are evidenced by sidewise motions of the vertical bar of the cross-pointer meter from the center of the dial. The vertical bar thus directly gives the pilot left–right steering directions for keeping the airplane on the selected radial. The same principle may be employed for actuating an automatic pilot from tacan bearing signals.

The *ID-250* or the *ID-249* may also be used for position fixing, which requires knowledge of absolute or north-referenced tacan bearing. On the *ID-250*, this information is obtained by reading the pointer against the numbers printed on an inner movable dial card; this dial card is automatically positioned with reference to the meter case by the magnetic compass in accordance with the heading of the airplane. On the *ID-249*, the tacan bearing is obtained by rotating the course-selector knob until the vertical bar of the cross-pointer is centered on the dial, and then reading the numerical indicator.

3.4 Fine-Bearing System

The fine-bearing feature of the tacan omnirange function produces very greatly improved accuracy over any simple cardioid system. Errors in omnirange bearings arise from two main sources: imperfection of the phase-measuring circuits, which have only some finite limit of accuracy; and, more seriously, radio propagation effects known as site errors. Both errors are significantly reduced by the technique to be described, which requires an increase in antenna dimensions over that for the cardioid or coarse system.

In the case of the tacan antenna, the necessary increase in size still leaves a quite-compact assembly. Referring to Figure 4, the inner cylinder has a diameter of about 5 inches (12.7 centimeters). Now attention is directed to the outer cylinder, which is approximately 33 inches (84 centimeters) in diameter. It is constructed of fiber glass like the inner cylinder and rotates integrally with it 15 times per second. The outer cylinder, however, has 9 wires embedded in it. The wires are spaced uniformly at 40-degree intervals. These wires also are parasitic elements and have a distorting effect on the heretofore-considered cardioid pattern produced by the central antenna and inner-cylinder wire. The resulting composite pattern is plotted in polar coordinates in Figure 6A. The over-all cardioid or single-lobed variation is still present, and predominant in fact, but superimposed on it are 9 secondary variations or ripples. The maxima of these ripples or minor lobes are spaced 40 degrees apart.

To indicate the nature of the cyclic variations in pulse amplitude received by an airplane at a given bearing, the composite radiation pattern is transformed into rectangular coordinates in Figure 6B. For simplicity, only the envelope of the pulse amplitudes is shown, since pulse operation, peak-riding detection, et cetera, have been explained in connection with the coarse-bearing system.

This envelope signal has a basic 1/15-second period, as before, because of the predominant fundamental component due to the rotation of the inner cylinder. The outer cylinder also makes one complete turn in 1/15 second, which causes 9 ripples or minor lobes to sweep past the airplane. Hence the composite envelope wave also contains a 9th-harmonic sine-wave component, having a frequency of $15 \times 9 = 135$ cycles per second. The 135- and 15-cycle sine-wave components are separable by filters, and electric phase measurement is performed on each.

To furnish a suitable reference for measuring the phase of the 135-cycle component of the envelope wave, the ground equipment transmits appropriately timed and coded reference signals similar to those for the coarse system. In distinction to both the distance-measuring replies and the *coarse-bearing* reference signals, the 9th harmonic or *fine* reference signal is a precisely regular group of 6 pulses, each a 12-microsecond twin, spaced exactly 24 microseconds apart. In one rotation of the antenna, 8 of these groups are transmitted, separated by 40 degrees of rotation. The 9th position is occupied by the 15-cycle reference signal.

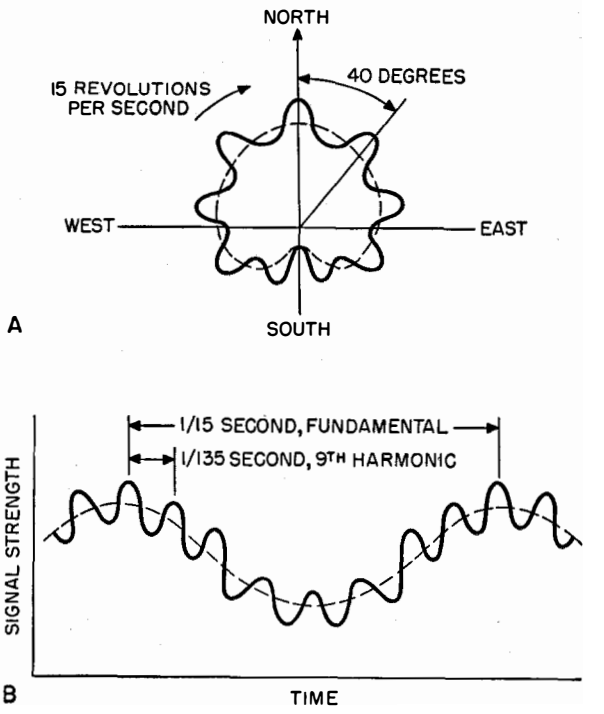

Figure 6—The solid line at *A* represents the composite radiation pattern produced by both cylinders. (Broken line indicates the elementary cardioid pattern.) *B* is the wave received as a result of the rotation of the antenna.

The important point is that in the case of the 135-cycle signal component the relation

between electric phase and geographic bearing is quite different from that of the 15-cycle signal component. Referring to Figure 6A, as an airplane progresses through a 40-degree arc of bearing, which is the angular width of a minor lobe, the phase of the received 135-cycle signal will move through a complete cycle or 360 electric degrees. Thus, each *single degree* of bearing change results in a 9-degree change in the measured phase of the 135-cycle signal. This ratio of 9 electric degrees per single space degree gives a pronounced magnifying effect in the process of detecting changes in bearing and is the basis for calling this the *fine* bearing system.

If the bearing indication were given by a pointer that made one dial revolution to indicate 360 degrees of bearing, then the circuits should be arranged to produce a 9-to-1 gearing reduction from the phase measurement to the bearing pointer. One degree of phase shift would then produce 1/9-degree of pointer movement. If the phase-measuring circuits were accurate to within one degree of phase on either side of the correct value, then the bearing-meter indication resulting from measurement on the coarse signal would also be correct to within one degree; however, the bearing-meter indication resulting from phase measurement on the fine system would be correct to within 1/9 degree.

By itself, the fine system has a 9-fold bearing ambiguity. From inspection of Figure 6A, it is evident that along any of 9 directions that are exactly 40 bearing degrees apart, airplanes will receive 135-cycle signals with identical phase. A measurement on this signal would indicate location accurately within some 40-degree bearing sector, but it would not be known *which* sector. This is analogous to the situation in a clock where the fast-moving minute hand (fine indicator) gives the exact minute but after any one of 12 hours. The slow-moving hour hand (coarse indicator) reveals the correct *hour sector* but only roughly tells the minutes.

To resolve the ambiguity of the 135-cycle phase measurement, the 15-cycle phase measurement is used. The 15-cycle measurement has more than enough accuracy for this purpose. However, a two-pointer clock-type bearing indicator with one dial revolution of one pointer corresponding to 360 degrees of bearing and one dial revolution of the other pointer corresponding to 40 degrees of bearing is not employed. For convenience and simplicity of interpretation, pilots prefer a conventional 360-degree bearing dial with a single pointer. Consequently, the 15-cycle coarse phase measurement initially moves the pointer to within the correct 40-degree bearing sector and thereafter ensures that it remains in the proper sector. The exact positioning of the pointer within that sector is under control of the 135-cycle fine phase measurement, suitably geared down. The very-accurate 135-cycle bearing information may also be employed for operation of radio–magnetic indicators, left–right meters, automatic pilots, computers, et cetera.

3.5 Site Errors

The most-troublesome source of errors in bearing systems is not instrumental but rather propagational. The elementary principles of site errors are explained with the aid of the illustrative example of Figure 7. In Figure 7A, it will be seen that energy reaches the airplane not only via the direct path D but also via indirect paths Q and R. The airplane being at a 128-degree bearing, it receives a 128-degree phase of the cardioid modulation along the direct path. Some large building, hill, or other prominence, which is at a 20-degree bearing (for illustrative purposes) also intercepts some energy from the beacon via path Q. This energy will have a 20-degree electrical phase. A weak but appreciable portion of this energy may reach the airplane along path R by reflection or reradiation. The composite signal $(D + R)$ will have an electric phase that in general differs from the phase of the desired direct signal, and since the airplane receiver can only respond to the composite energy that reaches it along all paths, an appreciable error in bearing can result.

Since electric waves are concerned, the characteristics of the composite signal $(D + R)$ are determined by vectorial addition, performed by taking into account the phase and the magnitude of the individual signals. In Figure 7B, it is seen that the composite signal has a phase that differs by 18 degrees from the phase of the desired direct signal. The bearing meter in the coarse omnirange would therefore indicate

a geographic bearing that is 18 degrees in error. As the airplane moves about, the geometry of an actual situation changes in a very complex manner. Different reflecting objects in different directions may all simultaneously interact with the direct signal. The bearing meter may fluctuate in quite an erratic manner.

To minimize such effects, the ground beacon should be located on very flat terrain having no large buildings, metallic structures, hills, or other prominences in the immediate vicinity. In practice, such an ideal location cannot often be found. It is not obtainable on board a ship with its complicated superstructure. The location of suitable sites has always been a difficult problem for omnirange installations especially in rough terrain.

Site error is greatly reduced by use of the 9-lobed fine-bearing operation of tacan. The ultimate theoretical improvement is 9-fold. It may be shown by mathematical analysis that for objects of the same reradiating power, the *maximum electric* phase error between a direct signal and a composite signal in a multilobed system is the same as in a single-lobed system. It is clear that the difference in phase between the *direct signal* and the *reflected signal* (denoted by the angle ϕ in Figure 7B) will depend on the particular geometrical configuration of the beacon, airplane, and reflecting object. Further, for the identical geometrical configuration, the angle ϕ will be generally different in a cardioid and a multilobed system because of the different relation between bearing angle and signal phase. In either system, however, considering all possible geometrical configurations, the range of all possible values of the angle ϕ is still effectively the same, that is, from 0 to 360 degrees, since we are dealing with phase angles. This is indicated by the dash-line circle, which represents the locus of all possible orientations of the reflected-signal vector R compared to the direct-signal vector D in either type of system, for a given small value of reflection coefficient. This is a justifiable assumption in practice.

It is evident that the largest possible value of the angle ϵ (which represents the error in phase between the *direct* and the *composite* signals) occurs when the geometrical configuration is such that the angle at the vertex V in the vector diagram equals 90 degrees. In a cardioid system, the corresponding geometrical configuration might be, as shown in Figure 7A, a 108-degree relative bearing between airplane and reflecting object. In a 9-lobed system, the geometrical configuration might be a 108/9 or 12-degree relative bearing between airplane and

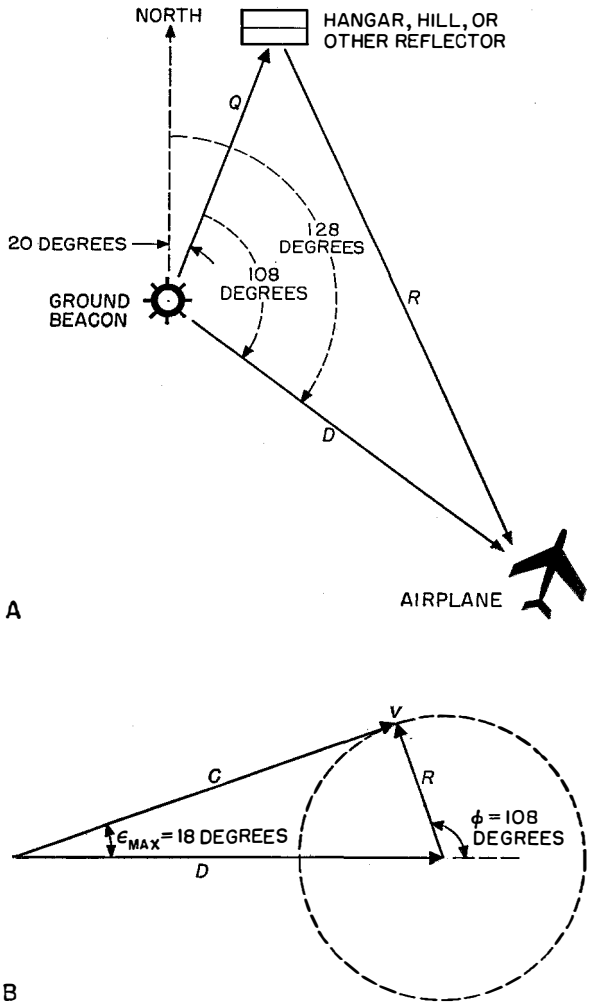

Figure 7—Site errors in a geometrical configuration are illustrated at *A* and in a vector diagram at *B*. C = composite signal, D = direct path or signal, R = reflection path or signal, V = vertex, and ϵ = error angle.

reflecting object. But *in either system*, if (for illustrative purposes) the reflected signal R is 1/3 the magnitude of the direct signal D, the *maximum* value of angle ϵ is the *same*, that is, approximately 18 degrees.

In a cardioid system, this maximum value of ϵ would produce a maximum bearing-indication

error of 18 degrees. In 9-lobed system, however, each degree of electric phase angle of the signal corresponds to 1/9 degree of bearing; hence, the fine-system maximum bearing-indication error would be only 2 degrees. To use the analogy offered previously, suppose that by accident (simulating a site error) one were to displace both the hour and the minute hands of a clock by 90 degrees of *dial angle* (a full quarter turn). The coarse or hour-hand reading would be in error by 3 full hours or 180 minutes of *indicated time*. The fine or minute-hand reading would be in error by only 15 minutes of *indicated time*; that is, a 12-fold smaller time-indication error is produced from the same mechanical disturbance.

The bearing-indication error produced by a given reflecting object in either a cardioid or a multilobed system may vary from some maximum value down to zero depending on the particular bearing of the airplane. It is significant, however, to note that as the airplane flies around the beacon some average value of error will be experienced, and that the statistical average error is approximately 64 percent of the maximum error in either system. In other words, a multilobed system will accomplish the same percentage reduction in *average* bearing-indication errors as it does in *maximum* bearing-indication errors, as compared with a cardioid system. Hence, the site-error improvement comes into play not only for isolated extreme errors but also for the statistical or average behavior, which is of greater practical importance.

The improved site freedom of the tacan omnirange due to the fine system is one of its most useful attributes. With the present equipments, comparative experimental tests at various locations have shown very substantial reduction in average and extreme bearing errors caused by site effects, as compared to cardioid systems. At sites where a very-high-frequency omnirange is practically useless, a tacan beacon can still give good service.

3.6 Vertical Directivity

In radio systems, it is possible to provide a greater range of service without increased transmitter power by concentrating the energy in a desired direction by means of directional antennas. In a point-to-point communication system, both horizontal and vertical directivity may be used. In an omnidirectional navigational system, it is obvious that only vertical directivity may be used for increasing the service range.

Airplanes that are distant from a beacon, although at a considerable altitude, are located on a line-of-sight that is very close to horizontal with respect to the beacon. Therefore, the radiation from the ground beacon should be concentrated along the horizontal direction. For a line-of-sight to be steeply inclined, the airplane must be quite close to the beacon; in this case adequate signal strength is no problem. Actually, the direction of maximum radiation should preferably be slightly above the horizontal. With such uptilting, there is less likelihood of strong energy striking nearby low-lying structures and hills and thereby producing site errors by reradiation

To achieve directivity in the vertical plane, the controlling factor is the vertical height of the antenna in terms of wavelengths. The application of this principle to 100-megacycle onniranges is difficult. With tacan operating wholly in the 1000-megacycle band, both bearing and distance functions make use of a considerable amount of vertical-pattern directivity, while maintaining antenna heights at very modest values. The central element of the tacan antenna is a vertical stack 4 feet (1.2 meters) in height, consisting of 7 discone radiators. The uptilt of the direction of major radiation is approximately 5 degrees above the horizon.

4. System Performance

Complete *system* errors include instrumental and propagational or site errors. The latter errors are quite variable depending on the location. All omnirange errors are very substantially reduced by the fine system. Average tacan omnirange complete-system errors are about 3/4 degree. Distance accuracy is fundamentally limited by the pulse width but in practice depends largely on the refinement of the time-measuring circuits employed in particular models of airborne equipment. Tacan distance-measurement accuracy is within about

±600 feet (183 meters) plus 0.2 percent of the distance measured.

In the very- and ultra-high-frequency bands, service range is limited not only by transmitter power and receiver sensitivity but more practically by line-of-sight consideration as determined chiefly by the altitude of the airplane. Tacan bearing service extends to 200 nautical miles (371 kilometers) or more, subject to line-of-sight limitations. Distance-measuring service, in practice, is additionally limited by the built-in maximum search range of the strobe circuits and the associated maximum scale of the distance meter. It is designed to serve out to 200 nautical miles (371 kilometers) to match the range of the associated bearing function.

5. Equipment Models

Thus far, only military-specification models have been produced in quantity. Under development for civil use is a less-expensive and smaller airborne set for private fliers. It gives bearing and distance with multichannel service unde crystal control but some of the automatic refinements of the military equipment are omitted. The distance reading is displayed on a number wheel as in the *AN/ARN-21*, but bearing indication and channel tuning require some additional manual control. A preliminary model (Figure 8) has already been flight tested. Also under development is an airborne model conforming to the type of construction favored by the civil airlines.

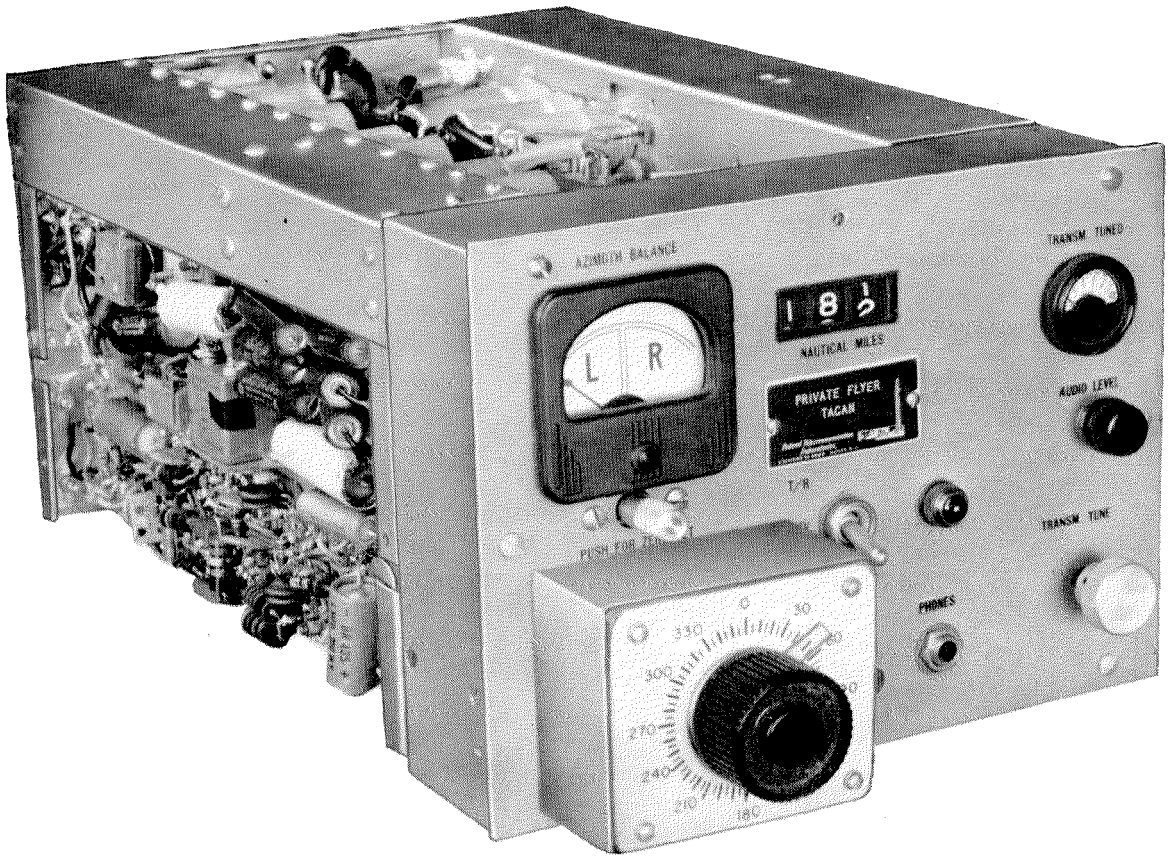

Figures 8—Experimental model of tacan airborne equipment for civil use on small aircraft.

Tacan Ground Beacon AN/URN-3

By HENRY B. SCARBOROUGH

Federal Telecommunication Laboratories, a division of International Telephone and Telegraph Corporation; Nutley, New Jersey

TACAN is a radio navigational system that provides meter indications of the distance and bearing of an equipped aircraft from a ground beacon. This article covers the ground equipment, *AN/URN-3*, with the exception of the antenna, which is described in a separate paper.

1. Equipment

A tacan ground-installed beacon consists of a receiver–transmitter, such as the *AN/URN-3*, and either a shipboard or a shore antenna.

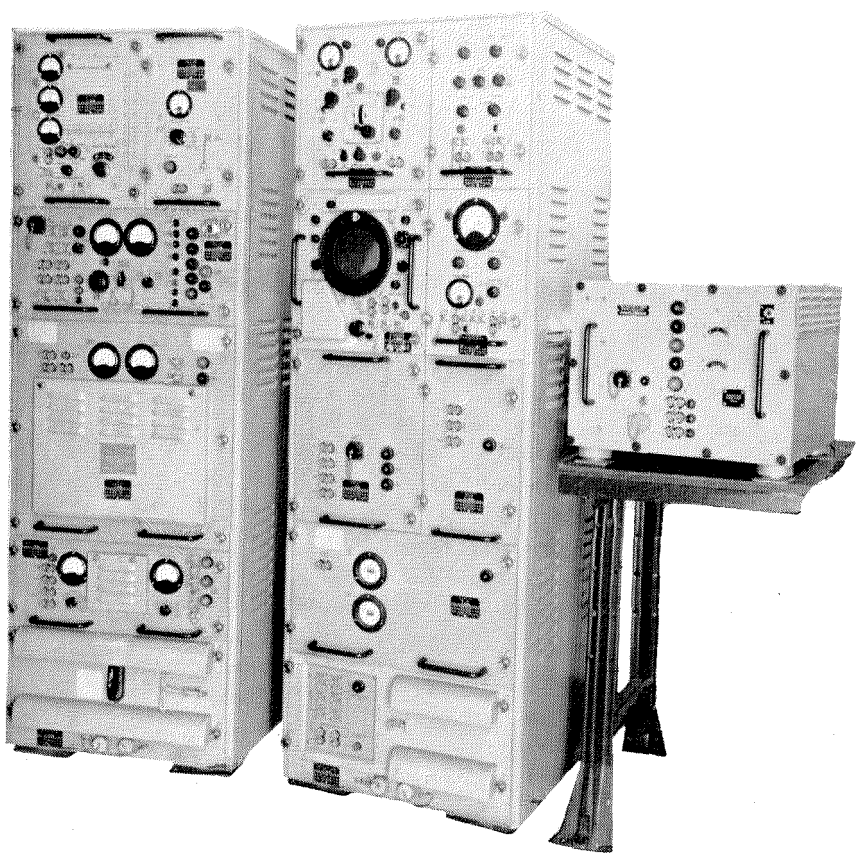

Figure 1—The *AN/URN-3* receiver–transmitter, special test equipment, and monitor. The over-all cabinet dimensions are 72 inches (1.83 meters) high, 25 inches (0.64 meter) wide, and 26 inches (0.66 meter) deep. There is a 2-inch (5-centimeter) extension in front and a 6-inch (15-centimeter) extension at the rear. The upper four drawers in the righthand cabinet are test equipment. The separate unit on the table is a monitor for independently checking beacon operation.

Figure 1 is a photograph of the *AN/URN-3* receiver-transmitter, which is housed in two cabinets, each 72 inches (1.83 meters) high by 25 inches (0.64 meter) wide by 26 inches (0.66 meter) deep, with a 2-inch (5-centimeter) front and 6-inch (15-centimeter) rear extension. The width and depth, after removal of the rearward extensions, permit passage through surface-vessel hatches. The top four drawers of the right cabinet are specialized test equipment, while the smaller unit on the table is an independent monitor.

It was decided to make a single installation in 2 cabinets, including the special test equipment; thus a dual installation will consist of only 4 cabinets if the transfer equipment replaces the test equipment in the second set.

The cabinet at the left houses the radio-frequency, video-frequency, and control circuits; the other cabinet contains the power supplies for the transmitting circuits and in the upper half the special test equipment.

Front access is provided by slide-mounted pull-out assemblies. For ease of handling, the circuits have been compartmentalized into drawer assemblies, each weighing 100 pounds (45 kilograms) or less, with the exception of the klystron amplifier–modulator assembly, which weighs 222 pounds (101 kilograms). When withdrawn from the cabinet, as illustrated in

Figure 2—Two of the slide-mounted drawers pulled out fully to demonstrate the accessibility provided by the design.

Figure 2, the drawers rest on the slides. When fully engaged in the cabinet, the drawers are lifted off the slides and are supported by large taper pins in the rear and pickup pads in the front. The drawers are interconnected through flexible cables.

Kel-F insulated wire, silicon-rubber-insulated high-voltage cable, and Teflon-insulated radio- and video-frequency coaxial cables are employed throughout the transmitter and cabinet wiring. The receiving and coding circuits at the top of the main cabinet employ standard wire and cable insulation.

Epoxy-resin-encased transformers contribute to space saving. Three of these are used in the high-voltage circuits of the transmitter: a 3-phase unit for high-voltage-rectifier plate power, filament transformer for the rectifiers, and low-capacitance unit for the klystron filament.

From a component standpoint, the Sperry *SAL-39* high-power klystron used in the final amplifier presented some problems since it was in the process of development. The *SAL-39* was incorporated in the *AN/URN-3* design after it became apparent from preliminary investigations that a rugged tube of this type was well-suited for this service.

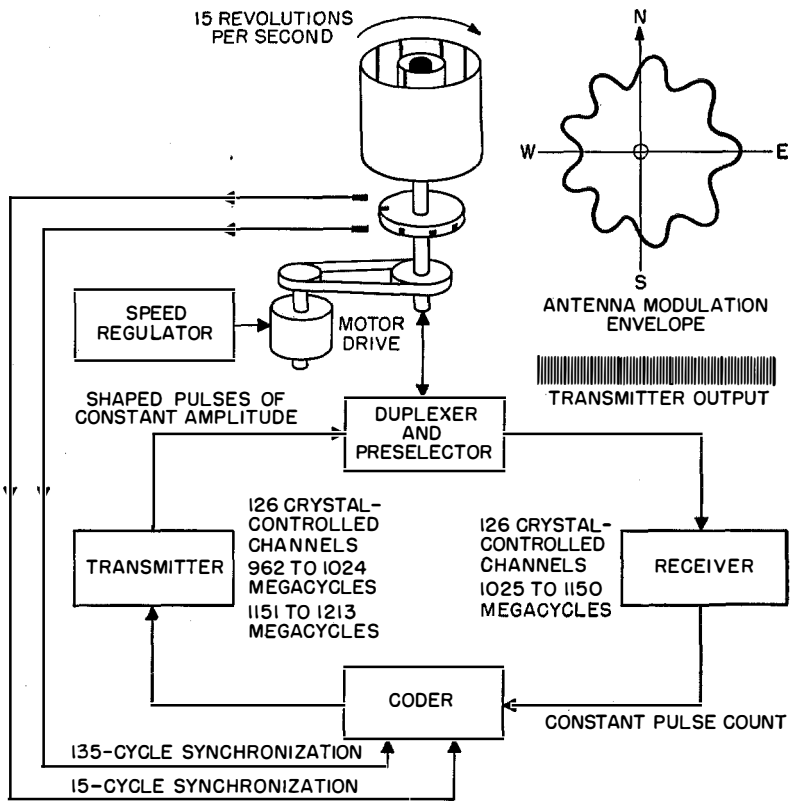

Figure 3—Block diagram of tacan beacon.

2. *Principles of Operation and Design*

The principles of operation and design of the *AN/URN-3* are shown in the block diagram of Figure 3. Essentially the tacan beacon is a high-performance distance or range transpondor on which the bearing function has been superimposed through the addition of a rotating directional antenna.

Any of 126 clear frequency channels are available for operation. The receiving frequencies are spaced at 1-megacycle-per-second intervals in the range from 1025 to 1150 megacycles and the transmitting frequencies are similarly spaced in either of two ranges from 962 to 1024 and from 1151 to 1213 megacycles. A high-stability narrow-band receiver and a high-stability transmitter with a controlled narrow-band spectrum provide the necessary channels. The essential requirements for bearing indications are a constant average duty cycle and a constant-amplitude pulse output from the transmitter together with high-accuracy multilobe directional modulation by the rotating antenna. These bearing requirements are superimposed on the requirements for range operation, namely accurately fixed beacon delay, traffic capacity for 100 aircraft, and a service range of 200 nautical miles (371 kilometers).

The design allows for a transmission-path loss of 146 decibels. The air-to-ground path comprises the airborne transmitter with a peak power output of 1 to 2 kilowatts (+30 to +33 decibels referred to 1 watt) and the ground

receiver with a sensitivity of −125 decibels, making a total propagation path allowance of 155 to 158 decibels. The ground-to-air path comprises the ground transmitter with peak power output of 5 kilowatts minimum (+37 decibels) and the airborne receiver with sensitivity around −120 decibels, with a total propagation-path allowance of 157 decibels. If 10 decibels are allowed for airborne and ground cable losses and safety factors, the permissible loss from antenna terminal to antenna terminal of the receiver–transmitter equipments is around 146 decibels.

A common antenna receives and transmits all information. The amplitude modulation produced by the rotating directional elements of the antenna is acceptable in both the receiving and transmitting paths. Incoming signals pass to the receiver-transmitter duplexer with a transmission-line loss of 1 to 3 decibels, depending on antenna height and type of line employed.

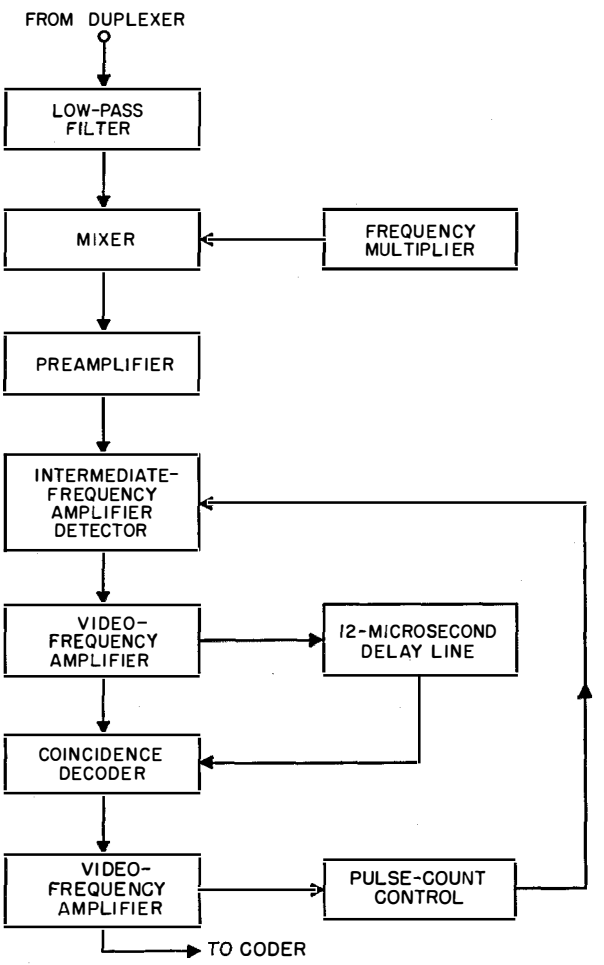

Figure 4—A block diagram of the receiver.

The 63-megacycle separation of receiving and transmitting frequencies permits the use of a passive duplexer. It consists of a rigid air-insulated coaxial line and 3 quarter-wavelength coaxial cavities in cascade constituting the receiver band-pass filter. A folded open-ended stub is tuned for optimum performance at the transmitter frequency. The loss caused by the duplexer is 0.5 decibel to the transmitted and 1 decibel to the received signal.

The receiver, block-diagrammed in Figure 4, triggers replies to properly coded range interrogations arriving on the selected channel. In normal traffic, 70-percent replies occur for signal levels better than −125 decibels at the receiver terminal.

The local-oscillator input to the mixer, which is a balanced-tee arrangement employing crystals, is derived from the crystal oscillator of the transmitter, near 45 megacycles, followed by a 24-fold frequency multiplication in the receiver. The injection of the local-oscillator signal at the final frequency and the use of a balanced mixer result in high sensitivity.

A low-noise intermediate-frequency preamplifier with a cascode input circuit precedes the main intermediate-frequency amplifier that has 5 single-tuned stages and a Ferris discriminator detector. The novel features of the intermediate-frequency circuits, aside from the Ferris discriminator that gives 80 decibels of adjacent-channel rejection, are grid-leak "droolers" in several grid circuits to ameliorate the effects of echoes following strong signals, operation over the wide dynamic range of received signal levels experienced in actual operating conditions, accurate determination of the leading edges of pulses, and automatic gain control to maintain a constant average 2700-per-second pulse-count output from the receiver as a means of maintaining constant transmitter duty cycle and a smooth envelope for modulation by the antenna.

The decoder is a conventional coincidence type employing an inductance–capacitance delay line for the 12-microsecond spacing. The decoded output is integrated and used to control the gain of the intermediate-frequency amplifier. In the absence of decoded range interrogations, the amplifier gain is high and the receiver output is

random noise. Interrogations above the threshold level are decoded and the number of noise pulses correspondingly reduced, up to the maximum of 2700, which is sufficient for 100 aircraft.

The block diagram in Figure 5 shows how the coder performs the following operations on the 2700 pulses per second supplied by the receiver.

A. Periodically substitutes for the receiver output a 2700-pulse-per-second identity signal keyed in continental Morse code. The gaps in range replies are too short to interrupt that service, and the constant count preserves the bearing modulation envelope.

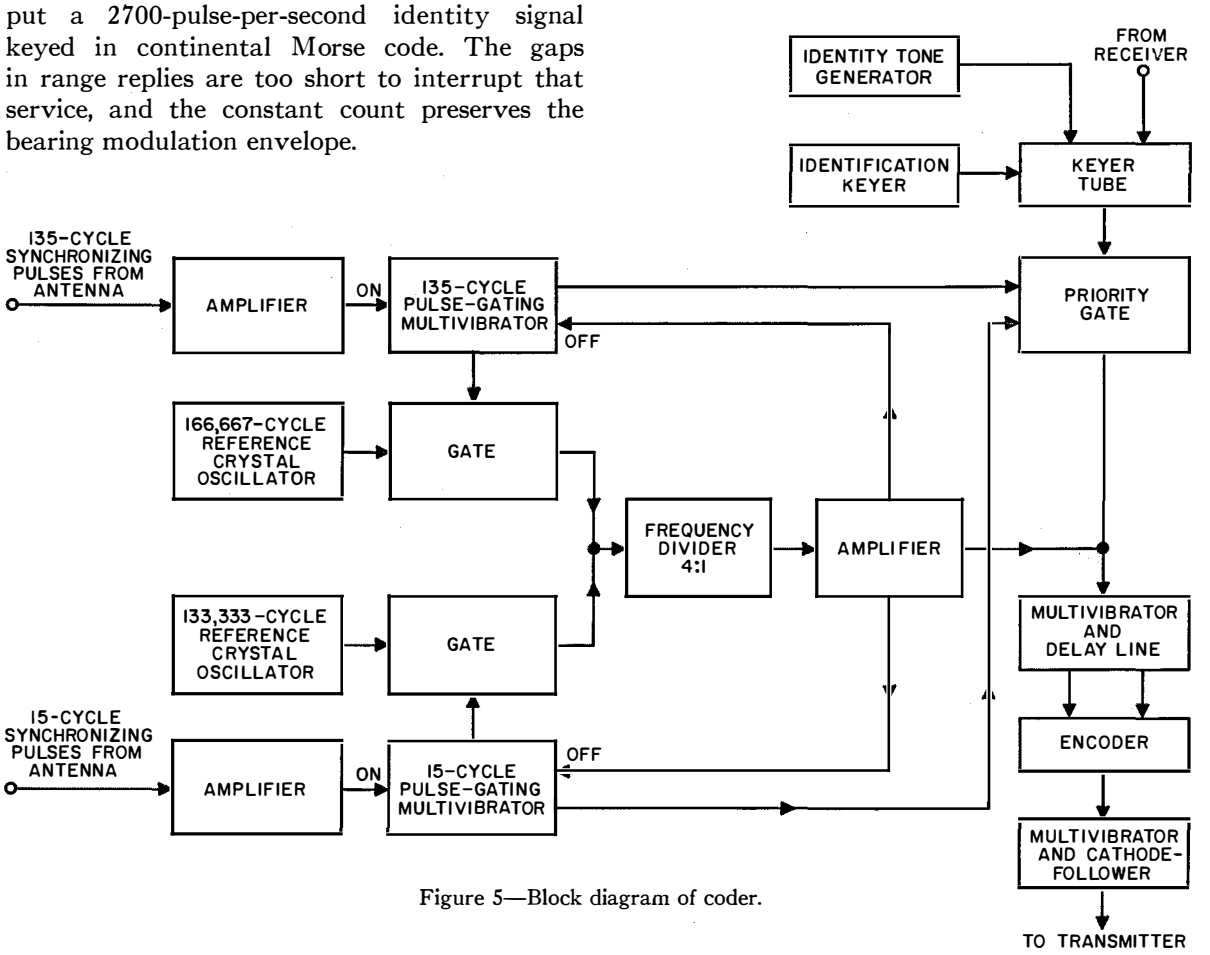

Figure 5—Block diagram of coder.

B. Generates 2 sets of bearing reference-pulse groups in response to synchronizing trigger pulses from the rotating antenna and gives them priority over all other information. Before encoding into pulse pairs, the 15-cycle reference groups consist of 12 pulses spaced 30 microseconds apart that are derived from a 133.33-kilocycle oscillator followed by 4:1 frequency division. Similarly, before encoding into pairs, the 135-cycle reference groups consist of 6 pulses spaced 24 microseconds apart that are derived from a 166.67-kilocycle oscillator followed by 4:1 frequency division.

C. Delays range interrogations (and, incidentally, all other pulses) by a temperature-stabilized inductance–capacitance delay line adjusted for a 50-microsecond over-all beacon delay between the receipt of an interrogation and the transmission of a reply.

D. Converts each pulse into a pair of pulses with the prescribed spacing of 12 microseconds (a tap on the delay line does this) and passes the 3600 rectangular pulse pairs to the transmitter circuits.

The transmitter, diagrammed in Figure 6, delivers more than 5 kilowatts of peak power at a duty cycle in excess of 2 percent with pulses 3.5 microseconds wide and shaped to limit spectrum content to permit beacon opera-

tion on channels of only 1-megacycle spacing. The output tube is a 3-cavity high-gain klystron amplifier with electrostatic focusing (as contrasted with magnetic focusing) and integral cavities (as contrasted with separable external cavities).

The basic circuits are grouped into two drawers. The 3600 pairs of rectangular pulses from the coder are applied to two paths; one through the pulse-shaping network and radio-frequency modulation stage of the oscillator–multiplier system and the other through the high-level video modulator that gates on the beam of the klystron final amplifier. The signals come together again in the klystron amplifier, the former as shaped radio-frequency pulses at the final transmitter frequency that are applied to the klystron input cavity at a peak power level near 50 watts, and the latter in the form of wide negative trapezoidal video pulses applied to the klystron cathode at a peak level near 11 kilovolts. Because of delays in the radio-frequency and shaping circuits, pulses employed in the various operations are timed and sequenced by tapped delay lines and pulse wideners. The important sequences and shapes are illustrated in Figure 7.

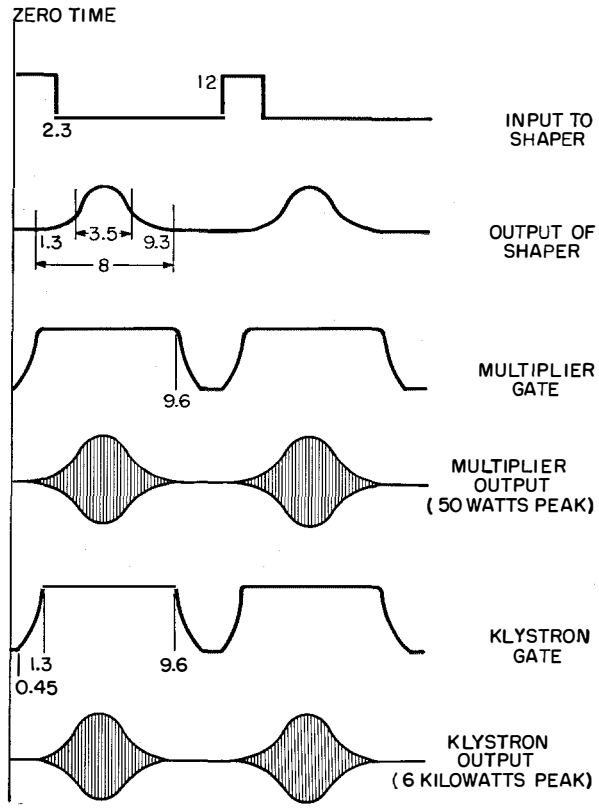

Figure 7—Transmitter pulse sequence. The notations are time in microseconds.

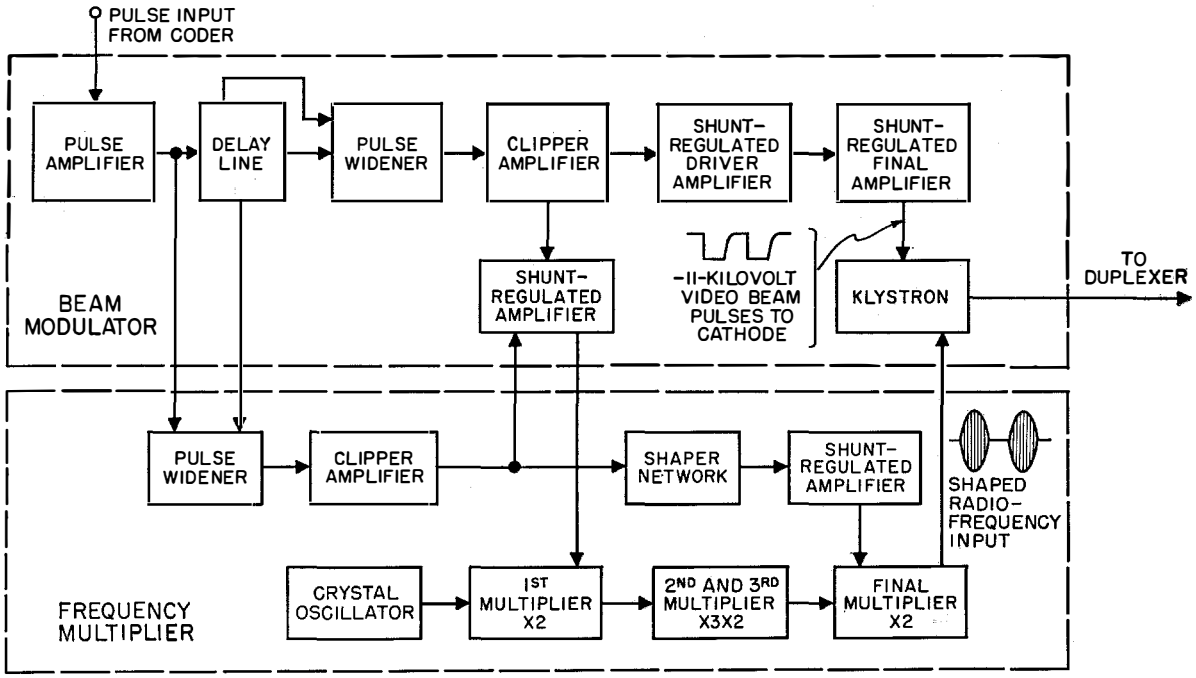

Figure 6—Block diagram of transmitter.

In the frequency multiplier, the output of the crystal oscillator, which operates near 45 megacycles, is multiplied to the final operating frequency by 1 miniature tube and 3 coaxial cavity stages utilizing *4X150G* tetrodes. The first multiplier stage is gated with rectangular pulses to save power in later stages. The final multiplier has the gated radio-frequency pulses and the shaped video pulses superimposed on its grid and consequently delivers shaped radio-frequency pulses to the klystron. The video pulses are shaped in an inductance–capacitance filter.

The modulator employs *6AR6* tubes as heavy-current shunt-regulated amplifiers to key the frequency multiplier and high-level beam modulator. The klystron beam pulses are created in two steps as shown in Figure 8. First a large storage capacitor is charged to 12 kilovolts through a *5D22* tetrode and a *371B* diode, the *4-1000A* shown being in the cutoff plate-current condition. Discharge takes place through the *SAL-39* klystron and *4-1000A* when the *4-1000A* is driven to a low plate impedance by positive grid pulses.

Figure 9 shows diagramatically the operating structure of the *SAL-39* klystron, the elements

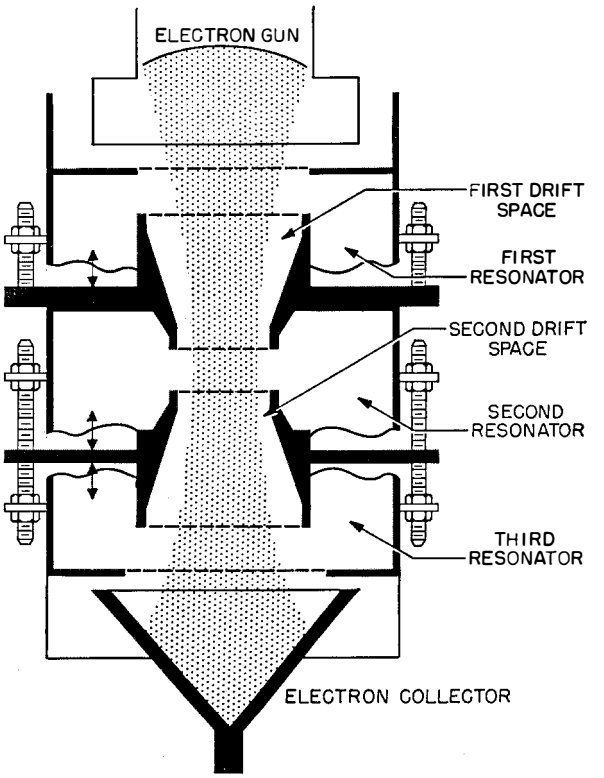

Figure 9—*SAL-39* space-charge-focused pulse klystron.

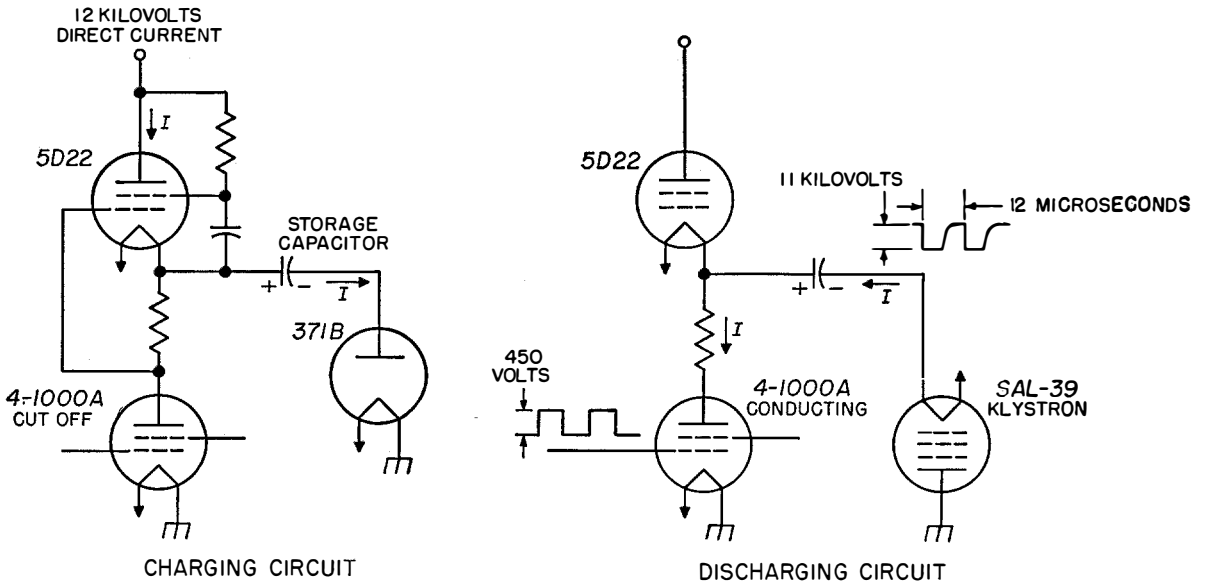

Figure 8—Beam modulator for the klystron amplifier. The storage capacitor is charged through the *5D22* and the *371B* diode while the *4-1000A* is in plate-current-cutoff condition. When the *4-1000A* grid is driven positive by a 450-volt pulse, the storage capacitor discharges through it and the klystron producing the indicated 12-microsecond 11-kilovolt waveform.

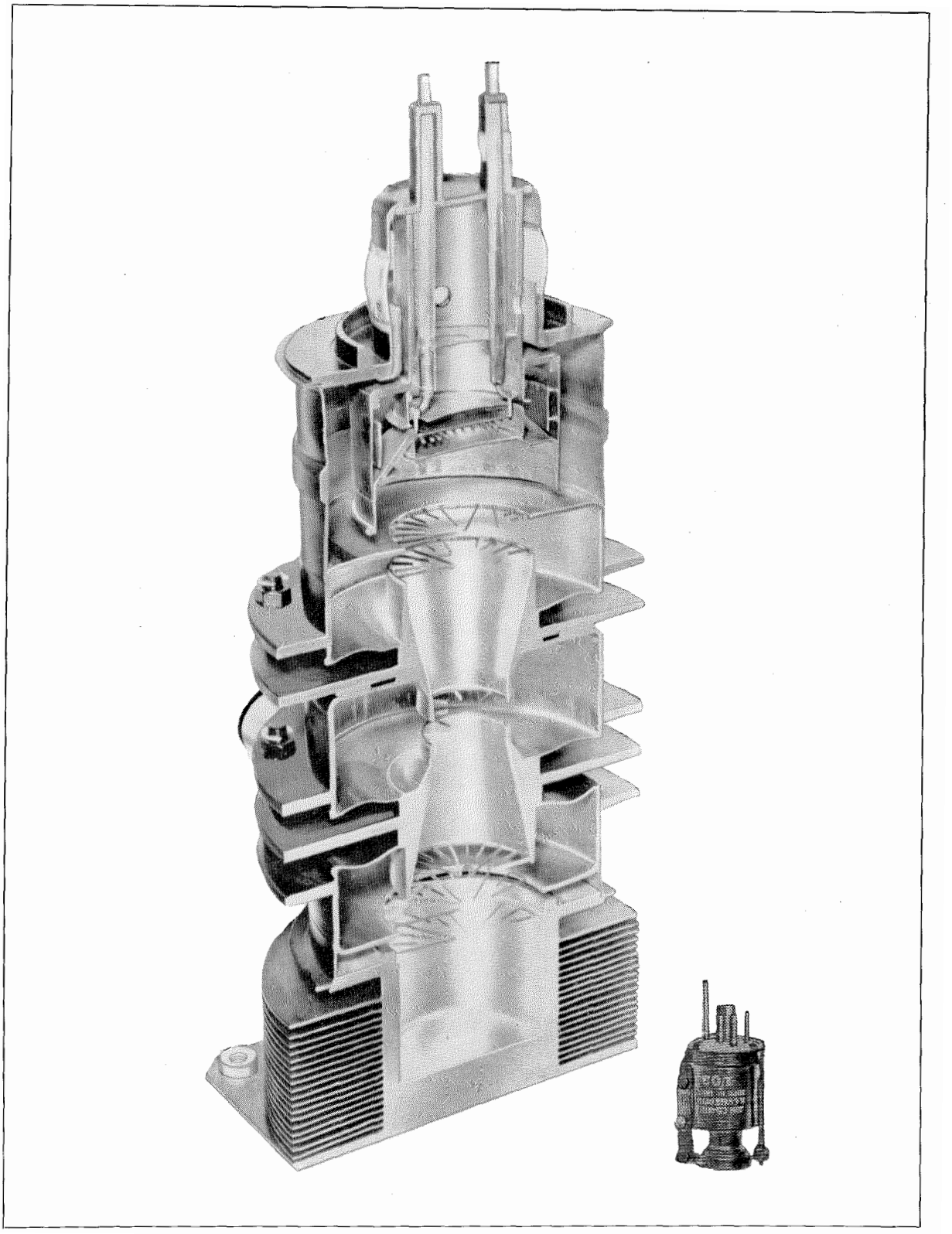

Figure 10—Cutaway view of the *SAL-39* klystron tube. A small reflex-klystron oscillator is shown for comparison.

of which are visible in the photographed longitudinal cross section of Figure 10. The 3 cavities integral with the tube use flexible diaphragms to permit tuning. The size of each cavity is determined by the adjustment of a nut-and-threaded-rod arrangement. Figure 11 shows typical tuning curves. The flange spacing for each cavity changes by about 0.3 inch (7.6 millimeters) in covering the 960-to-1215-megacycle band, giving a total change in length of 0.9 inch (23 millimeters).

The klystron beam-gating pulses delivered by the modulator have flat tops 8 microseconds wide and rise and decay times fast enough to permit 12-microsecond spacing within pulse pairs. The 7200 pulses at 11-kilovolt amplitude produce a peak current of 3 amperes and an average current of 0.2 ampere. The corresponding modulator peak and average powers are 33 and 2.2 kilowatts. Under these operating conditions, the klystron delivers about 6 kilowatts of peak power and 0.15 kilowatt of average power, giving an over-all beam-circuit efficiency of 7 percent, as against possible efficiencies above 25 percent now realizable with more-recent klystron techniques, which will be used in later models. This first major improvement scheduled for the *AN/URN-3* will result in an increase in power output, a decrease in the heat generated, and an increase in component life.

The major contributions of the tacan beacon to the advancement of the art are as follows.

A. In the integrated tacan system, the beacon performs the service of the former distance transpondor but provides more channels, larger service area, and higher traffic capacity. Simultaneously, the tacan beacon provides bearing information with higher accuracy and easier beacon siting than is allowed by the separate omnirange equipment operating in a lower frequency band. There is still a reserve capacity for addition of future functions on each channel.

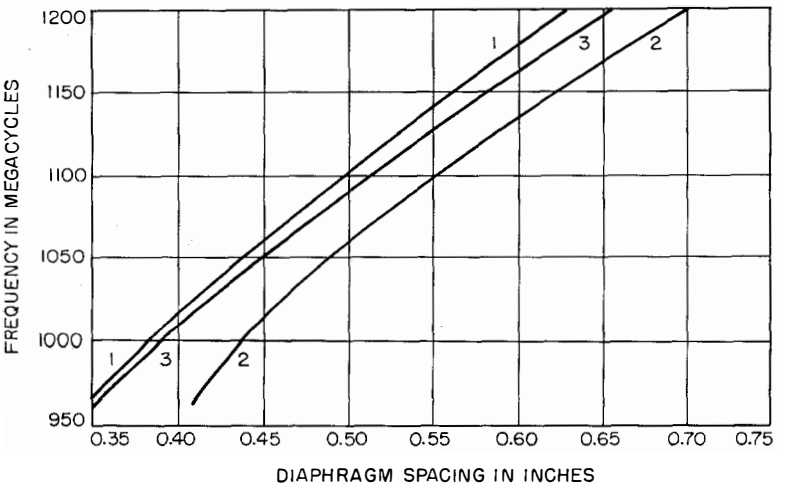

Figure 11—Cold tuning curves for a *SAL-39* klystron. Curves *1*, *2*, and *3* refer to the input, middle, and output cavities, respectively.

B. The receiver selectivity necessary for operation with a 1-megacycle channel spacing and the increase in receiver sensitivity resulting from narrow-band operation are important advances in the art. Under light traffic conditions, the sensitivity is still further enhanced as a result of the constant-duty-cycle principle, which allows high-sensitivity operation of the receiver.

C. The shaped-pulse transmissions, which permit 1-megacycle transmitter frequency spacing, set a new standard in spectrum utilization.

D. The transmitter final-amplifier tube supplies a peak power output sufficient for 200-nautical-mile (371-kilometer) service range, with traffic capacity for 100 aircraft, and a reserve capacity for future multiplexed functions. Yet this tube is rugged, simple to operate, requires low radio-frequency drive, and has long life.

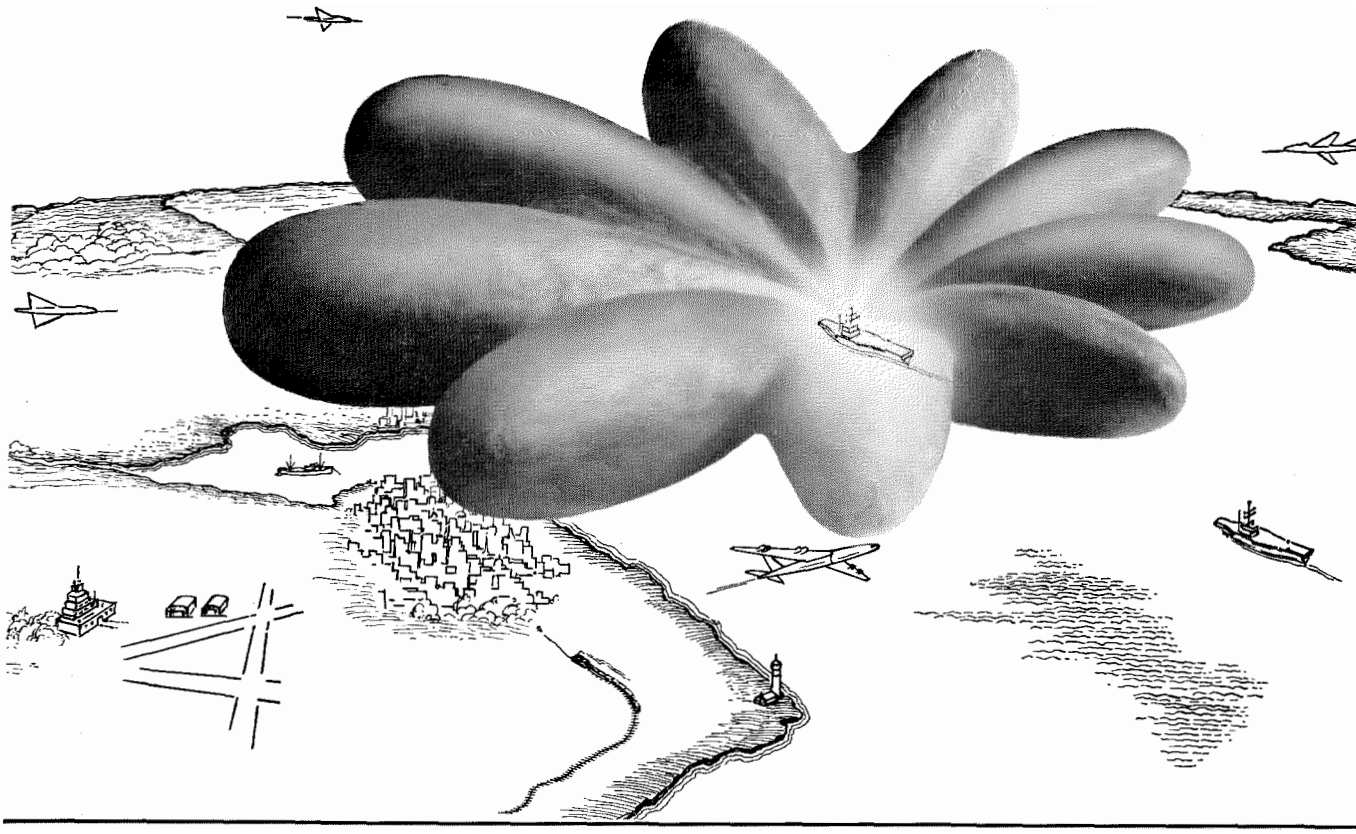

Idealized model of the 3-dimensional radiation pattern of the tacan antenna including both fundamental and 9th-harmonic components. In service, the pattern rotates as if the lobes were spokes of a wheel.

Antenna for the AN/URN–3 Tacan Beacon

By ANTHONY M. CASABONA

Federal Telecommunication Laboratories, a division of International Telephone and Telegraph Corporation; Nutley, New Jersey

THE *AN/URN-3* transmitter generates a constant-amplitude train of pulses that includes random noise pulses to maintain a constant duty cycle, regularized pulses for station identification, specially coded bursts for azimuth reference service, and accurately timed responses to interrogations for distance measurement. This train of fixed-amplitude pulses constitutes the input to the antenna. The antenna imposes certain amplitude modulation on the pulse train to produce azimuth information in the airborne *AN/ARN-21* equipment. It will provide the following functions.

A. 15-cycle amplitude modulation of the pulse train for a coarse indication of azimuth.

B. 135-cycle amplitude modulation of the pulse train for a fine indication of azimuth.

C. Reference trigger pulses in exact synchronism with both the 15- and 135-cycle modulation components.

D. Vertical directivity in the radiation pattern for maximum range.

E. Uptilt in the vertical pattern for increased freedom from siting errors.

F. Mechanism for rotating the antenna assembly at a constant speed.

G. Mechanism for stabilizing the antenna assembly in roll, pitch, and azimuth for shipboard installation.

H. Receiving antenna for interrogations originated by the airborne equipment for distance measurement.

While performing these specific electrical and mechanical functions, the antenna must be capable of withstanding such severe operational conditions as shock, vibration, variations in temperature, high wind velocities, and ice loading. In shipboard installations, the antenna is mounted atop the mast and is relatively inaccessible. Accordingly, the design must assure long periods of trouble-free operation without attendance or maintenance.

The tacan system includes two general antenna types, one for shipboard and the other for shore installations. The radio-frequency assembly of both antenna systems is identical. The shipboard antenna is mounted on a stabilized base that compensates for the roll and pitch of the vessel. A third stabilization system in azimuth is included so as to maintain the antenna pattern accurately oriented with respect to north regardless of the heading of the ship. For ground installations, the antenna is mounted on a simpler base mechanism that does not include roll and pitch stabilization. The azimuth stabilization system was maintained in shore installations to provide convenient adjustment for the initial orientation of the antenna.

Each of the ship or shore antenna assemblies may contain one of two radio-frequency rotating assemblies for low-band or high-band operation. In low-band operation, the antenna transmits over a frequency range from 962 to 1024 megacycles per second and receives from 1025 to 1087 megacycles. In high-band operation, the transmitting band is from 1151 to 1213 megacycles and reception is from 1088 to 1150 megacycles.

1. General Description

Four models of antennas are available for ship or shore and for low-band or high-band operation. In military nomenclature, these models are identified as follows.

A. Antenna group *OA-591/URN-3* for shore high-band use, consisting of antenna *AS-686/URN-3*, antenna control *C-1349/URN-3*, and antenna base *AB-361/URN-3*.

B. Antenna group *OA-592/URN-3* for shore low-band use, consisting of antenna *AS-685/URN-3*, antenna control *C-1349/URN-3*, and antenna base *AB-361/URN-3*.

C. Antenna group *OA-553/URN-3* for low-band shipboard use, consisting of antenna *AS-677/URN-3*, antenna control *C-1322/URN-3*, antenna base *AB-346/URN-3*, and radome *CW-320/URN-3*.

D. Antenna group *OA-554/URN-3* for high-band shipboard use, consisting of antenna *AS-678/URN-3*, antenna control *C-1322/URN-3*, antenna base *AB-346/URN-3*, and radome *CW-320/URN-3*.

The shore antenna includes equipment to maintain constant rotational speed irrespective of changes in power frequency. Such speed control is necessary since shore equipments are required to operate from portable engine–generator power plants.

Photographs of these various components are shown in Figures 1 through 5. Figure 1 illustrates the ship antenna whose base contains two motors to compensate for roll and pitch. Figure 2 illustrates the shore-type antenna utilizing an unstabilized base. Figure 3 illustrates the radome used as a weather protector only on the ship antenna. It permits much-smaller drive motors since wind forces are thus removed from the stabilized portion of the antenna. Figure 4 illustrates the shipboard-antenna control, which contains magnetic amplifiers for azimuth, roll, and pitch stabilization. Figure 5 illustrates the

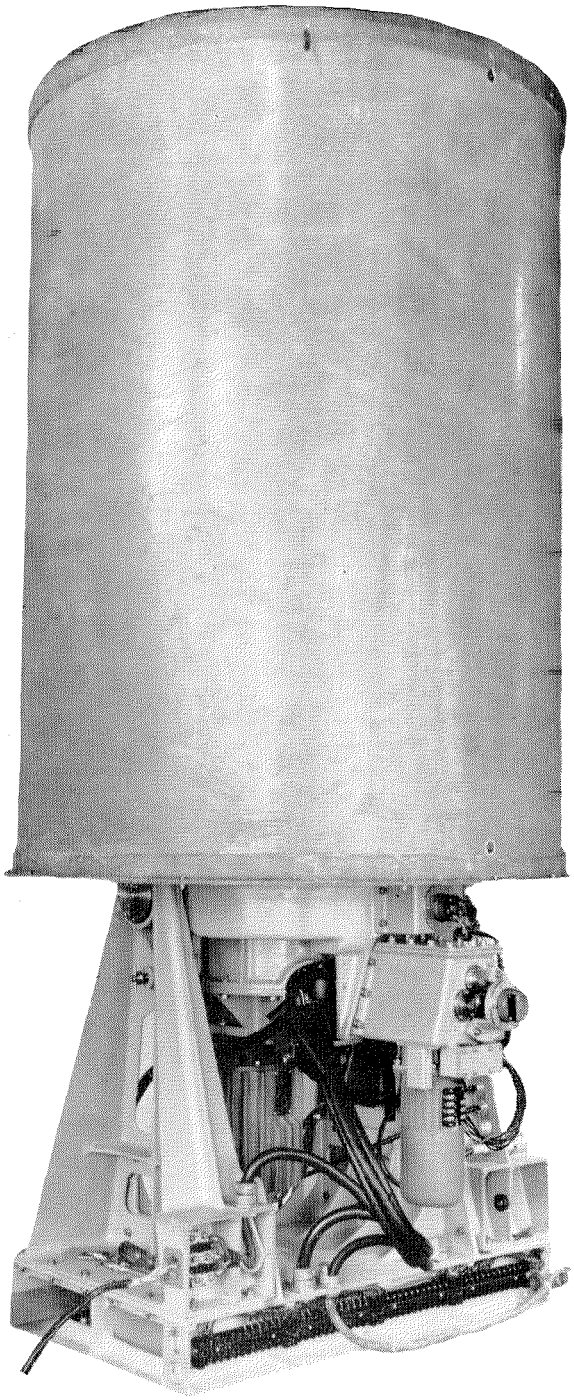

Figure 1—Shipboard antenna. The cylindrical fiber-glass cover protecting the rotating antenna is 45 inches (1.14 meters) in diameter. The over-all height of the structure is 96 inches (2.44 meters) for the low-band design and 88 inches (2.44 meters) for the high band. The motor that drives the antenna is mounted in a finned case just to the left of the bundle of cables, while the motor to the right of the cables is for pitch stabilization.

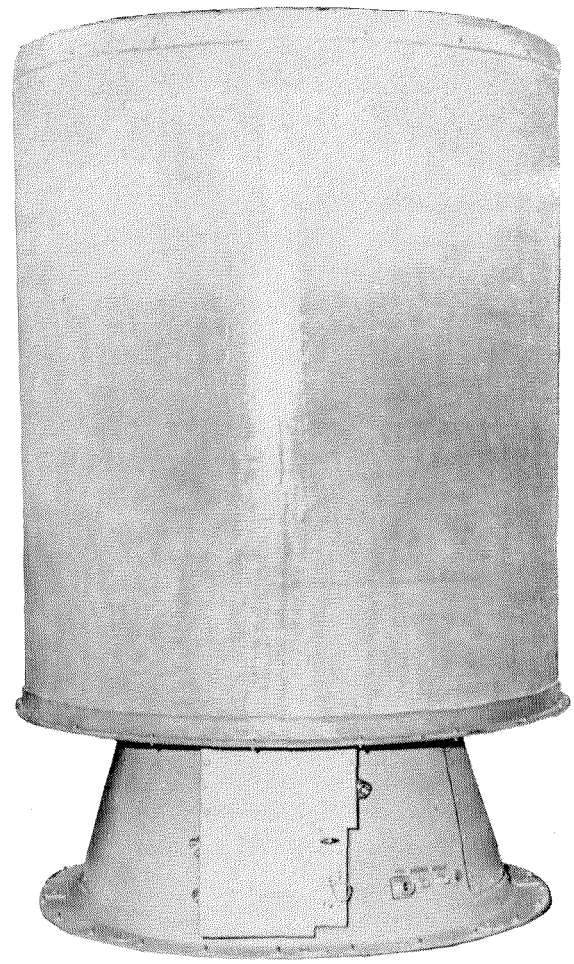

Figure 2—Shore antenna mounted on an unstabilized base that reduces the vertical dimensions by 18 inches (0.45 meter) from those for the shipboard design.

shore-antenna control, which includes magnetic amplifiers for speed control and azimuth stabilization.

1.1 Central Radiating Array

The radiating radio-frequency assembly of all antennas is identical. The dimensions differ slightly in the high-band and low-band units. The main radiating element of all antennas consists of a central antenna array composed of a stack of 7 biconical dipoles mounted within a supporting fiber-glass cylinder. The cylinder is approximately 4 inches (10 centimeters) in diameter and 48 inches (122 centimeters) long. All other components of the antenna are parasitically excited.

Figure 3—Radome for shipboard installation. Its maximum dimensions are 101 inches (2.57 meters) high by 77 inches (1.96 meters) in diameter.

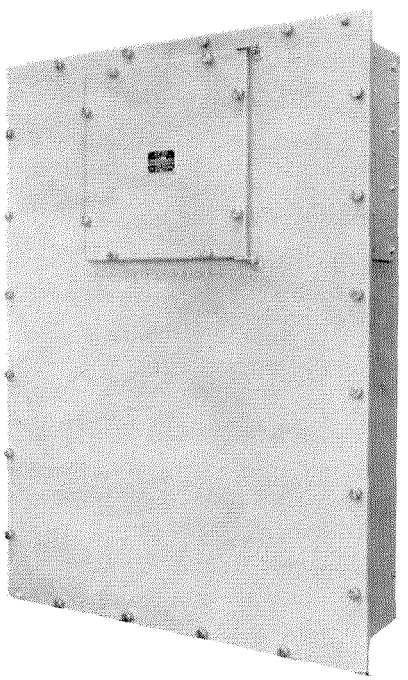

Figure 4—Antenna control unit for shipboard installations. The dimensions are 54 inches (1.37 meters) high by 39 inches (1 meter) wide by 12 inches (0.31 meter) deep.

The array is housed in a fiber-glass tube for rigidity and the space is impregnated with a polyfoam material to increase strength. The top

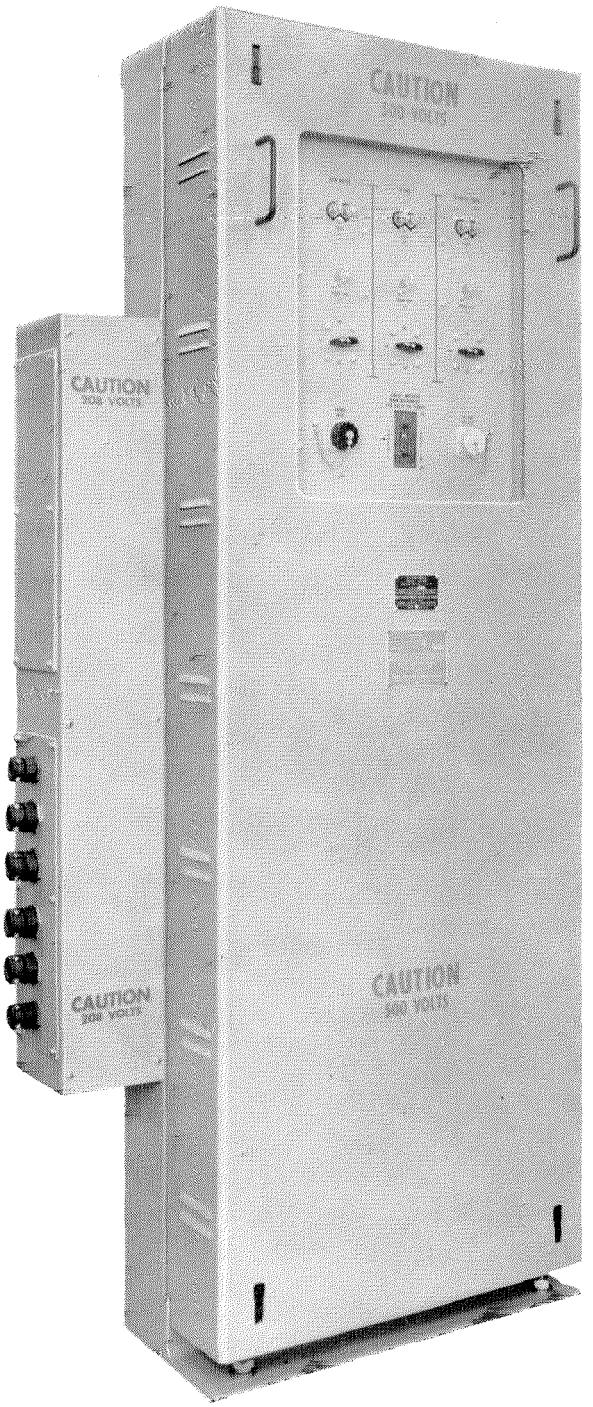

Figure 5—Antenna control unit for shore installations. Dimensions are 70 inches (1.77 meters) high by 31 inches (0.79 meter) wide over both cases by 13 inches (0.33 meter) deep.

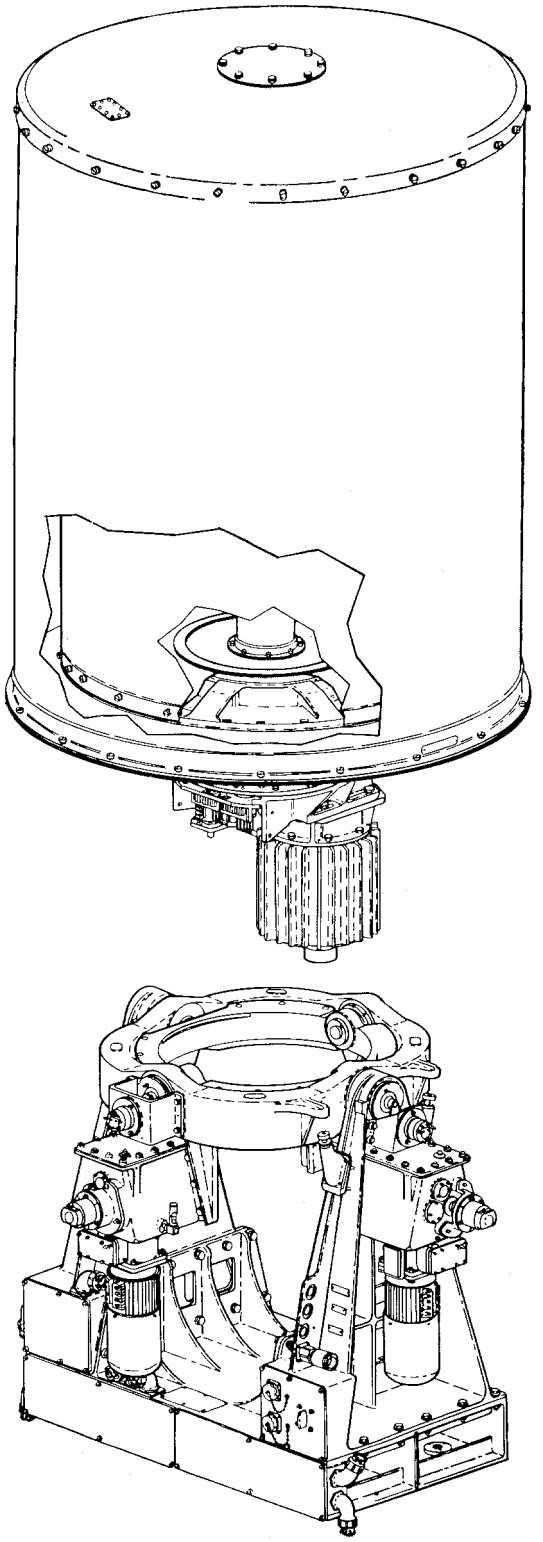

Figure 6—Shipboard antenna and base assembly.

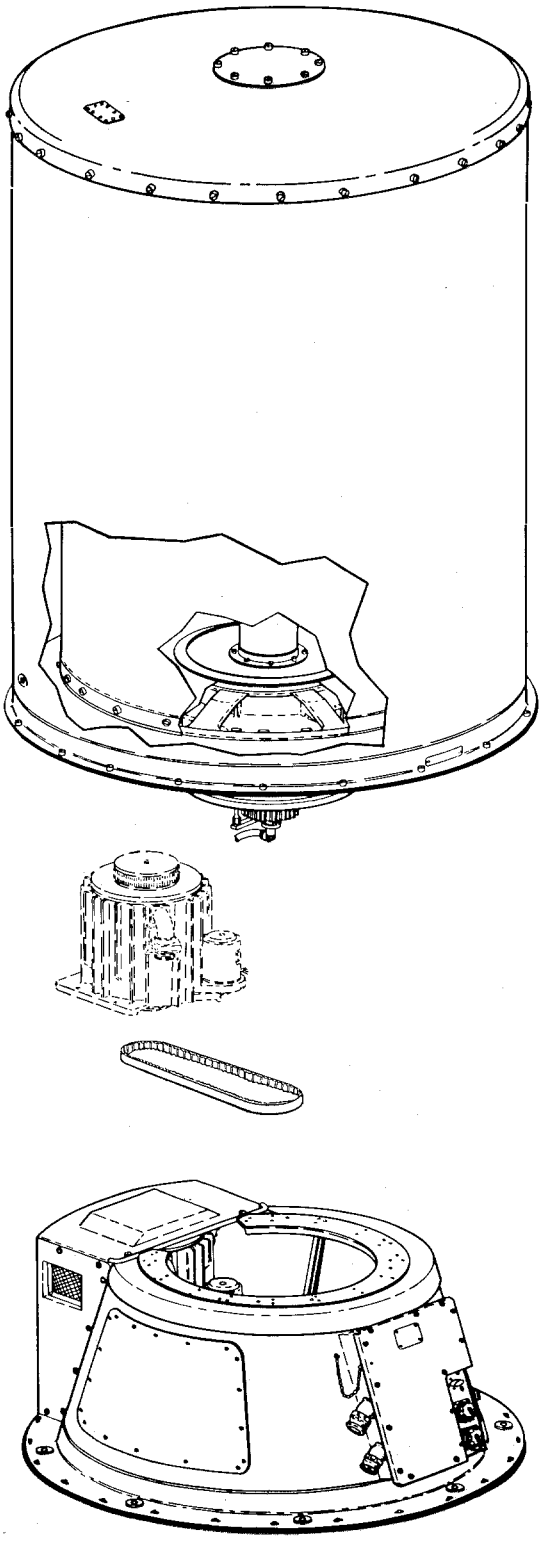

Figure 7—Shore antenna and base assembly.

and bottom of the array assembly contain bearings that center the rotating mechanism of the antenna.

1.2 Rotating Elements

The central array remains stationary while 2 coaxial cylinders that are rigidly secured together rotate about it. The general construction is indicated in Figures 6 and 7. The inner cylinder, approximately 5 inches (12.7 centimeters) in diameter, generates the 15-cycle modulation component by means of a single parasitic element. The outer cylinder has 9 parasitic elements spaced every 40 degrees and is 35 inches (89 centimeters) in diameter for high-band operation and 41 inches (104 centimeters) in diameter for low-band operation. It generates the 135-cycle modulation component. Both cylinders rotate as a unit at 900 revolutions per minute, which corresponds to a fundamental speed of 15 cycles per second. The rotating cylinders are protected by a stationary fiber-glass cover. The upper bearing for the cylinders is supported in the top of the cover. The lower bearing is included in the antenna base. The shaft of the rotating assembly is hollow to permit passage of the radio-frequency transmission line that supplies excitation to the central array.

1.3 Rotation Mechanism

The rotating cylinders are driven by a 2.5-horsepower synchronous motor operating at 1800 revolutions per minute in the shipboard model. A toothed timing belt transfers the motor drive to the antenna cylinders and introduces a 2:1 speed reduction. A similar drive system is used in shore bases except that a 1.5-horsepower speed-controlled motor operating at 1350 revolutions per minute is used.

1.4 Reference-Pulse Generator

The reference-pulse generator provides 2 sets of trigger pulses, one occurring once every complete rotation of the spinning cylinder and the other occurring at intermediate intervals spaced 40 degrees apart. These pulses, in exact synchronism with the 15- and 135-cycle modulation components, trigger the transmitter that generates the reference bursts. The reference-pulse generator is shown in Figure 8 and consists

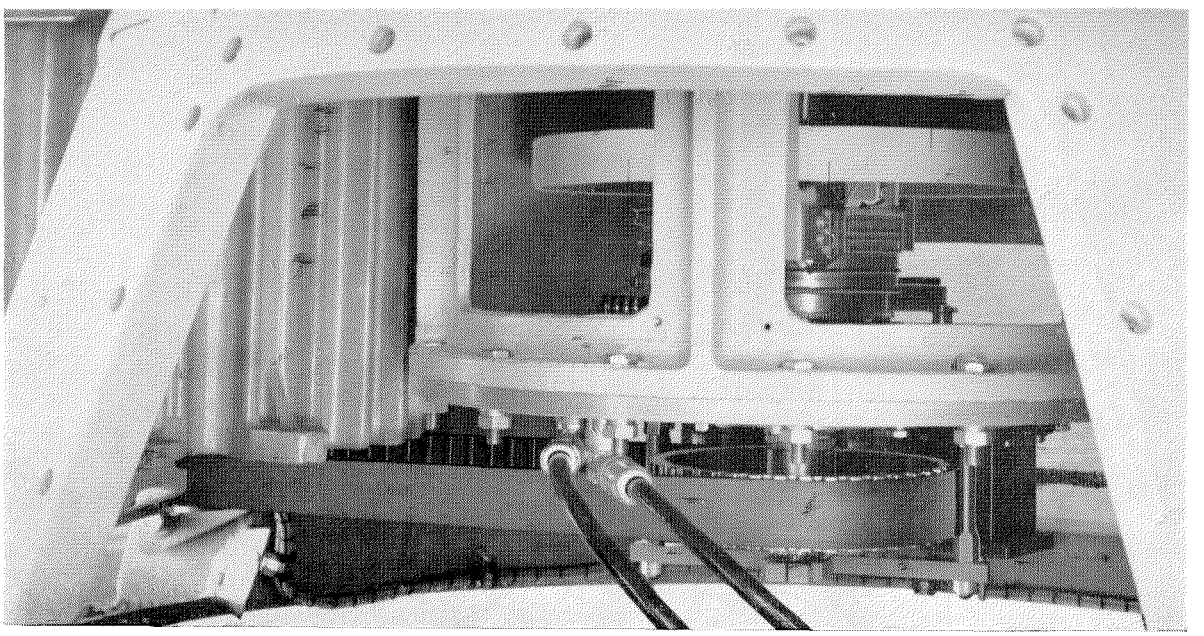

Figure 8—Reference-pulse generator. The iron slugs that produce the reference pulses are embedded in the periphery of an aluminum disk mounted on the shaft carrying the antenna elements. The slugs (retouched for visibility) for the 135-cycle pulses are in the lower half and the 15-cycle slug is in the upper half of the disk. The pulse-coil assembly is mounted just beneath the disk. The driving motor in its finned case is at the left of the picture.

of a rotary aluminum disk on whose outer edge are embedded soft-iron slugs that pass through a pickup-coil assembly. The iron slugs embedded in the wheel are approximately 0.015 inch (0.4 millimeter) in thickness and thereby produce a pulse of relatively short duration. The pulse is produced by the interruption of a magnetic field that induces a voltage in a pickup coil. It is possible to control the timing of the pulses with respect to the modulation by changing the relative position of the pickup-coil assembly with respect to the disk. The pickup-coil assembly is moved by the azimuth stabilization system, which can in turn be actuated by the magnetic variation assembly located in the transmitter. In shipboard use, the pickup-coil assembly is automatically oriented by means of the azimuth stabilization system, which translates information from the ship's gyrocompass system, thereby continuously compensating for changes in the heading of the ship.

The reference-pulse generator disk is mounted on the same shaft that rotates the radio-frequency parasitic assembly. Accordingly, no variation from absolute synchronism can occur.

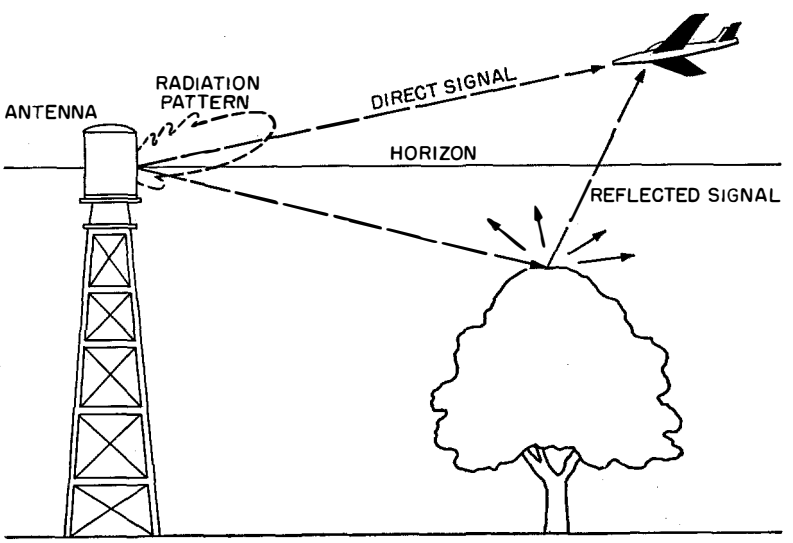

Figure 9—The uptilt of the radiation pattern of the antenna aids in producing the maximum ratio of direct-to-reflected signal at the aircraft.

1.5 Ship Control Unit

The ship control unit shown in Figure 4 contains circuits to compensate for the roll, pitch, and azimuth headings of the vessel, a line contactor, and a circuit breaker for the spin-motor 3-phase power. In addition, it contains switches for disconnecting these circuits for trouble-shooting purposes, relays for remote trouble indication, interlocks for safety to personnel, and 4 delta-connected phase-correction capacitors for the roll, pitch, and azimuth synchro stators.

The components are contained in a heavy steel box designed for deck mounting. The cover has an access door so that the switches and fuses can be reached conveniently. The whole unit is constructed to withstand high shock and vibration and is gasketed for spraytight operation. The outside dimensions are $56\frac{1}{2}$ inches high by $34\frac{1}{4}$ inches wide by $12\frac{1}{2}$ inches deep (144 by 87 by 32 centimeters) and the total power dissipation in the box is approximately 200 watts. The unit weighs 675 pounds (307 kilograms).

1.6 Shore Control Unit

The shore control unit shown in Figure 5 is a rack that mounts 5 chassis, a dust cover, and a junction box. Two chassis are used for speed-control service and one for the azimuth control. Another chassis serves as the front control panel and contains such components as switches, fuses, blown-fuse indicators, and an interlock. The final chassis contains various components for trouble indication, spin-motor starting, and synchro power-factor correction.

The azimuth amplifier is at the top of the rack and is electrically identical to the amplifier used in the ship control unit. The speed-control chassis are the bottom two on the rack since they are the heaviest, weighing approximately 290 pounds (132 kilograms) each.

The power dissipated in the rack is about 215 watts. It stands 70 inches high by $32\frac{1}{2}$ inches wide and is $12\frac{1}{2}$ inches deep (178 by 83 by 32 centimeters).

2. *Theory of Operation*

The antenna utilizes a harmonic-frequency system to improve accuracy; that is to say, the antenna generates both a fundamental and a 9th-harmonic component. The method of modulation is purely mechanical, involving no thermionic devices. Consisting essentially of parasitic wires that rotate about the stationary central array, it is completely contained in the antenna. The harmonic system increases accuracy by producing many electrical degrees of phase shift for each space degree.

2.1 Central Radiating Array

It is the purpose of the central array to accept the pulsed radio-frequency signal from the transmitter and radiate it efficiently into space. It must present a matched impedance over the frequency band to maintain radiation efficiency. In addition, the central array must generate the required vertical gain and uptilt. The vertical gain permits maximum utilization of the power in the vicinity of the horizon to obtain maximum range. Uptilt is a term used to indicate that the vertical lobe of the antenna pattern is directed slightly upwards so that a rapid gradient of signal exists at the horizon. This permits greater freedom in the choice of sites.

Figure 9 illustrates a typical vertical radiation pattern of the central array. An aircraft above the horizon receives a certain amplitude of direct signal. Because of the gradient, a reflecting obstacle at the same angle below the horizon will intercept appreciably less signal. The aircraft receives both the direct and reflected signals. If the ratio between these signals is high, the reflected signal will have least effect.

The uptilt is also an aid in minimizing the effect of null formations in the vertical pattern. Any radiating system above ground produces a lobed pattern in the vertical plane because the signal at any point in space is composed of a direct signal and a signal reflected from the ground. At certain discrete points, these two signals may be of equal amplitude and out of phase, thereby producing a signal null. The position of these nulls in the vertical plane depends on the frequency and the height of the antenna system above ground. Section 4.2 gives the derivation of this vertical pattern and indicates the location of the nulls for the frequencies being used. Uptilt reduces the reflected signal with respect to the direct signal and thereby lessens the amount of cancellation of the direct signal. Accordingly, the nulls become minimums of lesser depth and capable of being compensated for by the automatic-gain-control system of the receiver.

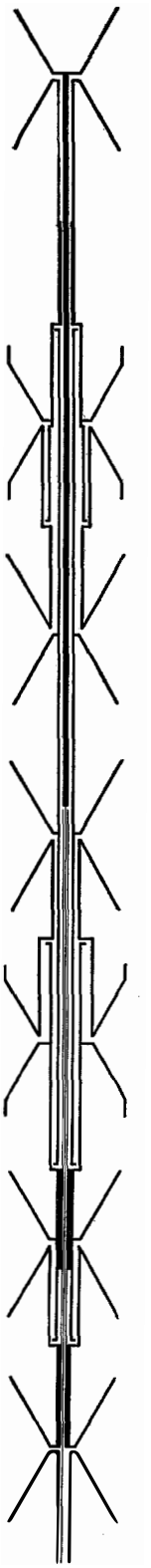

Figure 10—At the left is shown a cross section of the central antenna array of 7 biconical radiators that are mounted in a fiber-glass cylinder.

Figure 10 shows a cutaway view of the central array. It is composed of 7 biconical dipoles stacked vertically. The distribution system is self-contained in the array and consists of a number of series-driven transmission lines. The main transmission line proceeds to the center of the array, at which point it divides into the distribution network. A block diagram of the system is shown in Figure 11. The distribution network contains matching transformers at all junctions.

Considering first the lower 6 elements of the array, the central 2 elements are each supplied with 9 units of power. The 2 succeeding elements receive 4 units of power each, and finally, the end elements get 1 unit of power each. This distribution can be recognized as one tending to suppress minor lobes. To obtain uptilt, the elements are phased such that the lower 2 lead in current and the upper 2 lag in current with respect to the central elements.

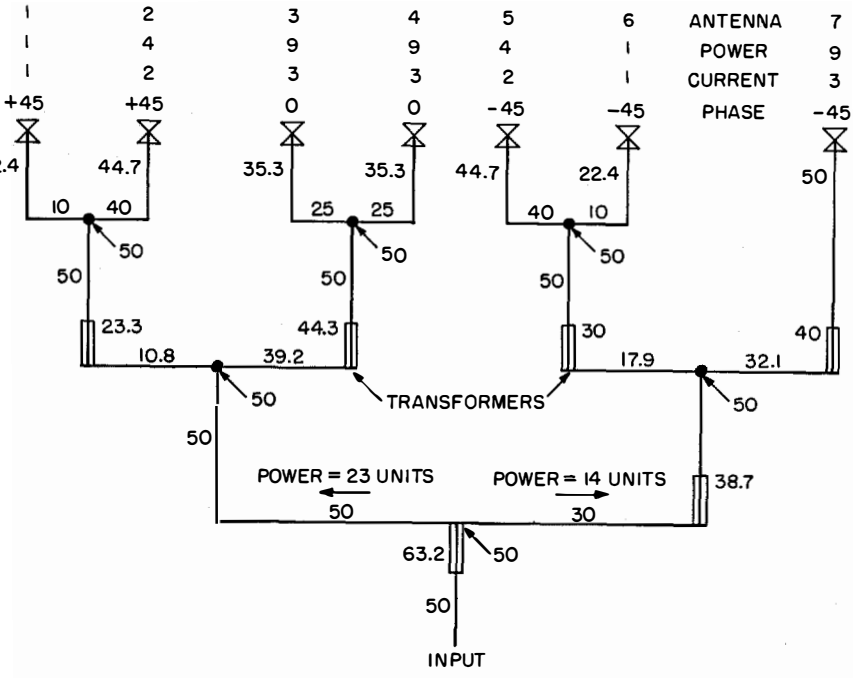

Figure 11—Method of distributing power to the 7 biconical antennas. This particular configuration is for the low-frequency band. Each biconical antenna has a characteristic impedance Z_0 of 50 ohms; the impedance values of the various transmission-line elements are indicated in ohms.

The 7th or top element was introduced to improve the vertical-angle coverage of the antenna. This unit operates in conjunction with a counterpoise that is placed between the 6th and 7th elements. The top element receives 9 units of power and contributes to the uptilt by virtue of the fact that its current is lagging. At high vertical angles, the counterpoise tends to mask the radiation from the lower 6-element array; therefore energy is received predominantly from the top element.

2.2 Modulating Mechanism

A sketch of the rotating mechanism of the antenna is shown in Figure 12. The stationary central array is surrounded by 2 cylinders that rotate about it. The inner cylinder contains a number of parasitic wires grouped in close proximity to produce the fundamental or 15-cycle modulation. The outer cylinder contains a number of parasitic wires spaced 40 degrees apart to produce the 9th-harmonic modulation. The patterns produced are shown in Figure 13.

The effect of the 15-cycle modulation produced by the single inner reflector is the typical cardioid pattern illustrated in Figure 13A. The horizontal pattern of the 9th-harmonic system is shown in Figure 13B. When these are combined, the

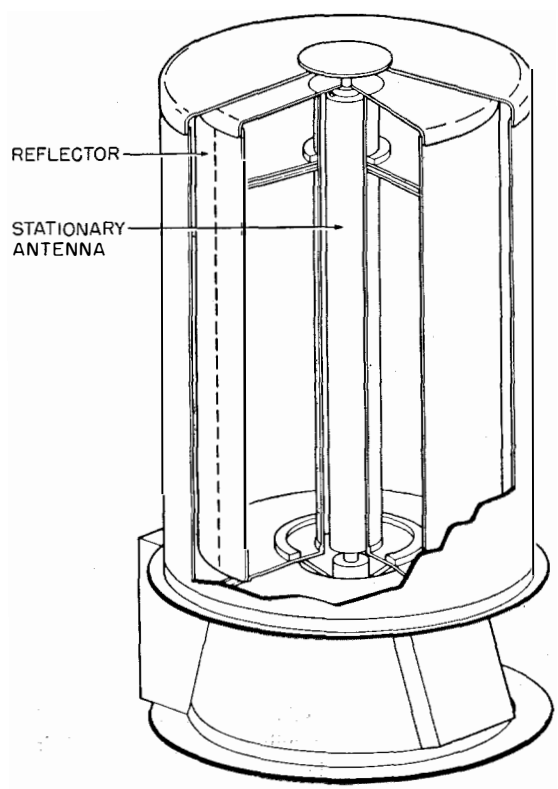

Figure 12—Cutaway drawing of typical antenna showing the stationary central fiber-glass cylinder housing the array of biconical radiating antennas. The outer cover is also stationary. The 2 intermediate cylinders rotate as a unit, the innermost having 1 reflector imbedded along its length to provide the 15-cycle modulation and the outermost having 9 reflectors to produce the 135-cycle modulation.

composite pattern of Figure 13C results. It is obvious that when this pattern is rotated, an observer fixed in azimuth will detect an amplitude modulation.

The parasitic elements produce the desired envelope in the horizontal pattern by reradiating energy that impinges on them from the central array. In space, the interaction between the central-array signal and the reradiated signals from the parasites produce the desired pattern. In general, the diameter of the cylinders controls the purity of the modulation while the resistance and number of the parasite wires control the depth of modulation. Section 4.1 shows these mathematical quantities and explains the choice of cylinder diameters.

During development of the antenna, it was found that ordinary copper wires, even of small diameter, produced excessive modulation. In addition, such highly conductive parasites exhibited relatively high Q values resulting in vast changes in modulation characteristics over the radio-frequency band. The design was directed at a constant percentage of modulation with as high a vertical angle as possible. This required that the vertical patterns of the parasites very nearly track that of the central array. Therefore, it was necessary that the current distribution in the parasitic wires resemble that of the central array of biconical elements. With parasites of high resistivity, this condition could be approached, since the standing wave on the parasite would be highly damped as it progressed from the point of generation. Hence, from all viewpoints, namely reducing modulation level, minimizing frequency sensitivity (Q), and obtaining the desired vertical pattern, parasites of high resistivity were indicated.

Accordingly, the parasitic wires are composed of nichrome, are approximately 1 mil (0.025 millimeter) in diameter, and offer a resistivity of about 700 ohms per foot (2300 ohms per meter). It was found that the percentage of modulation could be easily controlled by varying the number of wires in a group. In addition, each wire in the group could be adjusted in length so that compensations could be made for the desired vertical pattern. Accordingly, certain parasitic groups consist of 4 wires of 2 different lengths. The utilization of such wires also produced the desired broad-band effect.

For practical purposes, the phase between the 15- and 135-cycle components must be standardized so all receivers may be properly adjusted. In addition, it must be recognized that in this system, distance is simultaneously transmitted

Figure 14—Radio output received due south of the beacon. The envelope shows the relative depth of modulation for the 15- and 135-cycle frequencies and the heavy lines indicate reference-pulse bursts at 40-degree points. These two modulations are for bearing indications. By limiting, only the unmodulated central section is extracted for distance measurement. There are 3600 pairs of pulses transmitted each second on the average, including bursts of more-closely spaced reference pulses.

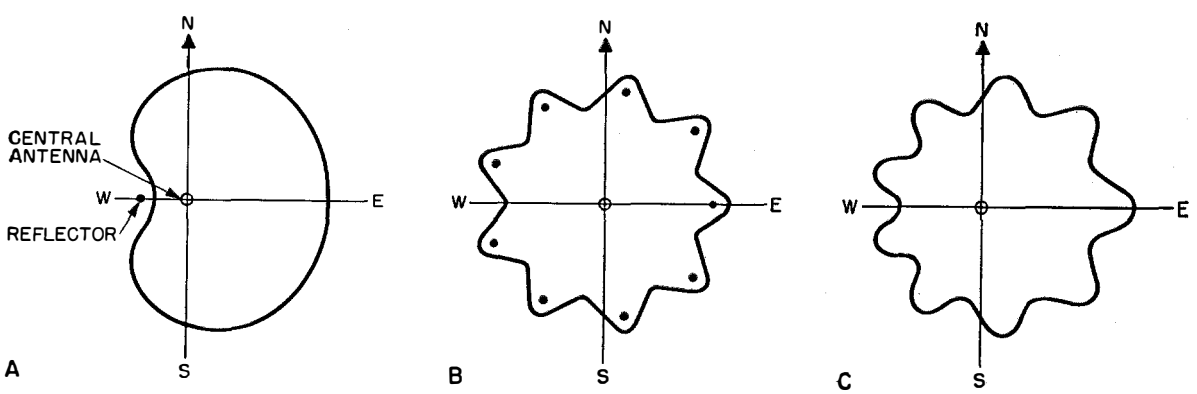

Figure 13—Antenna radiation patterns. A = with only single reflector of inner rotary cylinder. B = with only 9 reflectors of outer rotary cylinder. C = with both inner and outer rotary cylinders. The three-dimensional pattern is illustrated by the headpiece to this paper.

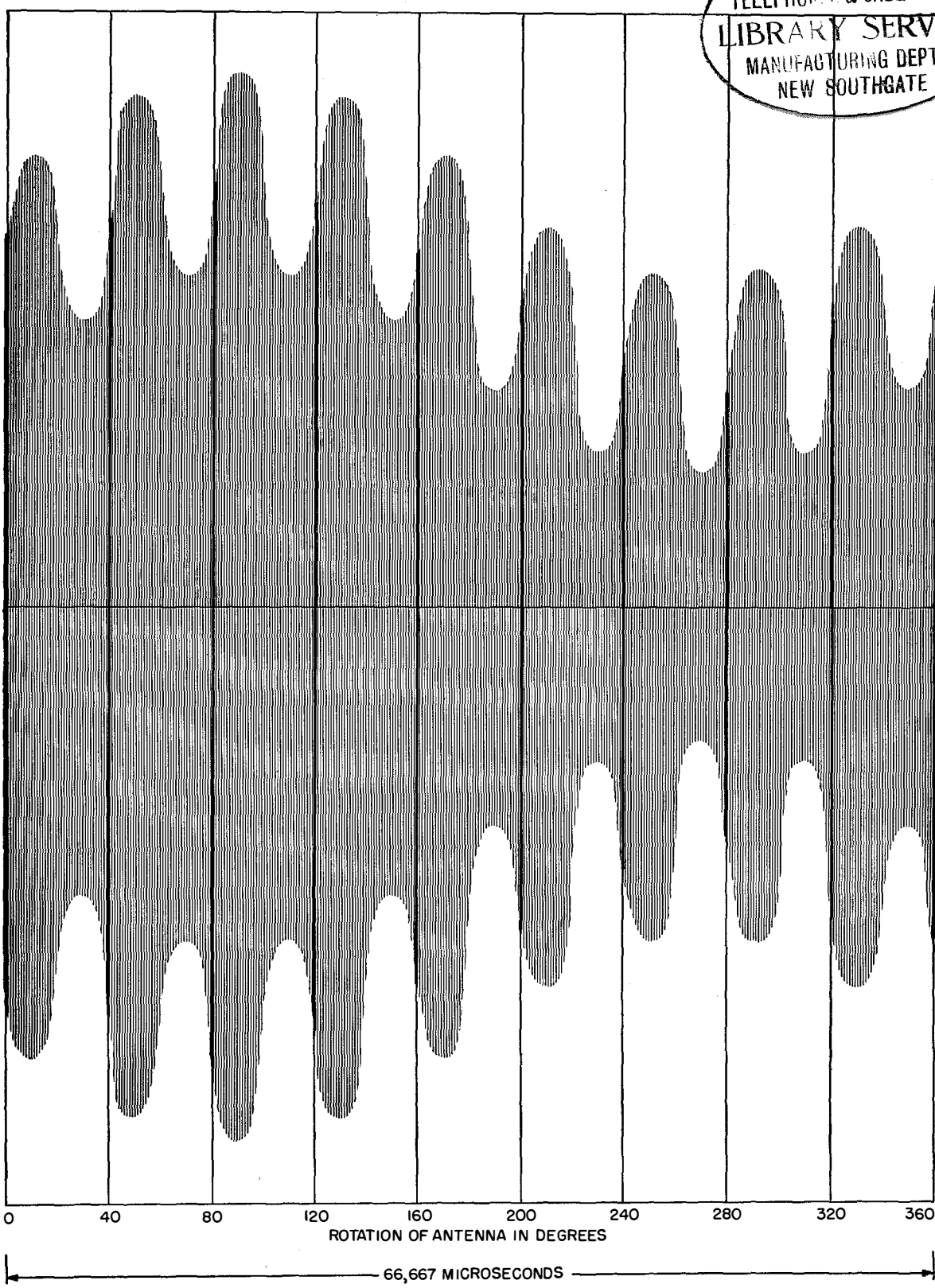

with the azimuth signal. In the receiver, this distance information is derived from the timing of certain response pulses after the modulation has been clipped. Accordingly, it would be impossible to use 100-percent modulation for the azimuth system without interruption or serious degradation of the distance indication. Therefore, the relative phase and amplitude of the 15 and 135 cycles have been standardized, resulting in the pattern shown in Figure 14. The 15- and 135-cycle cylinders are mounted on a common shaft and, after the phase adjustment has been made, are mechanically secured so that no further phase difference can accidentally occur.

2.3 Reference-Pulse Generator

The patterns discussed above are rotating about the central radiator at 15 revolutions per second. Accordingly, the phase of the modulation varies as the receiving system circles about the antenna. It is this shift in phase with azimuth position that determines the azimuth indication. However, this phase shift is not apparent until the signal is compared to a reference. Accordingly, a reference must be generated that is received simultaneously at all azimuths. Furthermore, this reference must be in exact synchronism with the modulating frequencies.

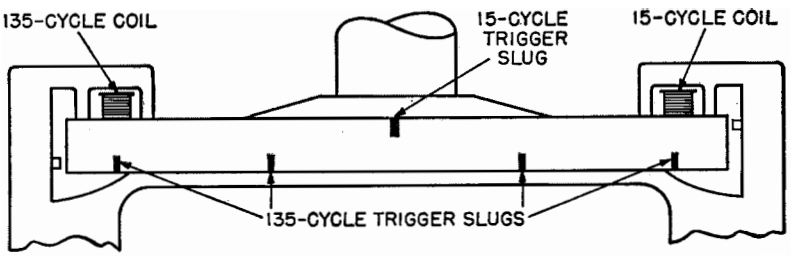

Figure 15—Reference-pulse generator. Soft-iron slugs are imbedded at 40-degree spacing in the lower edge of the periphery of an aluminum disk to correspond to the 9 parasitic reflectors and one in the upper edge for the single reflector. Pickup coils are energized when the slugs pass them and initiate the generation of the bursts of reference pulses.

For this purpose, an aluminum disk is attached to the rotating shaft of the antenna. Thin iron slugs are pressed into the edge of the rotating disk at 40-degree spacings. Note in Figure 15 that one of these slugs is located at the top edge of the disk and the others are at the lower edge. Two pickup coils are mounted near the periphery of the disk. These coils are wound on a permanent magnet and include a yoke that embraces the rim of the rotating disk. Hence, a constant magnetic field exists across the yoke gap. When the reluctance of the magnetic circuit is reduced by the passing iron slug, a pulse is induced in the coil. Since the upper edge contains only one slug, a 15-cycle repetition rate is developed in the corresponding coil and constitutes the fundamental reference. The lower coil carries the output of the remaining 8 slugs at a repetition rate of 135 cycles and thereby constitutes the harmonic reference.

For calibration, the reference-pulse-generator disk must be properly positioned with respect to the rotating parasitic elements and the base. This adjustment is called "north calibration." The standard is such that the fundamental or 15-cycle reference occurs when the common zero positive cross-over of the 15- and 135-cycle components sweep past south.

2.4 Roll and Pitch Stabilization

The block diagram of the amplifier for roll or pitch stabilization is shown in Figure 16, and the servo-system diagram in Figure 17. The amplifier is a conventional unit with 2 stages of gain and a tachometric feedback loop. To minimize the velocity error, the tachometric voltage is integrated by the acceleration feedback network. In addition, a heavy-duty tachometer is employed and loaded by a 500-ohm resistor so that simulated viscous damping is obtained.

A full-wave rectifier detects the synchro error voltage, which is then passed through a single-stage magnetic preamplifier. A small portion of this current is also used to operate a remote error indicator. The detector presents an input impedance of approximately 1200 ohms to the synchro and this may be reflected partially into the synchro bus if the error becomes excessive.

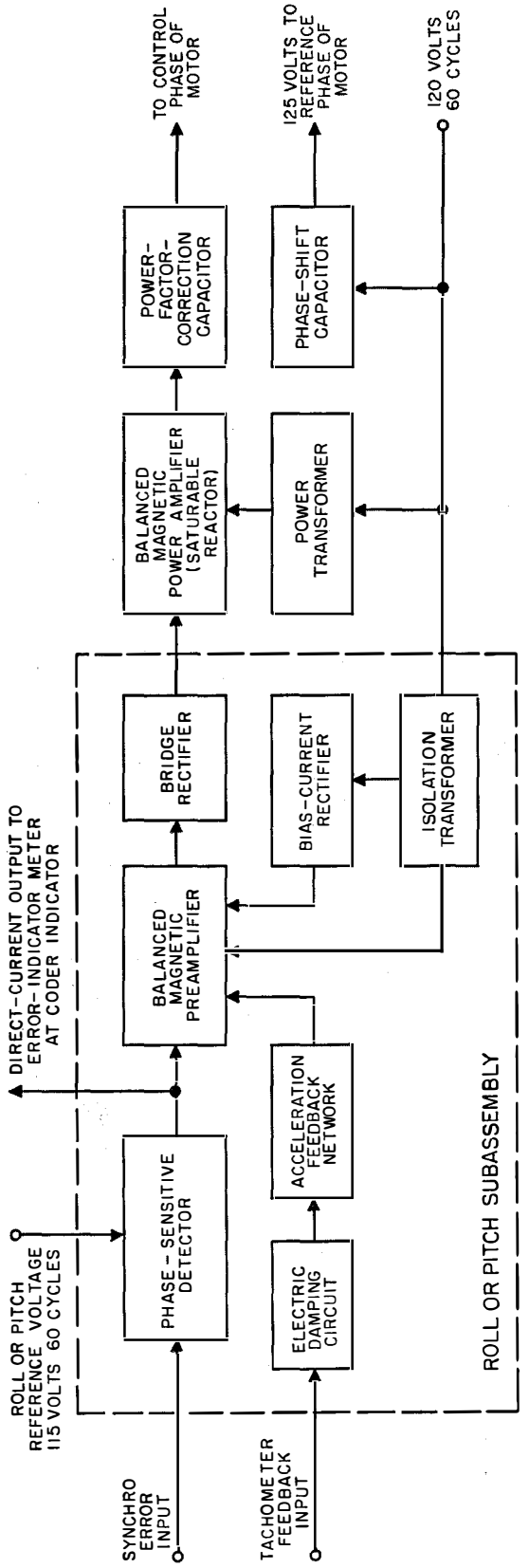

Figure 16—Block diagram of magnetic amplifier for roll or pitch compensation.

To keep this loading down, the synchros are disconnected from the amplifier by a relay whenever power is removed from the unit.

The roll and pitch amplifiers are identical except for the preamplifier forcing resistor. Since pitch is considerably less than roll, it is possible

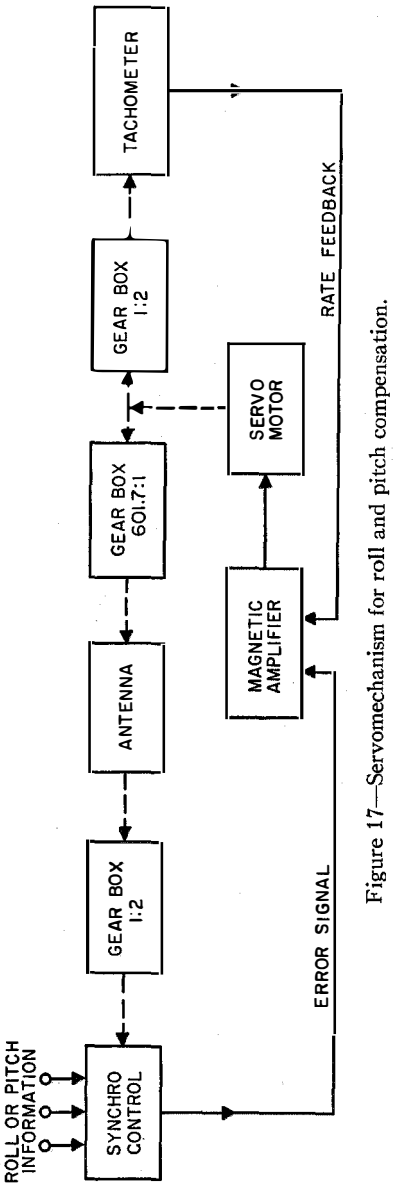

Figure 17—Servomechanism for roll and pitch compensation.

to have lower gain in the pitch amplifier. In fact, it was necessary to do this since with equal gains and the gyroscopic coupling between roll and pitch servos due to the antenna rotation, the system becomes unstable and precesses around the vertical axis.

Two other features of the amplifier are worth noting. First, by virtue of selected matched rectifier pairs and tight control on windings of the saturable elements, interchangeability of the subassemblies is possible. Thus, no adjustment or balancing is necessary should any one of the three components of the amplifier be replaced. The second feature is the local positive current feedback employed in each stage of magnetic amplification to increase the gain. The accuracy of stabilization is approximately $\pm$ 2 degrees for both axes.

2.5 Azimuth Stabilization

Figures 18 and 19 are block and schematic diagrams of the azimuth amplifier. Figure 20 shows the block diagram of the associated servo system. The amplifier drives a 5-watt motor and derives its error information from 2 synchro control transformers that are geared for a conventional 1-speed and 36-speed system. The amplifier detects each of these signals separately, operates on them to eliminate the possibility of false axis crossings, and mixes them magnetically in the output saturable reactor. The operation simply consists of limiting the high-speed signal so that the peak amplitude is not large enough to cause the combined signals to recross the zero axis. Nevertheless, the gain at crossover is not greatly reduced.

In Figure 19, the 2 rectifiers connected back to back in series with the 1-speed control current serve to de-emphasize the 1-speed signal in the region of normal operation (approximately $\pm$ 2.5 degrees) so that any error of this signal is minimized. Full gain is obtained outside this region so that control is maintained by the 1-speed signal.

Stable operation is insured by two networks. First, the capacitor C across the 36-speed forcing resistor constitutes a phase-advancing network. In addition, L helps reshape the locus of the open-loop gain phaser and acts similarly to an integral control network.

Positive feedback is used in the output stage to increase the gain. The error-indicator discriminator is separate in this amplifier so that no loading of the 1-speed control circuit is obtained. An accuracy of 0.1 degree can be maintained.

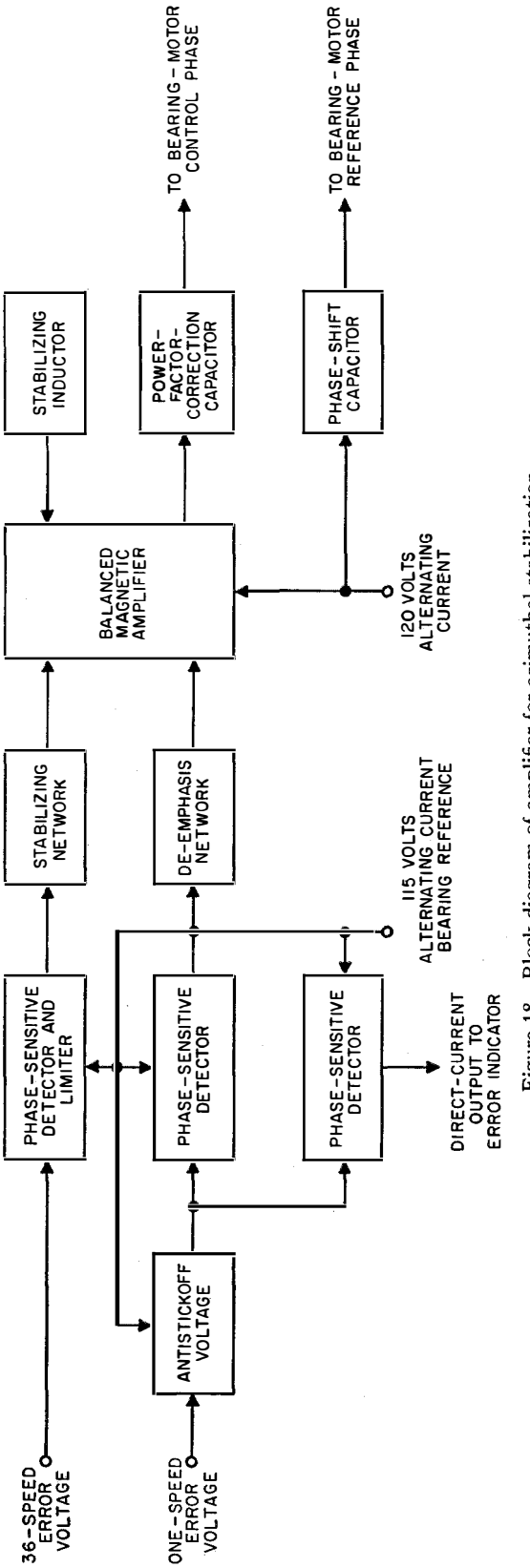

Figure 18—Block diagram of amplifier for azimuthal stabilization.

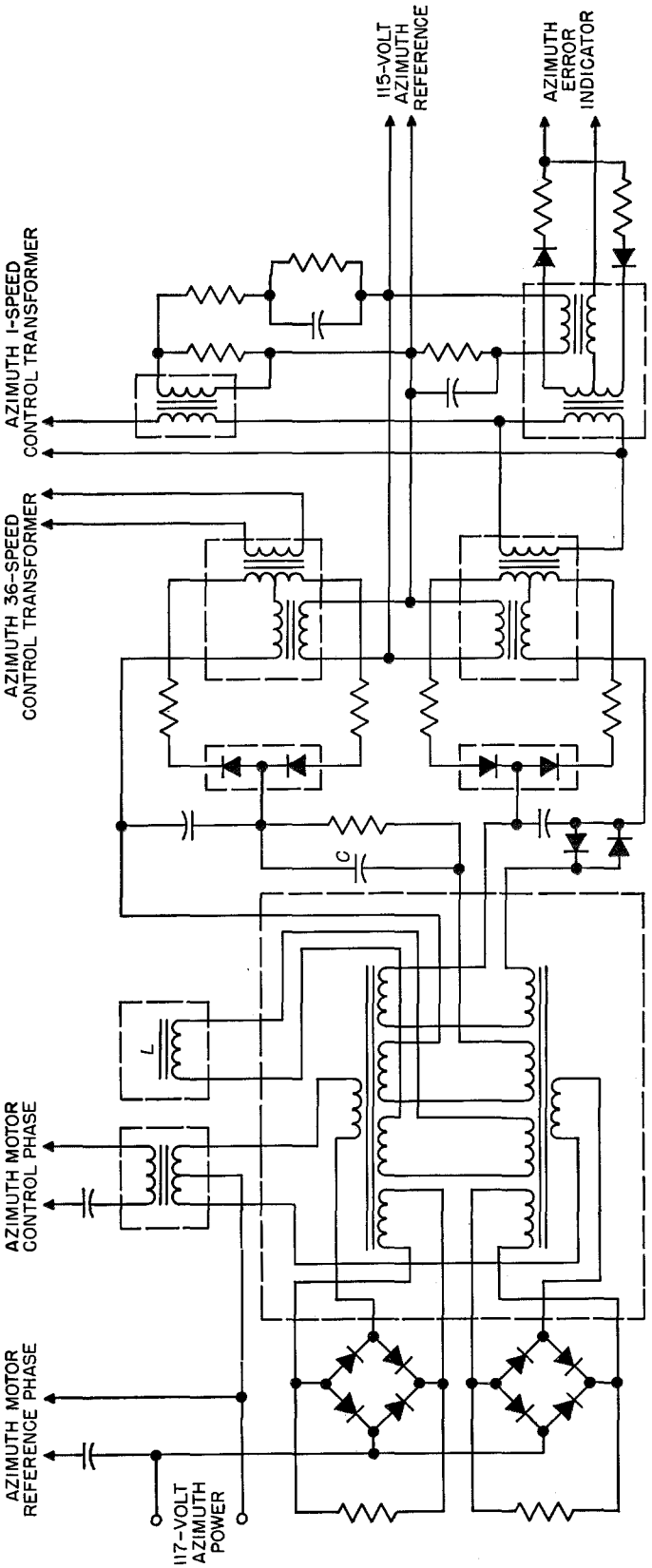

Figure 19—Schematic diagram of amplifier for azimuthal stabilization.

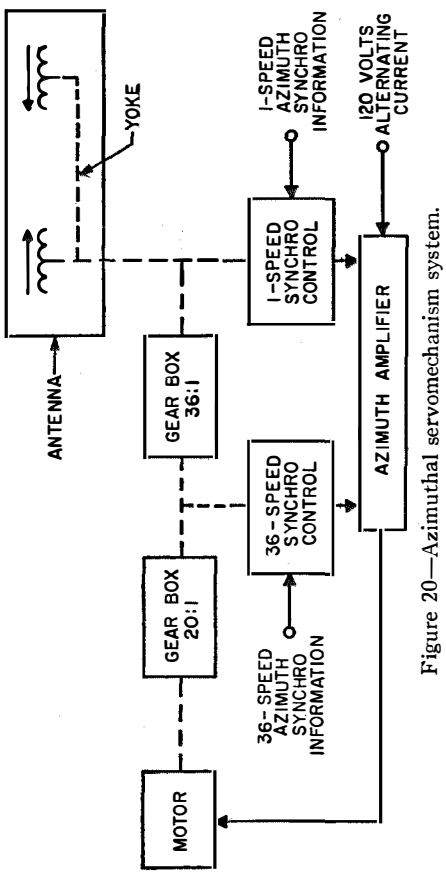

Figure 20—Azimuthal servomechanism system.

2.6 Speed Control

A block diagram of the speed-control amplifier is shown in Figure 21. Schematic diagrams of the pre-amplifier and power amplifier are shown in Figures 22 and 23. A block diagram of the speed-control servo system is shown in Figure 24. The tachometer signal from the rotating antenna passes through a frequency-discriminator circuit consisting of 2 series-resonant circuits tuned above and below the nominal tachometer frequency of 810 cycles per second. High-Q stable inductors and mica capacitors are used here since this circuit determines the accuracy of the system. The currents from the

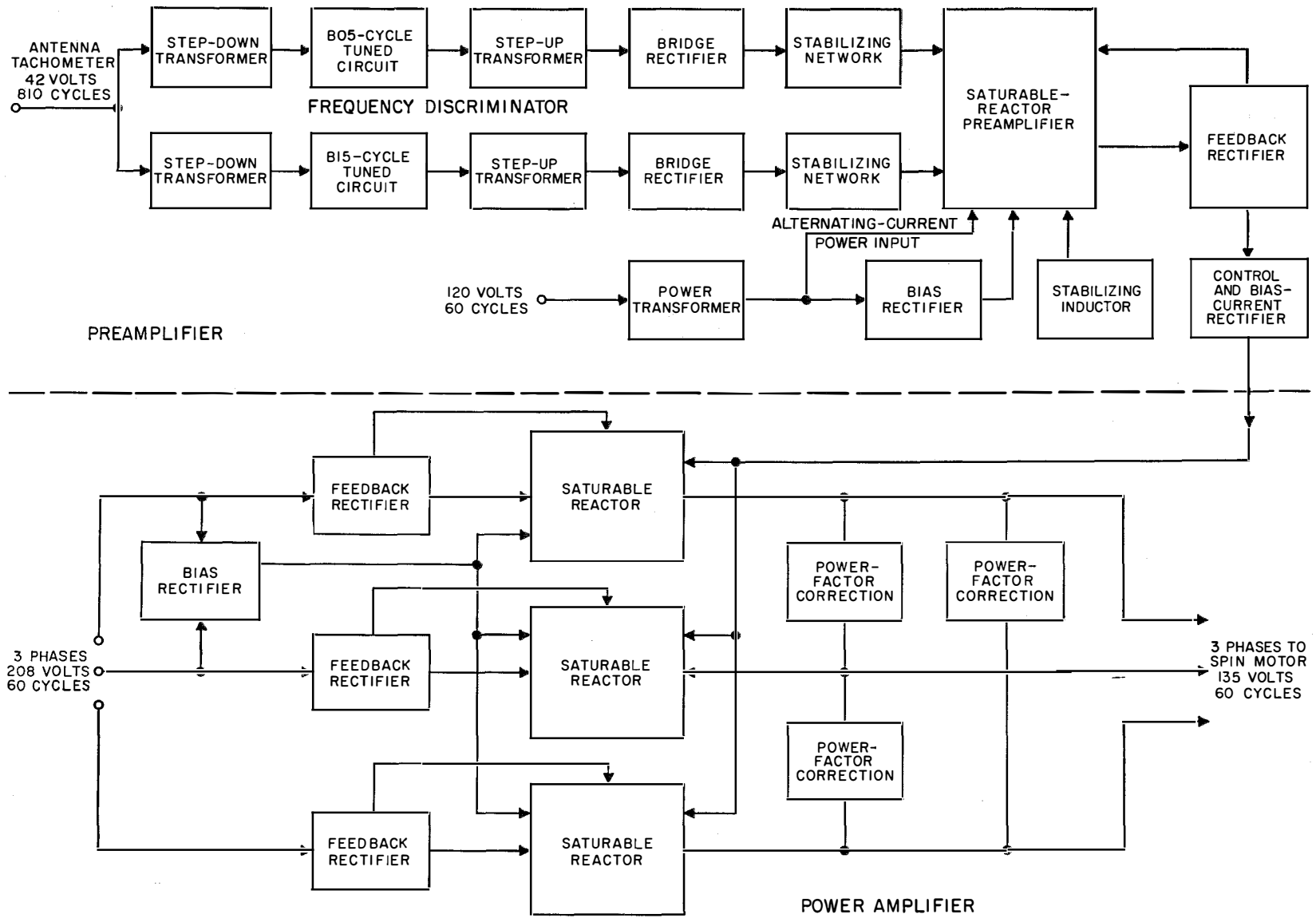

Figure 21—Block diagram of speed-control system.

high- and low-frequency circuits are rectified and mixed in the preamplifier reactor. Stabilization networks similar to those discussed in the section on the azimuth amplifier are also employed in the speed-control preamplifier.

The 3-phase power to the motor is controlled by 3 reactors each in series with a phase. The optimum operation of the reactor is obtained with a load whose power factor is close to unity. Accordingly, power-factor correction is accomplished by 3 wye-connected capacitors, transformed to increase their effective value. Thus, a smaller capacitor of a standard value can be used. The accuracy of the speed-control system is approximately 0.5 percent.

3. Electrical Operation

As in most production equipments, variations in operation can be expected from unit to unit. These variations are due in part to measurement error and in part to normal manufacturing tolerances and non-uniformity of components. Changes in operation are also encountered within a single unit over the frequency range. Therefore, in the discussion that follows, a certain range of data is given to define the limits over which the antenna may be expected to operate.

During initial test and calibration of the antenna, the following significant quantities are measured.

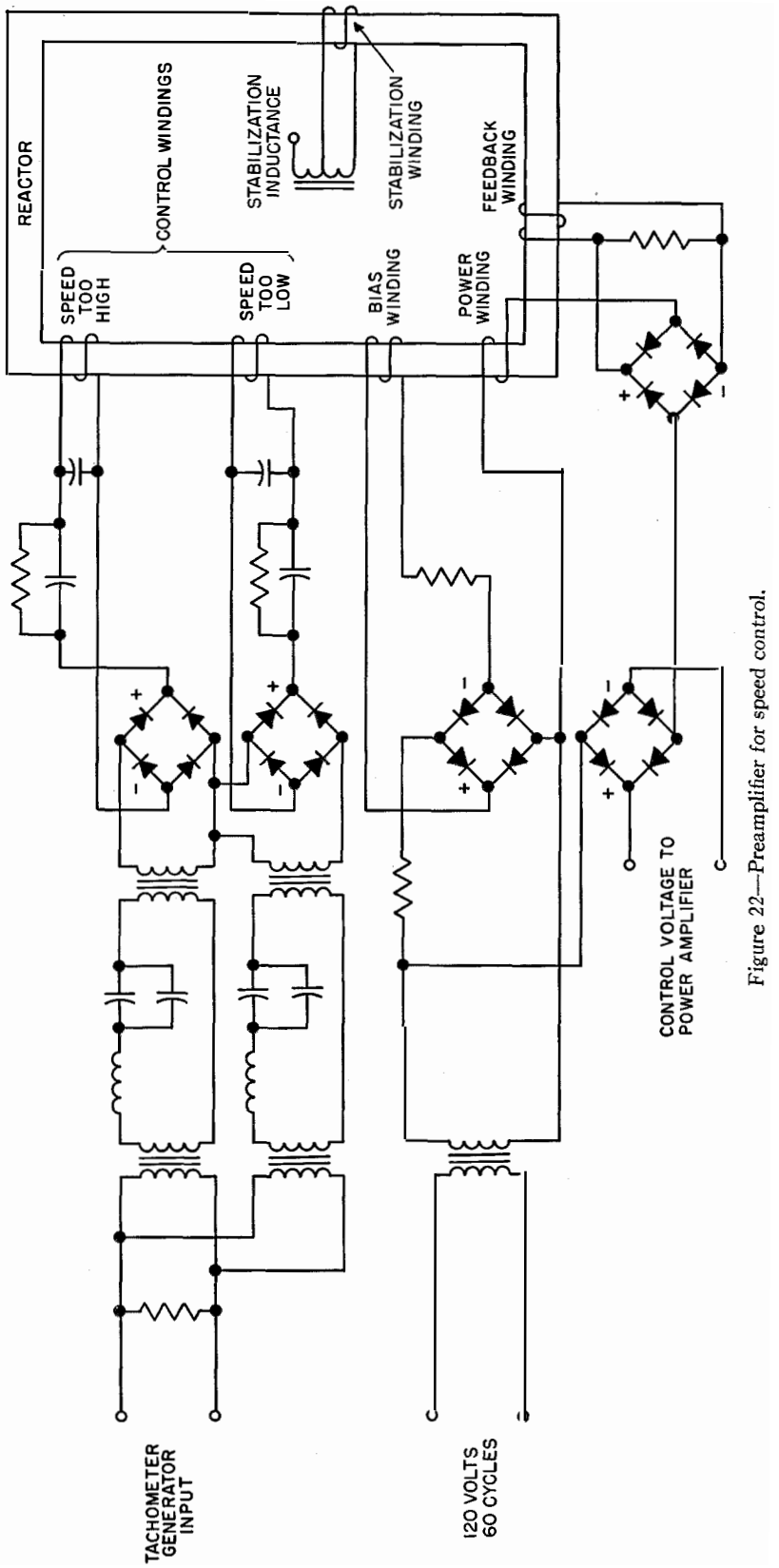

Figure 22—Preamplifier for speed control.

A. Impedance.

B. Horizontal radiation pattern.

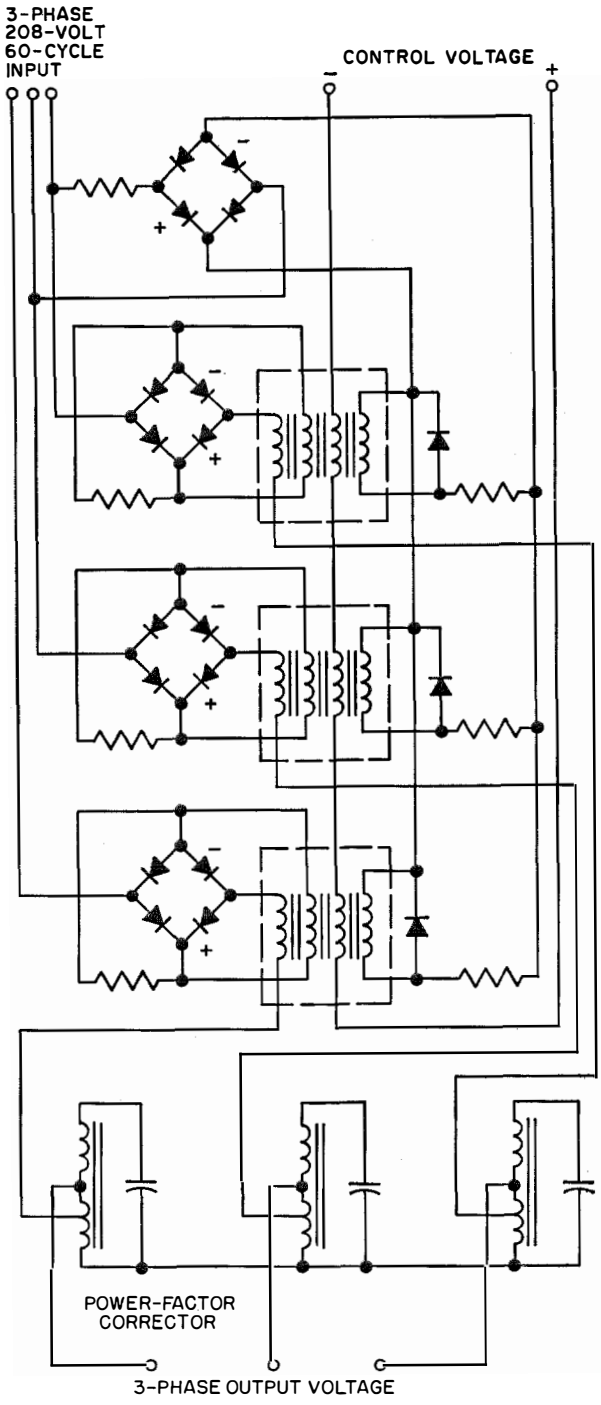

Figure 23—Power amplifier for speed control. The 4 windings on each saturable core are, from left to right, for power, feedback, control, and bias.

C. Vertical radiation pattern.

D. Relative phase between the 15- and 135-cycle components.

E. North calibration.

F. Harmonic content of the modulation components.

G. Depth of modulation.

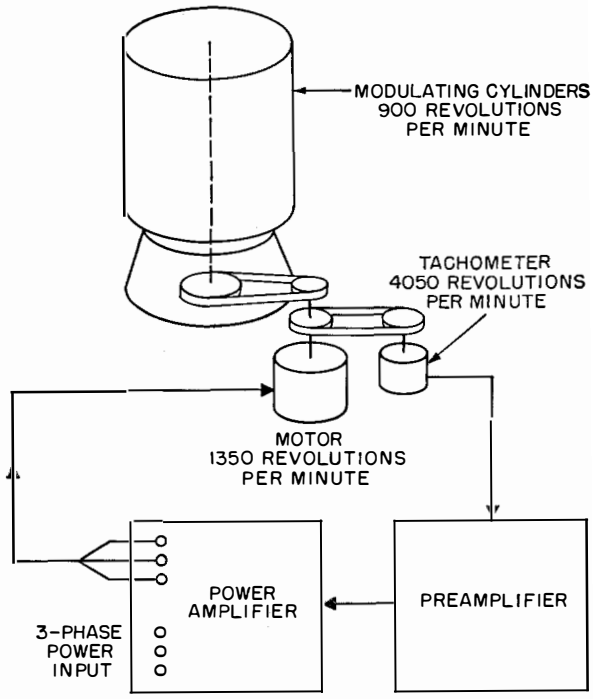

Figure 24—Servomechanism for speed control.

3.1 Impedance

In the measurement of many antennas, standing-wave ratios from 1.02 to 2.0 have been obtained, depending on frequency. In no case, does the standing-wave ratio exceed 2.0 and for 95 percent of the arrays, it does not exceed 1.6 over the frequency range.

3.2 Horizontal Pattern

The horizontal radiation pattern of the central array without the parasitic elements can be expected to be nearly circular. Such a pattern insures that equal range is obtained at all azimuths. It is emphasized, however, that slight

deviations from circularity do not affect the azimuthal accuracy because the central array is stationary and does not contribute to the modulation components. Therefore, substantial noncircularity could be tolerated without reducing the operational value of the equipment. Nevertheless, excellent circularity has been obtained and in the measurements taken on many antennas, the horizontal radiation pattern did not deviate from a circle by more than ± 5 percent.

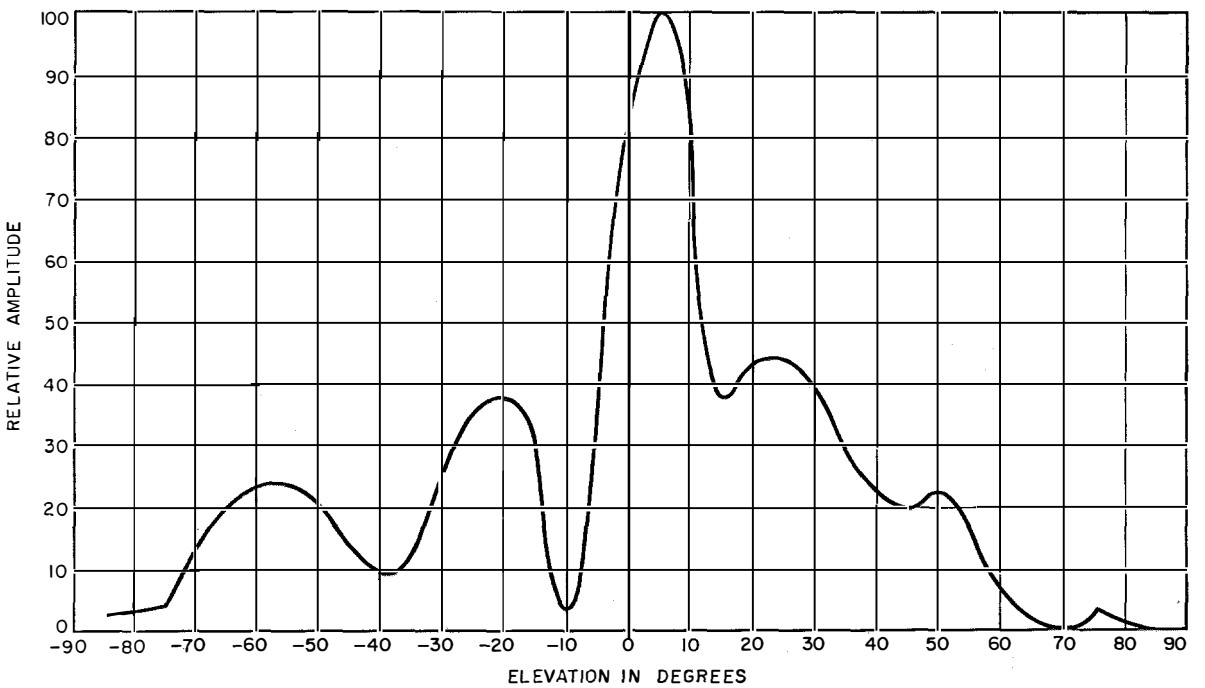

Figure 25—Typical vertical radiation pattern of central array.

3.3 Vertical Pattern

The central array was designed with a relatively large vertical aperture to obtain vertical gain and thereby maximum range utilization of the radio-frequency power. In addition, uptilt was introduced to minimize the effect of reflecting objects located below the horizon. To obtain greatest freedom from site errors, the uptilt should be as much as possible. During development, an increase of 0.5 decibel per degree in vertical angle was found adequate to effect a substantial improvement. Depending on frequency, the antennas tested exhibited uptilts from 0.5 to 1.5 decibels per degree.

Of interest in the vertical pattern is the presence of minor lobes. Because of the aperture on the antenna and of the relatively high power in the top cone, it can be expected that the radio-frequency distribution in the vertical plane will contain some convolutions. These convolutions are expressed as the magnitude of any nulls or minimums in decibels below the peak magnitude. In the first 15 degrees of vertical angle above horizontal, minimums of up to 9 decibels may be produced. Up to 50 degrees vertical angle, the worst null may reach a magnitude of approximately 16 decibels. However, at these rather high angles, the aircraft must necessarily be close to the transmitting station and can afford a relatively higher loss of signal and still be within the automatic-gain-control range of the receiver. In this regard, it is estimated that a 25-decibel reduction in signal can be tolerated without serious interruption in operation. A typical vertical radiation pattern of the antenna is shown in Figure 25.

3.4 Relative Phase

The relative-phase measurement consists of comparing the phase of the 135-cycle component with respect to the 15-cycle component; it depends on the relative position of the 15- and 135-cycle parasites. In actuality, the measurement is made as a normal factory test for adjusting the position of the cylinder of the 15-cycle parasite to the desired phase condition. Due to slight dissymmetry and to nonuniformity of the fiber-glass cylinders, the relative phase does not remain precisely constant at all azimuths.

However, it is emphasized that this condition does not affect the azimuthal accuracy. In north calibration, the reference pulses are accurately adjusted with respect to the 135-cycle component. The relative phase affects only the position of the 15-cycle reference within the *AN/ARN-21* fundamental gate, which is ± 20 degrees wide. This gate serves to eliminate the ambiguities in the harmonic system and the azimuth indication is not affected by movement of the reference pulse within the gate. The adjustment of cylinder position is such that the relative phase remains within ± 2.5 degrees at all points. This is the portion of the 15-cycle gate tolerance assigned to the antenna.

3.5 North Calibration

In north calibration, the position of the reference-pulse yoke is precisely adjusted with the azimuth servo system zeroed so that a standard signal will be received by an observer due south of the antenna. This north–south line is defined by a pair of calibration marks on the base of the antenna. Including all measurement errors, it is estimated that the calibration tolerance is within ± 0.2 degree.

3.6 Harmonic Analysis

Certain amounts of distortion of the 15- and 135-cycle components can be tolerated without affecting system accuracy since filters are incorporated in the *AN/ARN-21* for these components. It has been determined that values of 15 percent of second-harmonic distortion can be tolerated for both components. In practice, it has been found that in the worst case, the second-harmonic content does not exceed approximately 11 percent. In many cases, the second-harmonic distortion is so low as to be unreadable.

3.7 Depth of Modulation

Limits must be imposed on the variation of percentage of modulation to insure optimum operation of the *AN/ARN-21*. These variations occur as a function of vertical angle and of frequency. Modulation levels between 12 and 30 percent are considered satisfactory.

For increasing vertical angles, the percentage of modulation rises slightly and then begins to decrease. In the region near 20 degrees, the modulation generally reaches its maximum value. The vertical coverage of the antenna is defined as the point at which the 135-cycle modulation falls to a value too low to be properly processed by the *AN/ARN-21*. Investigations have indicated that this value is approximately 7 percent. Measurements indicate that for high-band antennas, vertical coverage to at least 35 degrees is always obtainable. Many antennas perform to beyond 40 degrees. Table 1 gives a vertical-coverage distribution of many sample antennas.

TABLE 1

Vertical Coverage

Vertical Coverage in Degrees	Percentage of Antennas
35.0 to 37.5	20.0
37.5 to 40	53.5
Over 40	26.5

Low-band antennas follow generally the same pattern so that it can be concluded that coverage above 35 degrees is always obtained. In some cases, the *AN/ARN-21* will operate satisfactorily for modulation levels below 7 percent. Hence, instances of better vertical coverage can be expected and have been reported in the field. Further, it should be noted that the above figures are based on data obtained at the worst measurement frequency and that an improvement can be expected at other points in the band.

4. *Appendix*

4.1 Derivation of Antenna Pattern

The form of the equation describing the desired 9th-harmonic pattern for proper operation of the *AN/URN-3* beacon is

$$E_\phi = [1 + k \cos (9\omega_m t - 9\phi)] \cos \omega_k t,$$

where

ω_m = angular rate of rotation of the space pattern

ϕ = azimuthal bearing of the beacon from the receiver

ω_k = carrier radio frequency $\times 2\pi$

k = constant determining percentage of modulation.

The expression indicates an amplitude-modulated wave with a modulating frequency of $9\omega_m/2\pi$ and with phase changing by an amount equal to 9 times the bearing angle.

The equation may be derived by initially assuming 9 equally spaced parasitic elements to be rotating about a central radiator. However, to reduce the number of terms to be handled and to clarify the steps taken, a single parasite will first be employed, for which case it will be shown that the 9th harmonic may be produced along with varying amounts of other odd harmonics. Then, by assuming 9 elements and using arguments of symmetry, it will be shown that harmonics other than the 9th may be virtually eliminated.

The development that follows assumes the receiving point to be in the same horizontal plane as the beacon and sufficiently remote so that lines drawn from the central radiator and the parasite to the receiver may be considered to be parallel. Attenuation terms are neglected and the radiation from each element is assumed to be circular. A simplification in the mathematics results if a quadrature initial phase is chosen between the central array and the parasite. Hence, these conditions are assumed in the calculation that follows.

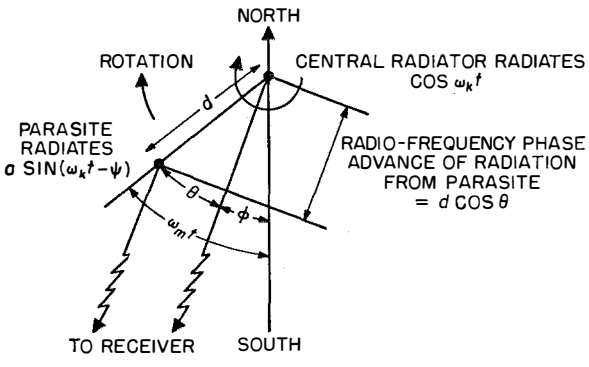

Figure 26—Symbols used in derivation of antenna radiation pattern.

The symbols used are shown in Figure 26 and are defined as follows

d = spacing of parasite from central radiator in wavelengths or radians

ψ = radiation phase of parasite relative to central array

θ = angular displacement of parasite from a line drawn to the receiver from the central radiator

$= (\omega_m t - \phi)$

ϕ = angular displacement of receiver from a point due south of the antenna

ω_m = angular rate of rotation of parasite about the central radiator

E_ϕ = total field at the receiver

a = ratio of parasitic voltage to central-array voltage

ω_k = carrier radio frequency $\times 2\pi$.

The radiations from the central radiator and the parasite will be combined at the receiver as follows

$$E_\phi = \cos \omega_k t + a \sin (\omega_k t - \psi + d \cos \theta). \quad (1)$$

Using the identity $\sin (A + B) = \sin A \cos B + \cos A \sin B$, where $A = (\omega_k t - \psi)$ and $B = d \cos \theta$, the second term of (1) may be expanded to obtain

$$E_\phi = \cos \omega_k t + a \cos (d \cos \theta) \sin (\omega_k t - \psi) + a \sin (d \cos \theta) \cos (\omega_k t - \psi). \quad (2)$$

It can be seen that the two complex modulation terms are periodic with θ and as such may be harmonically analyzed. Since θ is related to the rotational rate and bearing angle through $\theta = (\omega_m t - \phi)$, it will be seen that harmonics of θ must be harmonics of the rotational rate ω_m

with phases varying according to multiples of receiver bearing angle ϕ. The analysis may be made by expanding the coefficients into a Bessel series using the identities

$$\cos(d\cos\theta) = J_0(d) - 2J_2(d)\cos 2\theta + 2J_4(d)\cos 4\theta \ldots - 2J_{18}(d)\cos 18\theta \ldots$$

$$\sin(d\cos\theta) = 2[J_1(d)\cos\theta - J_3(d)\cos 3\theta + J_5(d)\cos 5\theta \ldots + J_9(d)\cos 9\theta \ldots J_{27}(d)\cos 27\theta \ldots].$$

It may be seen from (2) that the relative phases of the two modulation terms are in time quadrature while the Bessel expansions show that the cosine term contains only even, while the sine term contains only odd, harmonics of θ. Since it is desired to optimize the 9th harmonic, the spacing d is chosen so that $J_9(d)$ is near maximum (see Figure 27) and the radiation phase ψ for the parasite is adjusted so that the phase of the odd-harmonics term coincides with that of the central radiator. This avoids odd-harmonic phase modulation of the carrier. The adjustment is made by establishing proper current phase in the parasite. In practice, this is accomplished by the use of high-resistance parasites of certain lengths.

The resulting waves are thus amplitude modulated principally by the odd-harmonic terms and phase modulated by the even-harmonic terms.

With current phase adjusted as indicated, the relative radiation phase ψ will be zero. Setting the relative phase equal to zero and collecting terms, the expression becomes

$$E_\phi = [1 + a\sin(d\cos\theta)]\cos\omega_k t + a\cos(d\cos\theta)\sin\omega_k t \quad (3)$$

or, substituting the Bessel expansions,

$$E_\phi = \{1 + 2a[J_1(d)\cos\theta - J_3(d)\cos 3\theta\cdots + J_9(d)\cos 9\theta\cdots - J_{27}(d)\cos 27\theta\cdots]\}\cos\omega_k t + 2a\{[J_0(d)/2] - J_2(d)\cos 2\theta + \cdots - J_{18}(d)\cos 18\theta\cdots\}\sin\omega_k t.$$

The expression is now of the desired form but contains many undesirable harmonics. A calculated pattern of the coefficient of $\cos\omega_k t$ (odd-harmonic terms) is shown in Figure 28A.

It may be proved that for a symmetrical array, the lowest harmonic that may occur in the pattern will correspond to the space repetition rate of the parasite system. Further, the only higher harmonics to appear will be multiples of this harmonic. As a result, if 9 equally spaced parasites be arranged around the central array,

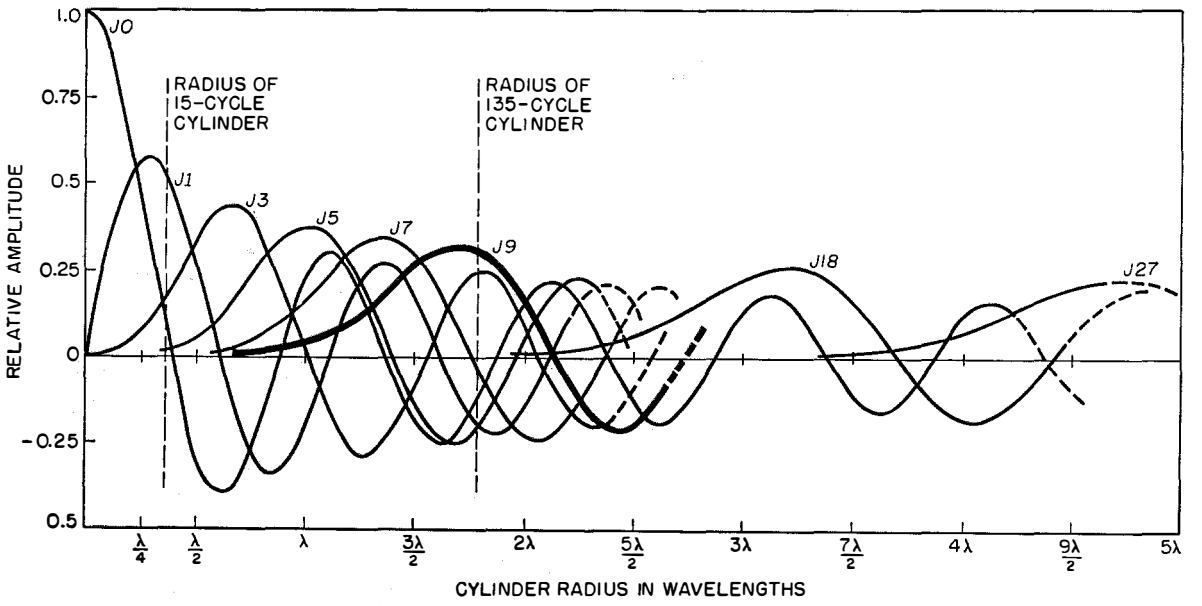

Figure 27—Bessel coefficients of harmonic terms as a function of radius of parasitic elements.

the only harmonics present will be the 9th, 18th, 27th, et cetera.

A plot of the pattern for 9 elements may be obtained by superimposing 9 plots similar to that in Figure 28A each progressively shifted 40 degrees with respect to the other. A curve thus obtained is shown in Figure 28B. It can be seen that the pattern is essentially sinusoidal, having a period corresponding to 40 degrees of azimuth.

Mathematically, the expression for 9 parasites may be obtained by retaining only the possible harmonics and multiplying their coefficients by 9, thus

$$E_\phi = \{1 + 18a[J_9(d)\cos 9\theta - J_{27}(d)\cos 27\theta\cdots]\}\cos\omega_k t + 18a\{[J_0(d)/2] + J_{18}(d)\cos 18\theta\cdots - J_{36}(d)\cos 36\theta\cdots\}\sin\omega_k t. \quad (4)$$

Reference to the Bessel curves of Figure 27 will disclose that for the value of d at which $J_9(d)$ is maximum, the value of the J_{18}, J_{27}, et-cetera terms are so small that they may be neglected. The $J_0(d)$ term is not insignificant. However, the only effect of this constant quadrature term is to produce a small phase shift in the carrier term that can be compensated for by slight readjustment of the radiation phase of the parasite ψ. If this is done, then the quadrature carrier term may be neglected. The expression may now be written

$$E_\phi = [1 + 18a\,J_9(d)\cos 9\theta]\cos\omega_k t, \quad (5)$$

or substituting $\theta = \omega_m t - \phi$,

$$E_\phi = [1 + 18a\,J_9(d)\cos(9\omega_m t - 9\phi)]\cos\omega_k t. \quad (6)$$

Equation (6) represents a carrier modulated by a frequency of 9 times the rotational rate and whose electrical phase will change at 9 times the rate of the bearing angle of the receiver.

The fundamental 15-cycle pattern may be derived in a similar manner if d is chosen to provide a maximum value for $J_1(d)$. In this case, only a single parasite is required. The final equation becomes

$$\text{Total } E_\phi = [1 + 2a\,J_1(d)\cos(\omega_m t - \phi) + 18a\,J_9(d)\cos(9\omega_m t - 9\phi)]\cos\omega_k t. \quad (7)$$

Equation (7) defines the total desired radio-frequency pattern for proper azimuth operation of the *AN/URN-3* beacon.

The factor d is intentionally chosen to be greater than that required for a maximum value of $J_9(d)$. As the vertical angle increases, the effective argument of J_9 becomes smaller, as follows

$$d_v = d\cos\theta_v, \quad (8)$$

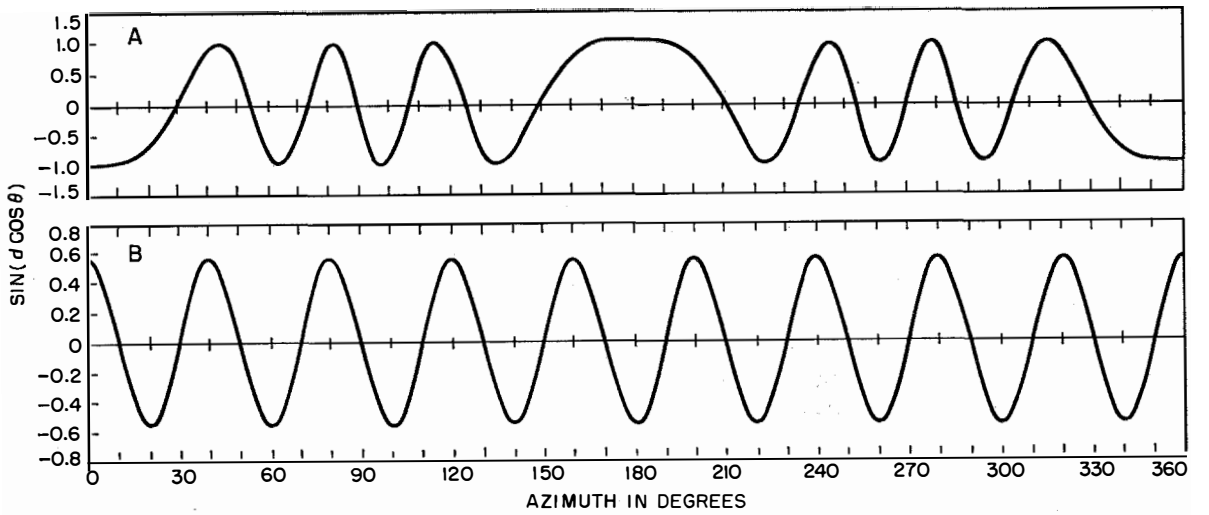

Figure 28—*A* = space pattern for a single parasite rotated in azimuth about the central array. At zero degrees, the parasite is directly between the radiator and the receiver, d = 630 degrees. *B* = resulting space pattern for 9 equally spaced parasites.

where d_v is the effective argument of J_9 and θ_v is the vertical angle. To obtain an expression for the performance with the vertical angle, the term $(d \cos \theta_v)$ is used as the Bessel function argument in (7), resulting in

$$\text{Total } E_\phi = [f_c(\theta_v) + f_p(\theta_v)\, J_1(d \cos \theta_v) \times \cos(\omega_m t - \phi) + f_p'(\theta_v)\, J_9(d \cos \theta_v) \times \cos(9\omega_m t - 9\phi)] \cos \omega_k t, \quad (9)$$

where

$f_c(\theta_v)$ = vertical pattern of central array
$f_p(\theta_v)$ = vertical pattern of 15-cycle parasite
$f_p'(\theta_v)$ = vertical pattern of 135-cycle parasites.

From the above, if d is initially chosen so that $J_9(d)$ is beyond maximum, an improved vertical coverage will result. As d_v decreases with elevation, the value of $J_9(d_v)$ will go through maximum and thereby remain relatively constant over a wider range of elevations. This operation results in a slight increase in modulation level in the first 20 degrees of elevation, after which the modulation falls off as defined by the Bessel function.

4.2 Calculation of Vertical Pattern of Antenna Above Ground

The calculation shown below derives the equation for the vertical pattern of any antenna above ground. It should be understood that the derivation applies to the field strength or carrier level and not to the antenna modulation characteristics with elevation. This latter characteristic is discussed in 4.1. The assumed conditions for the calculation are shown in Figure 29. Let

$\omega = 2\pi f$, where f is the radio frequency
θ_v = vertical angle in degrees
h' = height of the antenna in feet
$h°$ = height of the antenna in electrical degrees $= (h'/\lambda) \times 360$
A_D = magnitude of direct signal
A_R = magnitude of reflected signal
A = ratio of reflected to direct signal $= A_R/A_D$
λ = wavelength in feet
α_R = phase shift imposed at the reflecting point
F_p = total field of the receiving point.

It is assumed that the receiver is sufficiently remote from the antenna that all wave fronts travel parallel paths to the receiving point.

$$\begin{aligned} F_p &= A_D \sin(\omega t + h° \sin \theta_v) + A_R \sin(\omega t - h° \sin \theta_v + \alpha_R) \\ &= [\sin \omega t \cos(h° \sin \theta_v) + \cos \omega t \sin(h° \sin \theta_v)] \\ &\quad + A[\sin \omega t \cos(h° \sin \theta_v + \alpha_R) - \cos \omega t \sin(h° \sin \theta_v + \alpha_R)] \\ &= \sin \omega t[\cos(h° \sin \theta_v) + A \cos(h° \sin \theta_v + \alpha_R)] \\ &\quad + \cos \omega t[\sin(h° \sin \theta_v) - A \sin(h° \sin \theta_v + \alpha_R)]. \end{aligned}$$

Neglecting the radio-frequency terms, the magnitude of the field becomes

$$F_p = [\cos(h° \sin \theta_v) + A \cos(h° \sin \theta_v + \alpha_R)] + j[\sin(h° \sin \theta_v) - A \sin(h° \sin \theta_v + \alpha_R)]. \quad (10)$$

Equation (10) represents a complete statement of the vertical pattern including the effect of

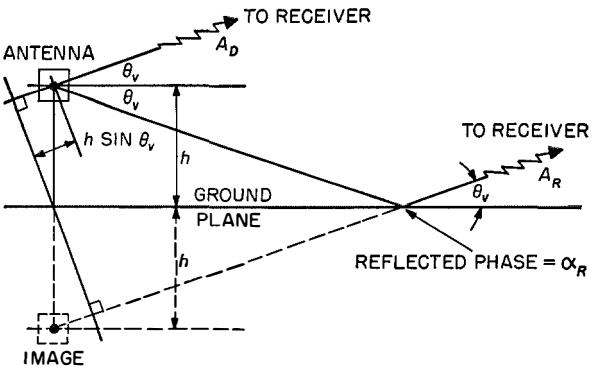

Figure 29—Conditions assumed for calculation of vertical radiation pattern of an antenna above ground.

uptilt and ground attenuation A and phase shift at the reflecting point α_R. At low angles, the ground attenuation can be neglected and the reflection phase $\alpha_R = 180$ degrees. Assuming no uptilt or ground attenuation, $A = 1$. This permits the following simplification of (10)

$$F_p = [\cos(h° \sin \theta_v) - \cos(h° \sin \theta_v)] + j[\sin(h° \sin \theta_v) + \sin(h° \sin \theta_v)]$$

$$F_p = j\, 2 \sin(h° \sin \theta_v).$$

Neglecting the constant and substituting for $h°$

$$F_p = \sin [360\ (h'/\lambda) \sin \theta_v]. \qquad (11)$$

In (11), the nulls occur when $[360\ (h'/\lambda) \sin \theta] = 180, 360, 540$ degrees, et cetera, and the maxima occur when $[360\ (h'/\lambda) \sin \theta] = 90, 270, 450$ degrees, et cetera.

Equation (11) was used to obtain the information shown in Figure 30. The graph indicates the positions of the 1st, 2nd, and 3rd nulls as a function of the height of the antenna above ground at a frequency of 1000 megacycles. It should be noted that these nulls occur only when $A = 1$ or when no difference in magnitude exists between the direct- and reflected-radiation components. With uptilt, the signal reflected from the ground is appreciably less than the direct signal, hence complete cancellation cannot occur and minimums result instead of nulls. This can be shown by reference to (10) which, when α_R is assumed to be 180 degrees, becomes

$$F_p = [\cos (h° \sin \theta_v) + A \cos (h° \sin \theta_v)] + j[\sin (h° \sin \theta_v) - A \sin (h° \sin \theta_v)]. \qquad (12)$$

Neglecting radio-frequency phase, the magnitude of the field F_p' is the square root of the sum of the squares of the quadrature components, or

$$F_p' = 1 + 2A + A^2 - 4A \sin^2 (h° \sin \theta_v). \qquad (13)$$

It can be shown that (13) cannot equal zero unless $A = 1$, which is a condition of no uptilt.

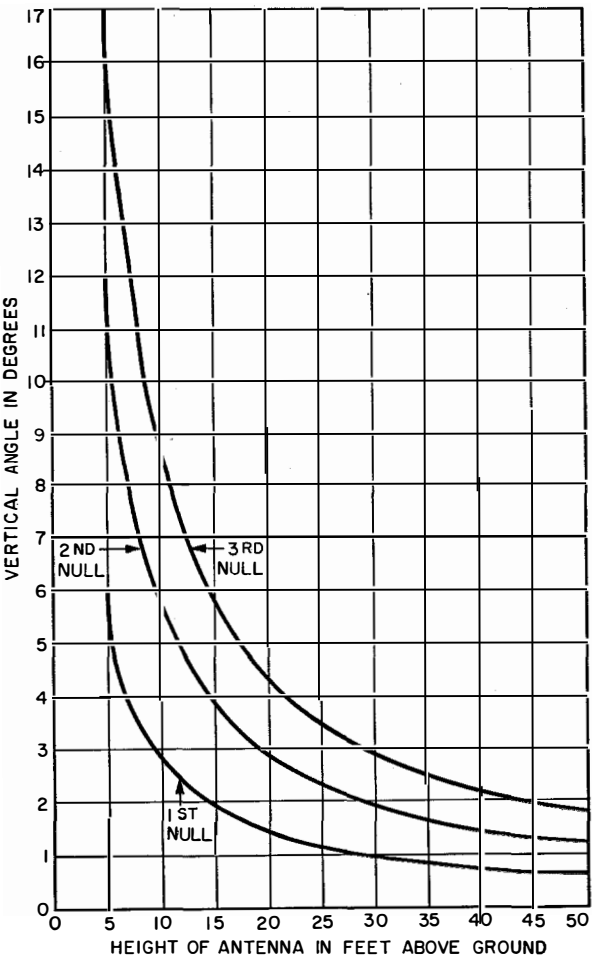

Figure 30—Location of nulls or minimums in the vertical radiation pattern of an antenna above ground at approximately 1000 megacycles.

Airborne Tacan Equipment AN/ARN-21

By SVEN H. DODINGTON

Federal Telecommunication Laboratories, a division of International Telephone and Telegraph Corporation; Nutley, N. J.

THE TACAN SYSTEM provides distance and bearing information to an aircraft from a selected ground beacon or transpondor such as the *AN/URN-3*. In furnishing distance-measurement service, this beacon always transmits a constant number of pulses regardless of the number of interrogations. It is designed to reply simultaneously to 100 aircraft. The constant-duty-cycle pulses are amplitude modulated by a rotating antenna system at both 15 and 135 cycles per second, providing rough and fine bearing information in much the same way that the hands of a clock give rough and fine indications of time without ambiguity. It has the novelty of providing both distance and bearing on the same channel and the use of a 2-speed system for bearing information.

The fundamental components of an airborne tacan equipment such as the *AN/ARN-21* are shown in Figure 1.

The local oscillator offers a selection of 126 crystal-controlled frequencies at 1-megacycle intervals from 1025 to 1150 megacycles. These frequencies are used directly to control the airborne transmitter and also to beat against the incoming signal from the ground transpondor at 962 to 1024 and 1151 to 1213 megacycles. The receiver intermediate frequency is 63 megacycles. The output of the receiver operates the airborne bearing circuits that in turn operate the bearing display. The receiver in cooperation with the transmitter also operates the range circuit that drives the range display. The main equipment is housed in a single package 17½ by 10 by 7½ inches (44 by 25 by 19 centimeters) weighing 56 pounds (25.5 kilograms) and powered by 450 volt–amperes from a 115-volt 400-cycle supply. External to this equipment are the two displays, the channel-selection control box, and the shock mount. An over-all view appears in Figure 2.

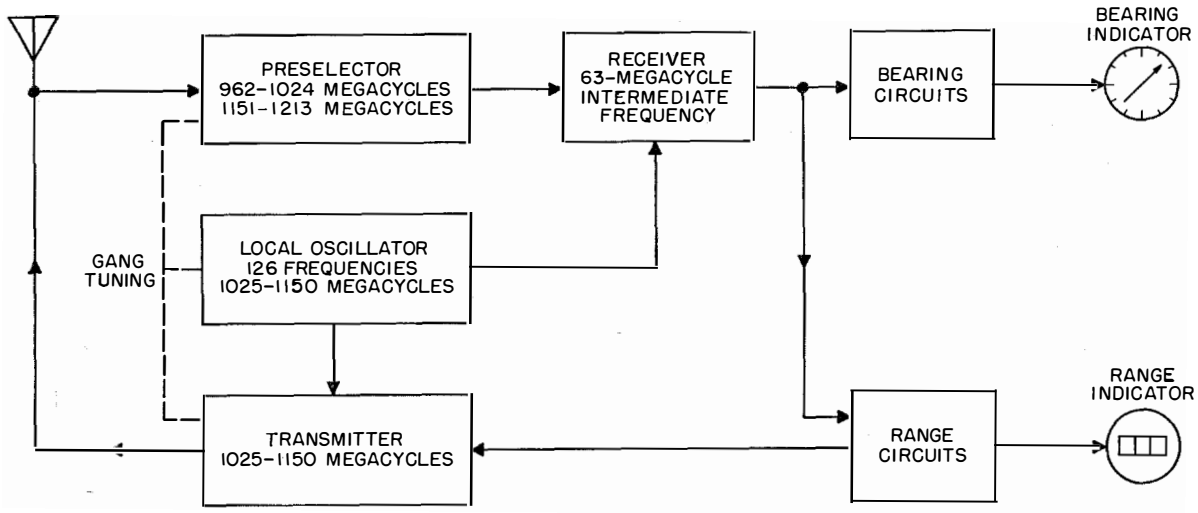

Figure 1—Block diagram of airborne equipment.

The signals received from the ground transpondor comprise pulses of 3.5-microsecond duration, in pairs spaced by 12 microseconds. Paired pulses are used to reduce the effect of pulse interference, mainly man-made. The constant-duty-cycle transpondor radiates 2700 pairs of pulses per second with random timing either in reply to range interrogations or as a

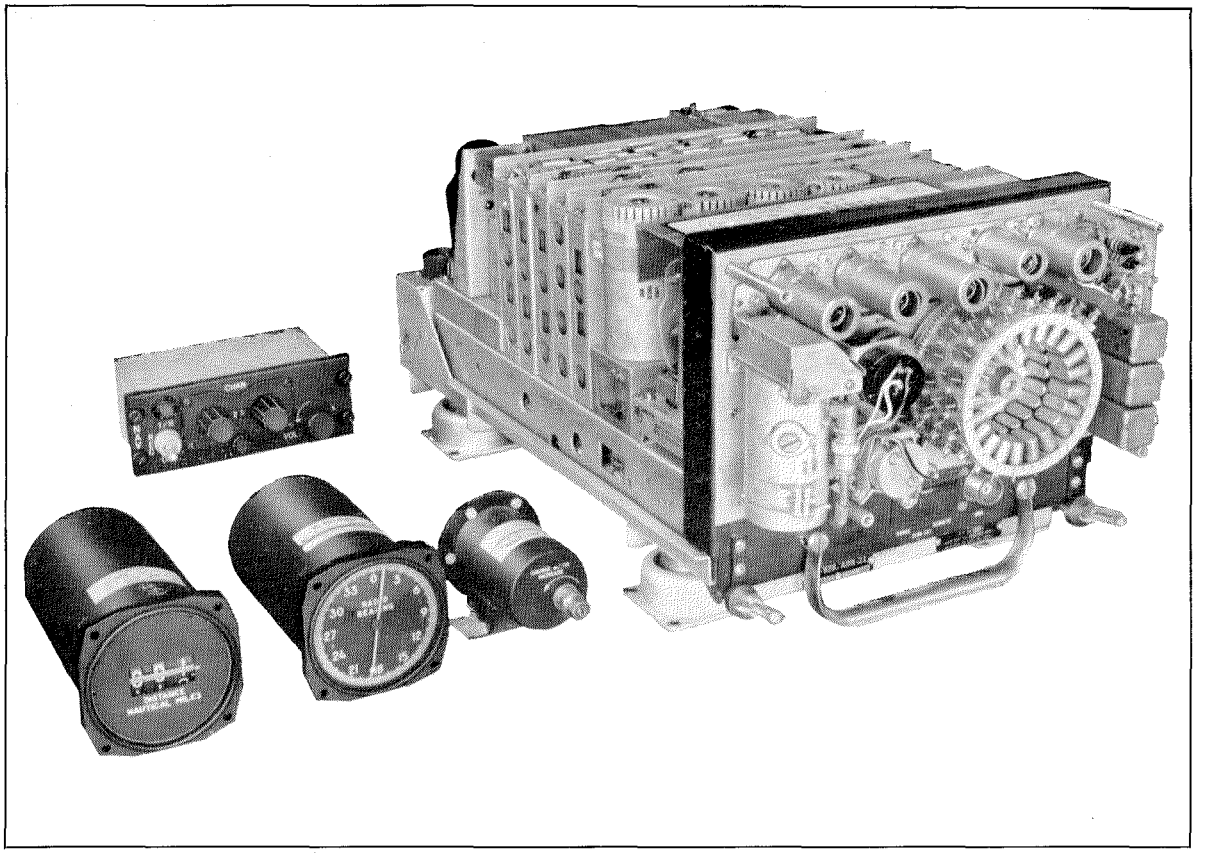

Figure 2—Airborne equipment.

substitute for such interrogations when fewer than 100 aircraft are being served. An additional 900 pairs per second are radiated by the transpondor to form 15- and 135-cycle reference bursts. The whole pulse train is amplitude modulated by the rotating transpondor antenna at 15 and 135 cycles.

Signals transmitted from the airborne equipment comprise range interrogation pulses of 3.5-microsecond duration in pairs spaced by 12 microseconds. They are of 1.5-kilowatt amplitude at a repetition rate of 27 pairs per second during range tracking and 130 pairs per second during range searching.

For bearing, the airborne equipment must display the phase difference between the amplitude-modulated sine waves and their corresponding reference bursts.

For range it must display in miles the time difference between interrogating pulses and reply pulses.

These problems, together with the channeling problem, would present little difficulty were unlimited space available. However, no electrical problem has been unaccompanied by space and power-consumption limitations. Therefore, it should be noted that many circuit choices were made not for performance alone but also because they represented the best over-all compromise.

1. Local Oscillator

Any one of 42 crystals that are mounted in a turret may be selected to provide a channel in the 1067-to-1109-megacycle band. A frequency multiplication of 27 is employed. Mixed with the output of this frequency multiplier is a fixed frequency of 42 megacycles, thus generating an additional 84 frequencies each either 42 megacycles above or below the output of the multiplier.

The local-oscillator chain is supplied with sufficient plate voltage to generate about 10

milliwatts for injection into the receiver mixer. The chain is also pulsed (exclusive of the first 2 stages) to generate about 5 watts peak for application to the final 3 transmitter stages.

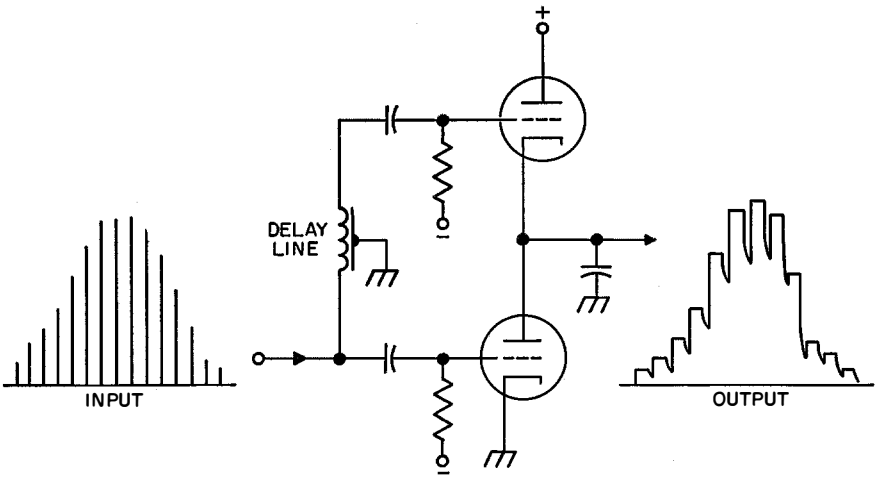

Figure 3—Typical peak-rider circuits.

2. *Transmitter*

The transmitter comprises 3 amplifier stages at the final local-oscillator frequency and employs *2C39A* grounded-grid triodes. They are anode pulsed at 2500 volts by a modulator using a *3D21A* vacuum tetrode driven by one *2D21* thyratron for each of the pulses in a 12-microsecond pair. The 3 stages are ganged to and track with the last stage of the local-oscillator chain, the preselector, and the crystal turret. The turret makes 3 revolutions as the frequency is varied over the 126 channels. The *2C39A* amplifier stages employ coaxial circuits, the anode–grid circuit being a quarter-wavelength long, resonated by a variable capacitor. The cathode–grid circuit is broad-banded over the necessary range. Above 30 000 feet, a barometric switch cuts the power to 800 watts, permitting unpressurized operation to 50 000 feet.

3. *Preselector*

The preselector protects the receiver mixer crystal from the transmitter and reduces spurious responses. Four quarter-wavelength circuits are used, a pair for the low band of 962 to 1024 megacycles and a pair for the high band of 1151 to 1213 megacycles. Both low-band and high-band pairs are permanently coupled to the antenna and to the receiver mixer, but the unused pair is short-circuited, raising its resonant frequency to the 2000-megacycle region. The preselector absorbs energy from the antenna only when resonant and therefore does not detract from the transmitter power output, which is 63 megacycles away.

Tuning is by varying the length of the quarter-wavelength sections, this resulting in the unusually high unloaded Q of about 2000 despite the cross-section of 1 square inch (6.5 square centimeters) per tuned circuit. Insertion loss with a 3-megacycle bandwidth is consequently less than 2 decibels.

4. *Receiver*

A *IN23B* silicon crystal is followed by an intermediate-frequency amplifier using a *2C51* twin-triode cascode input stage, followed by 5 conventional pentode stages using *6AK5* tubes. Automatic-gain-control voltage is applied to all grids except the second stage of the cascode and the last pentode.

5. *Bearing Circuits*

The received video pulses are decoded by conventional means employing a 12-microsecond inductance–capacitance delay circuit and a pentode tube with short suppressor-grid base. The signal is then split two ways: one portion retains its amplitude modulation and is supplied to the peak-rider and automatic-gain-control circuit. The other portion is amplitude-limited and goes to the range reply circuit, bearing reference-burst decoders, and identity-tone amplifier.

The peak-rider causes each decoded pulse to discharge a capacitor and then to charge it some 5 microseconds later. A "direct" voltage is thereby generated, proportional to the amplitude of the last-received pulse as shown in Figure 3. This direct current consequently closely follows the amplitude modulation im-

posed by the rotating transpondor antenna. After suitable filtering, it provides the 15- and 135-cycle bearing sine waves. Referring to Figure 4, these sine waves are phase-shifted by motor-driven goniometers in the bearing indicator and then compared with the reference

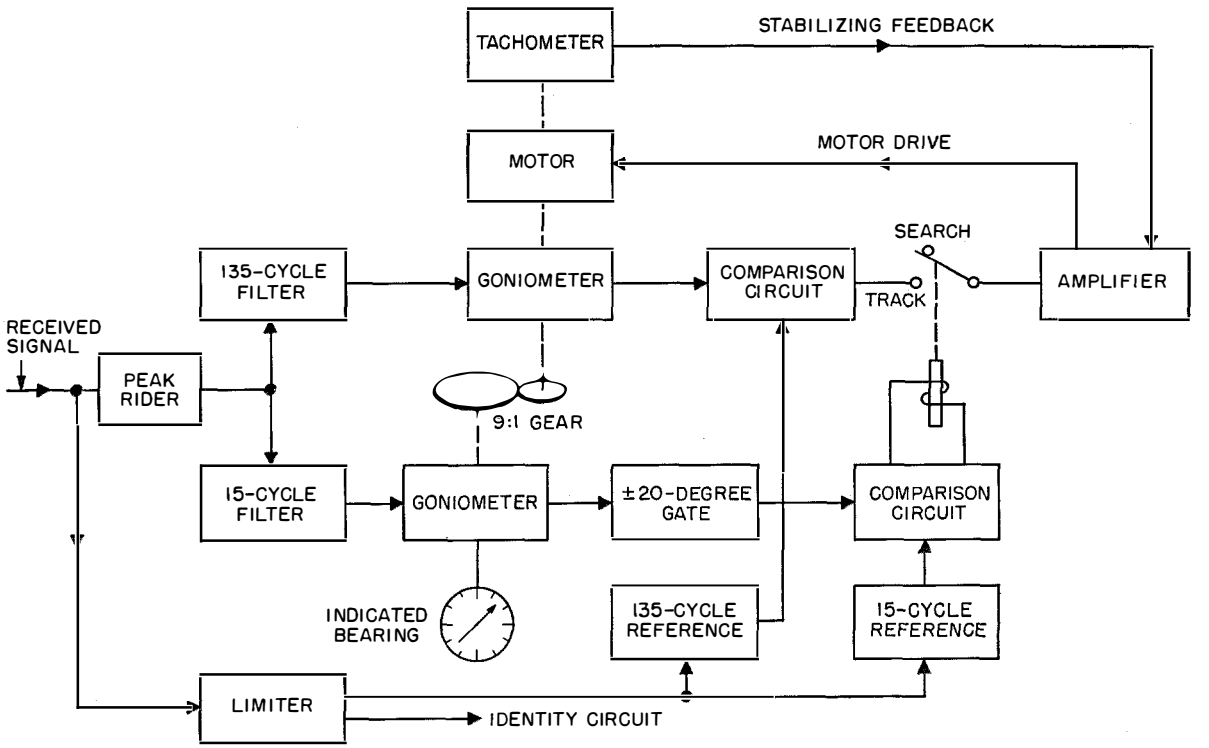

Figure 4—Airborne bearing circuits.

bursts. The resulting error voltage is amplified and used to drive the motor in the indicator towards minimum error, thus indicating true bearing.

Whenever the indicated bearing lies outside a range of ±20 degrees with respect to the receiver bearing, the 135-cycle information is removed and the indicator searches at 4 revolutions per minute. When it is within the ±20-degree sector, the indicator tracks the received bearing to within an accuracy of ±0.1 degree at rates up to 10 degrees per second.

Tachometer feedback is used to stabilize the servo system.

6. Range Circuit

The range circuit is fundamentally more complex than the bearing circuit since not only is the information rate somewhat less but this circuit must discriminate against the replies intended for up to 99 other aircraft. For this latter reason, the gate that determines the search-or-track operation covers a far smaller proportion of the range to be scanned, being 20 out of 2200 microseconds, compared with the 40 out of 360 degrees employed in the bearing circuits.

Aside from this major difference, many of the same principles will be noted. A 2-speed system is employed to gain accuracy and a similar motor-tachometer indicator drive is used.

Referring to Figure 5, fully half the circuit is taken up with the generation of a pair of 10-microsecond gates that during track straddle the received reply. This comprises the upper portion of the diagram. An oscillator having 1 cycle exactly equal to the round-trip time at a 20-nautical-mile (37-kilometer) range, generates accurately spaced pulses every 20 miles; these can be phase shifted by a goniometer driven by a motor, which also drives the Veeder

counter-type display. To avoid ambiguity every 20 miles, a 200-nautical-mile (371-kilometer) phantastron provides a single broad pulse, phase-shifted by a variable resistor geared 10:1 to the goniometer. The coincident 20-mile and 200-mile pulses then generate a pair of gates that can be shifted smoothly by the motor from 0 to 200 miles but with an accuracy some 10-fold better than could be obtained with the phantastron alone.

These gates are compared with the received signal and, when coincident, drive the motor so as to follow the signal. Whenever the signal is missing from the gate for more than 10 seconds, the motor amplifier is connected to the search voltage, which drives the display at 10 nautical miles (19 kilometers) per second.

During track, the display follows the true slant range to an accuracy of 0.1 mile (0.19 kilometer) ±0.25 percent up to speeds of 1000 knots (1900 kilometers per hour).

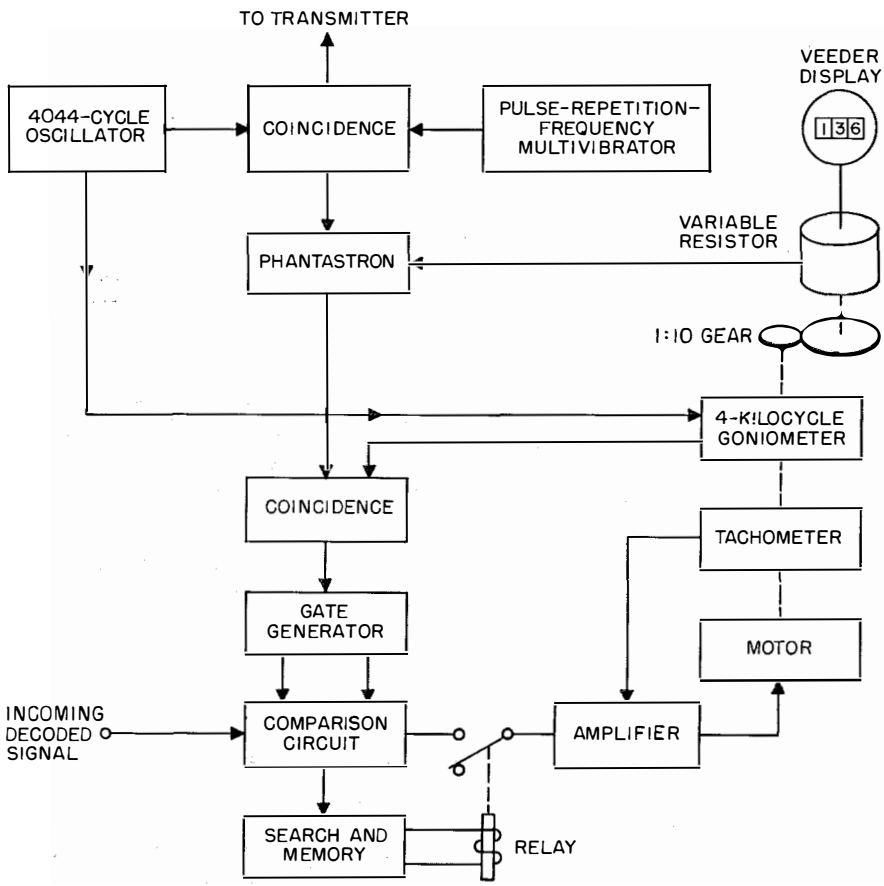

Figure 5—Range circuit.

7. Packaging

Of the 73 tubes used in all, 5 are disk-seal ultra-high-frequency triodes, 2 are octal-based units, 27 are miniatures, and the rest are subminiatures. Even with the use of subminiature tubes, the packaging problem would have been severe had it not been for the use of plug-in subunit construction. The equipment contains 10 such removable units, none of which has more than 9 tubes. Specifications of these units are held to close mechanical and electrical limits enabling the several manufacturers of the equipment to provide fully interchangeable units.

British Tacan Equipment

THE United Kingdom has been interested in the tacan development since 1950, when the British Services stated their requirements for a pilot-interpreted short-distance navigational aid. After demonstrations of the early tacan system operation to the British delegation late in 1950 and subsequent consideration by the Joint Communications Electronics Committee in 1951 the *AN/ARN-21* and *AN/URN-3* system was adopted as the tactical aerial navigational system for Canada, the United Kingdom, and the United States combined.

Since that time and in parallel to the development and production work in the United States, British versions known as the *STURN-3* and *STARN-21* were developed under contract with the British Ministry of Supply by Standard Telephones and Cables, Limited, an associate company of the International System.

Prototype models of the British designs have been flight tested together with American built equipment. Although there are differences in circuit details and components, the two versions conform to the same system specifications and are therefore functionally interchangeable. Some photographs of the British equipment are given on this and the following page.

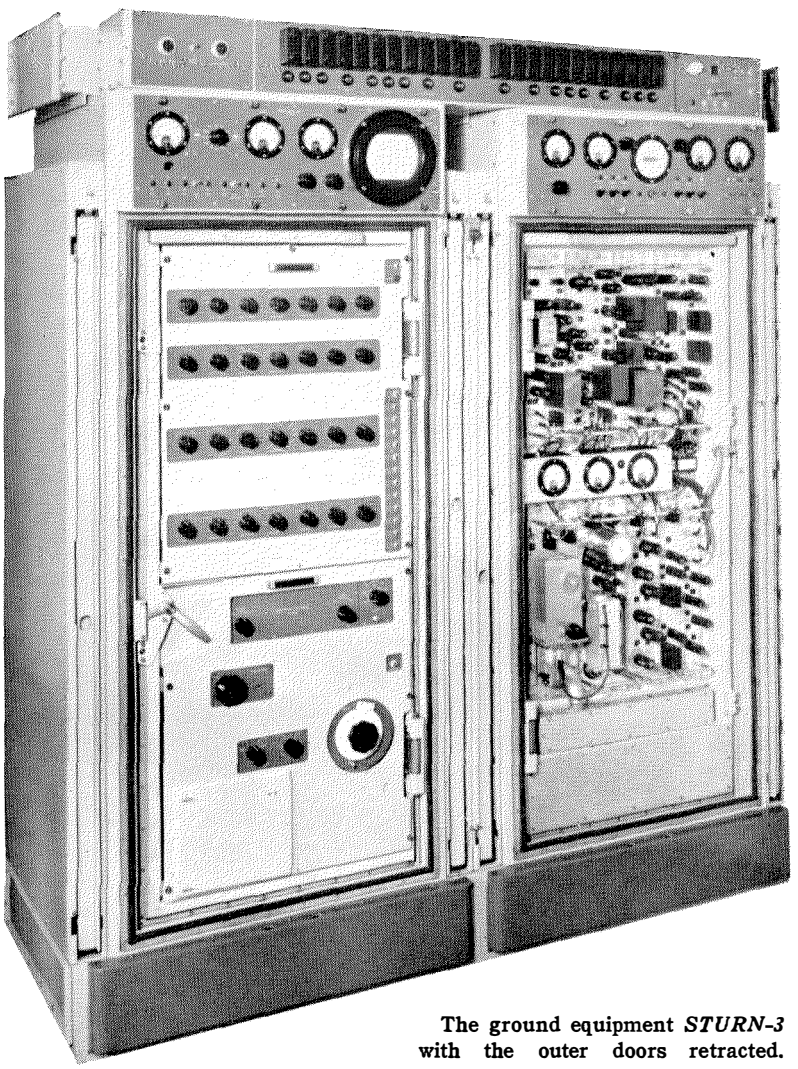

The ground equipment *STURN-3* with the outer doors retracted.

STARN-21 with the covers opened.

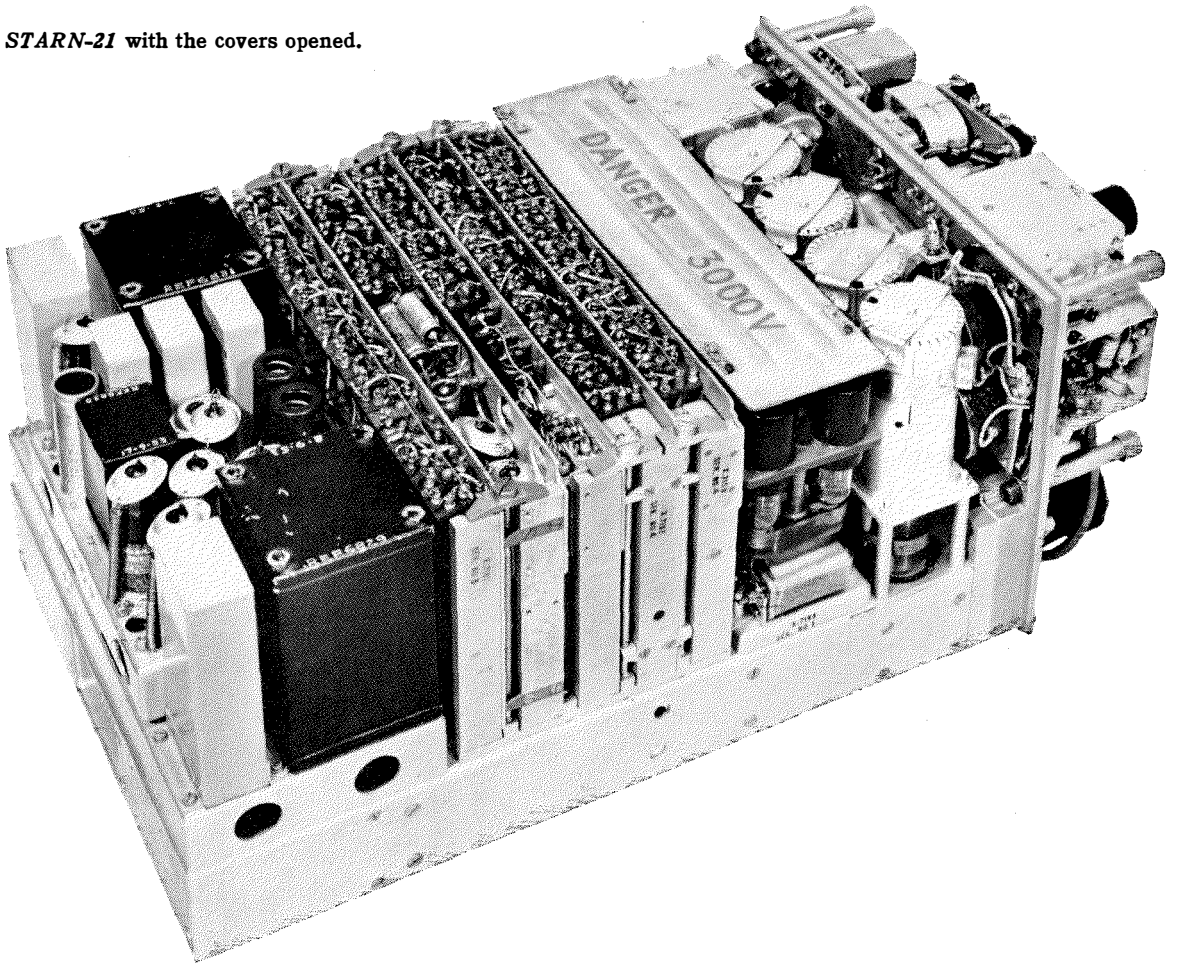

The airborne indicator gives bearing by a pointer and distance by a number display on a single instrument.

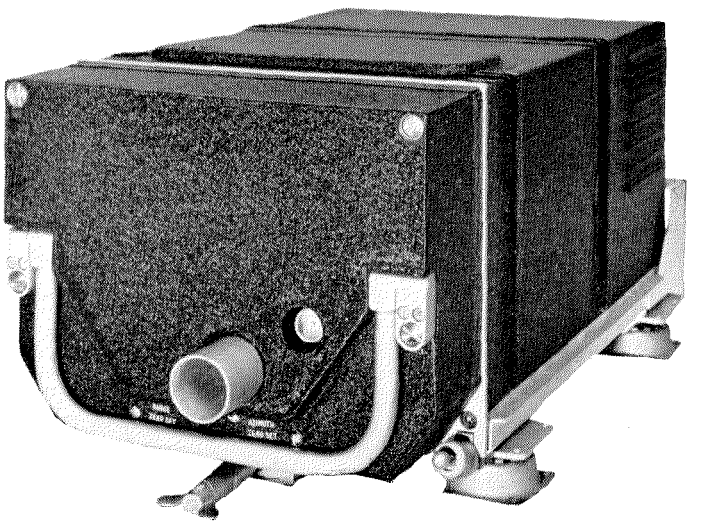

Airborne equipment *STARN-21*.

Experimental Determination of Tacan Bearing and Distance Accuracy*

By ETTIENNE DeFAYMOREAU

Federal Telecommunication Laboratories, a division of International Telephone and Telegraph Corporation; Nutley, New Jersey

TACAN is a radio navigational system that furnishes direct-reading meter indications of bearing and distance. Both functions make use of the same radio-frequency elements of the equipment, but the processes of measurement are different; hence the accuracies of the two functions are evaluated separately.

1. Bearing Accuracy

1.1 General Considerations

The bearing function in its use of multilobe antenna patterns, pulse transmissions, and physically rotating antenna elements presents a number of differences compared with other bearing systems. Each of these differences produces certain advantages, but the question that primarily interests the user is "What is the over-all improvement?" or more specifically, "What is the accuracy of the tacan bearing readings during actual service?"

Errors in radio bearing systems are due not only to finite accuracy limits of the equipments (instrumental errors), but also to disturbances of the radio signals in propagation from the ground station to the airplane (site errors). The multilobe operation of the tacan system has been designed to accomplish a significant reduction in both types of errors. Propagational errors are the most troublesome type in the practical operation of radio bearing systems; hence a realistic assessment of the accuracy of the system required not only laboratory tests of the equipment but measurements of accuracy during actual flights.

1.2 Experimental Setup

Systematic flight tests of bearing accuracies were performed in September 1954 in flights of the Laboratories' *DC-3* aircraft (Figure 1) orbiting around a ground beacon installed in the microwave research tower at Nutley, New Jersey. For systematic flight tests of a radio bearing system, three conditions are essential. One is that the geographic bearing of the airplane must be determined accurately by some independent method for comparison with the radio-derived information. Second, the ability of the observer to read and estimate subdivisions of a particular dial should not be a limiting factor; the full accuracy inherent in the received signals should be exploited. Third, both the check readings and the radio bearings should be recorded automatically and simultaneously.

For the check readings, the bearing of the airplane during its orbital flights around the beacon was optically tracked by a theodolite at the ground beacon. A separate radio communication link was used to transmit the theodolite readings to the airplane to actuate a pen on the same recorder that showed the tacan bearing indications. The theodolite operator advanced the bearing setting by exactly 5 degrees, and then transmitted a marker pulse when the nose of the airplane was seen to cross the vertical cross-hair in the field of view. Hence the airborne recorder chart was marked at every exact increment of 5 degrees of bearing. For ease of interpretation, the marks were made to occur when the recording was near the center of the paper chart; this chart was driven by clockwork in the usual manner of pen recorders.

The conventionally used cockpit indicators for radio bearing, namely the *ID-307* (north-referenced radio bearing indicator) and the *ID-250* (airplane-axis referenced or "radio–magnetic indicator") have 360-degree dials calibrated in increments of 2 degrees. Hence these instruments do not permit sufficient reading accuracy, so a more-accurate indicator was used. Figure 2 is block diagram of this setup.

* Reprinted from *IRE Transactions on Aeronautical and Navigational Electronics*, volume ANE-3, pages 32–36; March, 1956. The photographs did not appear in the original publication.

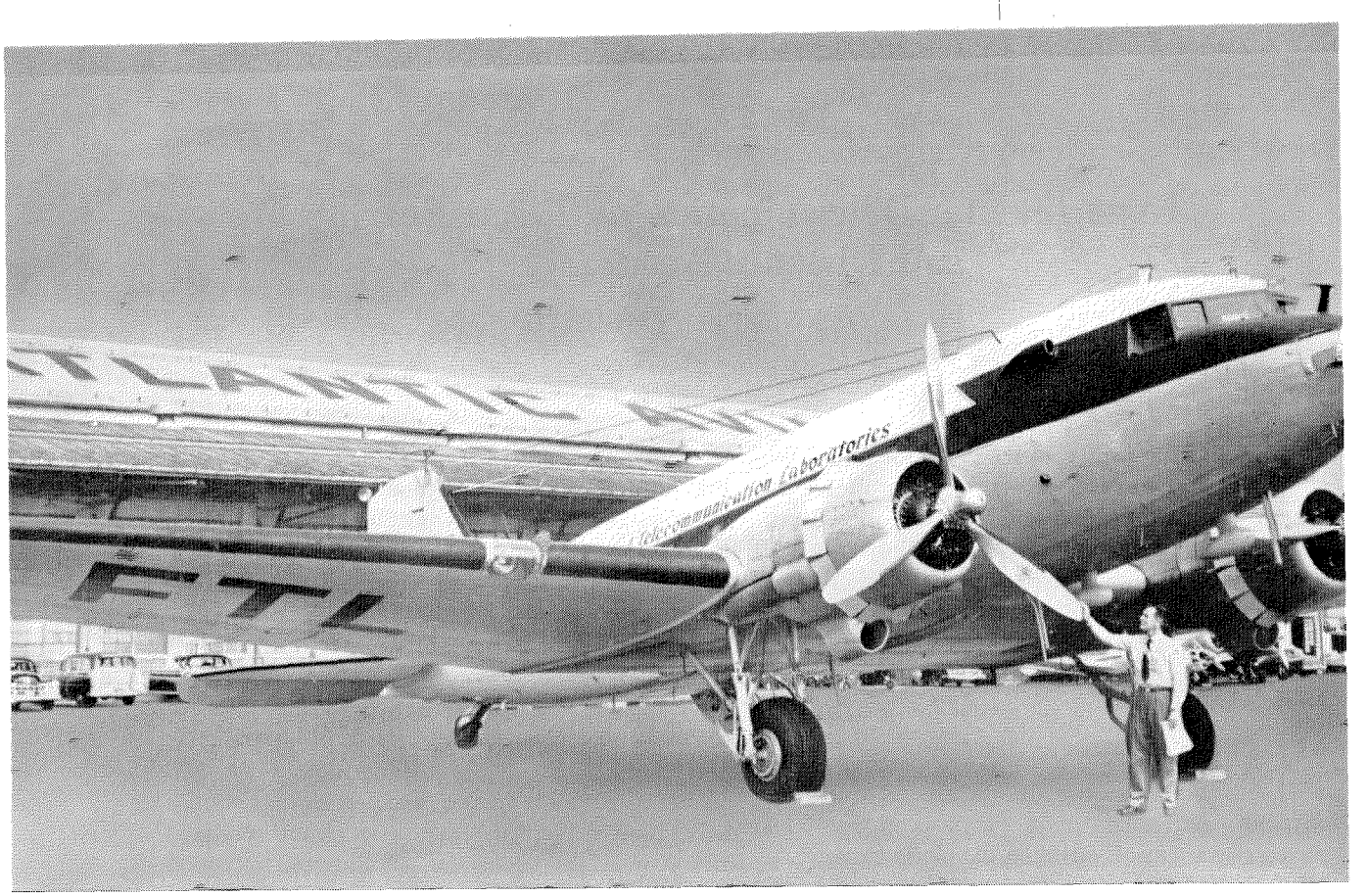

Figure 1—The *DC-3* "flying laboratory" used in tacan accuracy-determination flights.

A sensitive null-detection method of indicating and recording was built around the *ID-249*, which is a course-selector–deviation-indicator type of instrument. The deviations of the cross-pointer needle were recorded on the paper chart.

However, the null-detector coupler (instrument *CV-279* in the figure) was operated from the 9th harmonic shaft-resolver output of the *ID-307* instead of from the regular output, and from a fixed-phase resolver instead of from the bearing selector of the *ID-249*. The *CV-279* had its sensitivity set so that a variation of + 18 degrees of phase produced full-scale deviation of the crosspointer of the *ID-249*, and through the direct-current amplifier a deviation of ± 2 centimeters on the paper chart. This full-scale deviation produced by ± 18 electrical degrees corresponds to a geographical bearing deviation of ± 2 degrees. Thus, bearing indications can be read to within 0.1 degree with ease.

By the combination of 4 resolvers and an 8-position selector switch, the fixed-phase resolver provides 8 very-accurate reference phases, each evenly spaced every 45 degrees. Compared with the 9th harmonic output of the *ID-307*, an actual 5-degree geographical bearing increment is obtained. With this setup, a laboratory calibration run was first made on the *AN/ARN-21*, using the special test set (designated *AN/ARM-17*). A zero reading was set into the *ID-249* as well as the chart recorder; then the accurately calibrated dial of the *AN/ARM-17* was offset by ± 2 degrees in 0.2-degree increments, permitting accurate calibration of the *ID-249* and the paper recorder. Next, a full 360-degree calibration of the fixed-phase resolver was made in steps of 5 degrees. Then the complete equipment was installed in the airplane for the flight tests.

For normal navigational purposes, instruments such as the Veeder-type distance indicator, the cross-pointer meter, and the relative-bearing indicator (left to right in Figure 3) would give sufficient accuracy.

1.3 Flight Tests

The flight tests were made on September 14, 1954. The ground beacon consisted of an *AN/URN-3* installed in the tower at Nutley (Figure 4). A continuous paper-chart recording was made

in the aircraft during $2\frac{1}{2}$ orbits around the beacon at a 6-mile (11-kilometer) radius and at an altitude of 3000 feet (915 meters).

The chart writing speed was 12 inches (30 millimeters) per minute, with a deflection

equipment is entirely realistic and meaningful when performed on the equipment in the laboratory. The process relies solely on pulse timing, and propagation effects caused by reflections of radio energy do not produce any appreciable

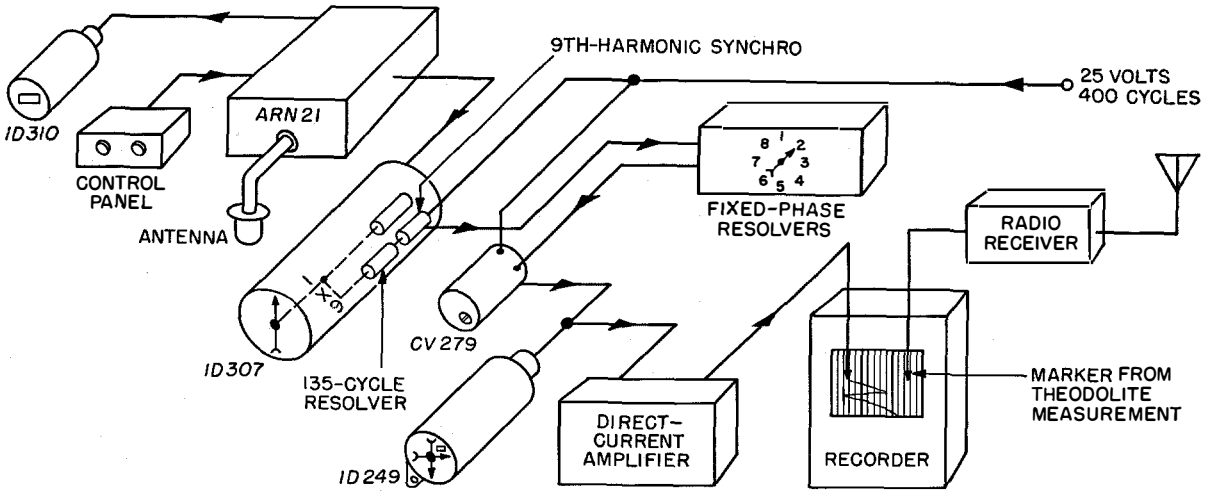

Figure 2—Airborne setup for evaluation of bearing accuracy.

sensitivity of about 0.5 inch (1.27 millimeters) per degree. The over-all time constant was under 1 second.

Analysis of the chart recording show no siting (propagational) or cyclical error. The only deviations from the mean appeared to be random and were different during the 2 orbits. Taking the actual recorded positions of the recording pen at the instants that the 5-degree theodolite marker pips were received, the distribution of errors is listed in Table 1.

TABLE 1

BEARING-SYSTEM ACCURACY

Deviation from Theodolite Bearing in Degrees	First Orbit		Second Orbit		Total	
	Points*	Percent	Points*	Percent	Points*	Percent
Above ± 0.2	5	8	4	6	9	7
± 0.1 to ± 0.2	13	21	8	12	21	16
Under ± 0.1	43	71	55	82	98	77

* Eleven points on the first orbit and 5 points on the second orbit were missed because of obstructions in visibility between the airplane and the theodolite station.

2. *Distance Accuracy*

2.1 General Considerations

In distinction to radio bearing, determination of the accuracy of radio distance-measuring

errors. The nature of the stroboscopic discrimination process that is used is such that sporadic false pulses due to almost any cause are rejected.

Another consideration that makes it actually *advisable* to determine distance accuracy in the laboratory is that flight tests would add considerable observational errors. These errors are due to the known fact that available maps cannot be relied on for sufficiently precise determination of distances between charted points, and that it is very difficult to fly over known landmarks with an accuracy appreciably better than a few hundred feet. The latter difficulty is compounded in practice because at extreme range from the beacon, around 200 nautical miles (371 kilometers) the airplane must fly at altitudes of 30 000 feet (9100 meters) or more to be in line-of-sight to the beacon.

To repeat, the accuracy of radio distance readings depends on the equipment and system parameters rather than on propagation disturbances. The equipment and system parameters that fundamentally limit distance-measurement accuracy are: accuracy of ground-beacon fixed delay, which is the delay between reception of an interrogation pulse and the

transmission of a response pulse; accuracy of airborne time-measuring circuits; reading accuracy of the airborne indicators; and the rise time of the pulses used in the system. These factors are next considered individually, and then the over-all effect is summarized.

2.2 Beacon Delay

The fixed or suppressed time delay of the ground beacon (which is calibrated out in the airborne indicator) is nominally 50 microseconds, with a tolerance of 0.4 microsecond. Present indications are that this tolerance is easily maintained in production equipments over the specified temperature range. Hence variations in this delay account for a possible error of ± 200 feet (61 meters) in the airborne distance indications.

Figure 3—In the pilot's compartment, the left meter gives distance and the center and right meters give bearing.

2.3 Pulse Rise Time

The radio-frequency channel spacing is 1 megacycle per second and requires a narrow transmitted spectrum for its pulses as well as narrow-bandwidth receivers. Interrogation and reply pulses are shaped so as to produce a radio-frequency spectrum that does not exceed 500 kilocycles. Such pulses have a rise time of about 2 microseconds.

The rise time of the pulses transmitted from ground to air is of little significance since under

normal operation these pulses are acted on by the airborne automatic-gain-control system so that they always have the same amplitude at the point at which their timing is measured. The rise time of these ground-to-air pulses, approximately 2 microseconds, is therefore not detrimental to range accuracy. In the opposite direction however, that is, air-to-ground, there is less opportunity to measure pulse timing at a constant pulse amplitude since the ground beacon will be receiving interrogation pulses from a number of airplanes at different distances. Theoretically, in a paired-pulse system such as is used in tacan, it is possible to devise a circuit in which the first pulse of the pair may set the gain for the following pulse. Such circuitry, however, has not yet been fully exploited in the *AN/URN-3*. A detailed study of such possibilities has been made but there are no immediate plans to improve operation in this respect. With the present equipment, an air-to-ground pulse rise time of 2 microseconds may contribute an error of ± 300 feet (91 meters) in distance measurement. (It should be possible, of course, to make the delay such that the accuracy is best with strong signals; the weaker signals would then be subject to an error from this cause of up to ± 600 feet (183 meters).)

2.4 Distance Indicator

The accuracy of reading the presently used distance indicator, the *ID-310* meter, is of the order of 0.1 mile (185 meters). This error is largely the result of using a Veeder counter type of display with rather small drums. The smallest divisions of the drum represent 0.25 mile (467 meters), but this apparent inaccuracy is not considered significant because fractions of a division may be estimated. This limitation is well compensated for by the lack of danger of ambiguity provided by the number-display type of indicator compared with two-scale dial indicators or their equivalent.

2.5 Airborne Ranging Circuits

Since 1949, all airborne distance-measuring sets built by the Laboratories have employed ranging circuits constituting a fine–coarse system. The fine system uses a timing reference sine wave of accurately maintained frequency, whose phase is shifted accurately by a resolver. The coarse system is used to eliminate ambiguity; it employs a potentiometer-controlled phantastron circuit to generate the required coarse time delays.

In the original 100-nautical-mile (185-kilometer) models of distance-measurement sets and tacan, use was made of a resolver that effectively generated 10 miles (19 kilometers) (in terms of time delay) per revolution. The accompanying phantastron accuracy therefore had to be better than ± 5 percent. In designing the 200-mile (371-kilometer) model of the present tacan system, there were two choices open. One was to retain the 10-mile-(19-kilometer-)per-revolution resolver and to use a phantastron circuit with ± 2.5-percent delay accuracy. The other was to employ a 20-mile-(37-kilometer-)per-revolution resolver with the phantastron delay accuracy retained at ± 5 percent. The latter choice was selected because it kept the phantastron circuit simple and involved no new risk in that direction. (The phantastron circuit had never been known to fail to perform with the specified accuracy.) This choice, however, resulted in doubling the requirement on accuracy for the fine or resolver system.

The voltage divider that controls the phantastron circuit has a linearity of 0.15 percent; therefore nearly all of the ± 5 percent tolerance is available for circuit tolerances. As far as has been determined, none of these circuits has ever failed to select the correct range sector. That being the case, the remainder of the ranging-circuit problem depends on the operation of the fine system.

The early distance-measuring sets constructed around 1949 for the United States Air Force, designated *AN/APN-34* (*XA-4* and *XA-5*), embodied what are probably the most-accurate automatic ranging circuits for distance measurement built to date. In an experimental evaluation of the type of ranging circuits used in these equipments conducted by the Civil Aeronautics Administration and covered in TDEC Report *212*, issued June 1953, it was stated that "The distance error is so small that it is difficult to measure accurately with present test equipment." In the *AN/APN-34* (*XA-4* and *XA-5*) equipments, space was not considered to be at the same premium as now considered. The

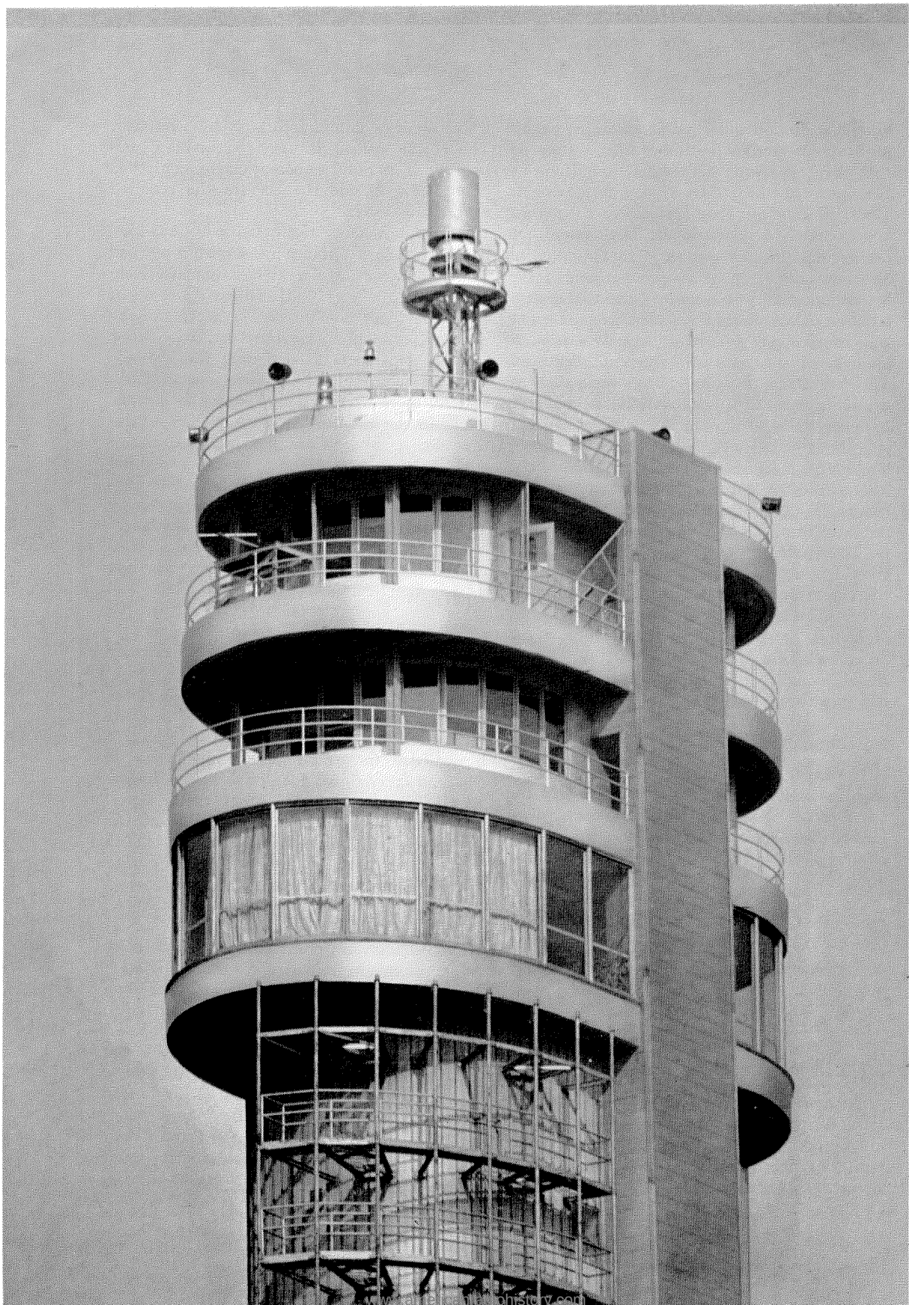

Figure 4—On the facing page, the ground beacon for the tests was mounted atop Federal Telecommunication Laboratories' microwave radio research tower.

distance-indicator dial was larger and the meter needle was driven directly by the servo. The resolver produced only 10-miles (19-kilometers) delay per revolution. The 8-kilocycle sine wave used as the timing reference was produced by a circuit that contained an oscillator coil that occupied 4 cubic inches (66 cubic centimeters) of space, thus permitting a very good Q value and a resultant large pure sine-wave output. All these features contributed to the extremely good ranging accuracy of these models.

The *AN/ARN-21* requirements were such that certain of the above features had to be compromised. These compromises are not inherent to the system but only to the specifications regarding range, space, and type of display that had to be met by the present models. For example, the Veeder counter indicator in comparison with a pointer-and-dial indicator has inevitable backlash; the last drum of the counter has only half the linear extent of the dial indicator of the *AN/APN-34;* the resolver in the *AN/ARN-21* is smaller and must produce 20 rather than 10 miles (37 rather than 19 kilometers) of delay per revolution.

However, in going to the *AN/ARN-21*, a number of partially compensating improvements are incorporated in the fine-ranging circuits. As one instance, the timing sine wave, which has a 4-kilocycle frequency rather than the earlier 8-kilocycle frequency used in the 100-mile (185-kilometer) system, is produced by a crystal-controlled oscillator. This improvement almost completely eliminates the frequency-drift problem. Second, even through the resolver used in the *AN/ARN-21* is smaller, it is of a new type and in conjunction with a new circuit has reduced the harmonic content of the timing wave to less than 2 percent. As a result, the ranging circuit in the *AN/ARN-21* produces an accuracy of ± 100 feet (31 meters) up to 10 miles (19 kilometers) and ± 300 feet (91 meters) for distances greater than 10 miles.

2.6 Over-All Distance-Measurement Accuracy

The situation as regards over-all tacan distance-measurement accuracy is summarized in Table 2.

TABLE 2

Distance-Measurement Accuracy

Source of Error	Plus-or-Minus Error	
	in Feet	in Meters
AN/URN-3 Transpondor Delay	200	61
Pulse Rise Time, *AN/URN-3* Receiver	300	91
Indicator Reading, *ID-310*	600	183
Thyratron and Delay-Line Drift	300	91
Airborne Ranging Circuits		
Close-in	100	19
Beyond 10 miles (19 kilometers)	300	91

These listed errors will generally not add arithmetically. From the statistical point of view, the root-mean-square value is significant and based on the errors given in Table 2 varies from 760 to 820 feet (232 to 250 meters) depending on the range. Experimental observations have shown that the over-all system error has not exceeded ± 700 feet (213 meters) for strong signals and ± 1000 feet (305 meters) for very-weak signals. These observations substantiate the present nominal specification for accuracy, which is ±600 feet (183 meters) plus 0.2 percent of the distance measured.

THE tacan development is based on three principal concepts: the provision of multiple services for air navigation and traffic control through coordinated system planning, provision for expansion of services by clear-channel operation of the radio transmissions, and high accuracy and freedom from site effects through use of a multilobe directional pattern. These three concepts must be understood if the tacan development is to have meaning, for they answer the often-asked question of "Why tacan?" They are discussed in the three papers that follow.

Coordinated-System Concept of Air Navigation

By PETER C. SANDRETTO

Federal Telecommunication Laboratories, a division of International Telephone and Telegraph Corporation; Nutley, New Jersey

ELECTRONICALLY, the most-important discovery of the second world war was not the one associated with the development of any single device such as antisurface-vessel radar, gun-laying radar, ground control of interception, et cetera. It is believed, rather, to have been the appreciation of the tremendous versatility of the vacuum tube. With this discovery, designers began to produce equipments performing feats that were never dreamed of before the war. To utilize this flexibility, however, the new devices have had to employ not a few, but a large number of, electron tubes. This increase in the number of vacuum tubes is particularly noticeable in airborne equipment. Before the war, an entire airborne installation employed but a handful of tubes, whereas, after the war, many airborne equipments placed in use and planned for the future utilize more than 100 tubes. Inexorably linked with the increase in the number of vacuum tubes is the law of the increase in the probability of failure of the equipment. This relation between the number of vacuum tubes in an equipment and the probability that the equipment will fail during a 10-hour flight is shown on

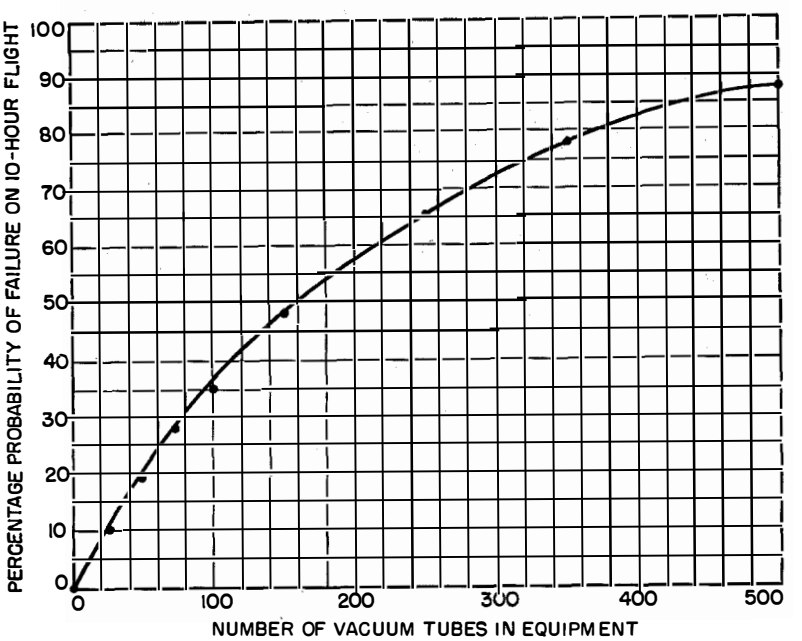

Figure 1—Probability of failure as a function of the number of vacuum tubes in equipment carried on a 10-hour flight.

Figure 1. This curve was plotted from the expression.[1]

$$P = 100[1 - \exp(3nt/2L)], \qquad (1)$$

where

P = probability of failure
n = number of tubes
t = time of mission in hours
L = mean life of tubes in hours.

The probability of failure is for a large number of samples and the mean life of the tubes in the environment in which they operate was taken as 3500 hours for the data plotted in Figure 1.

Figure 1 indicates that there is a limit to the number of tubes that can be carried aboard an aircraft without unduly jeopardizing the success of a mission. To increase the number of tubes that can be employed successfully, considerable effort has been expended in tube-reliability programs to increase the value of L. While such effort is certainly worthwhile, Figure 2 shows that this procedure does not necessarily constitute a complete solution.[1] An improvement in tube life of as much as 10 fold would not reduce the probability of failure of a 250-tube equipment to the point where it would be negligible; that is, where the probability of failure would be less than 10 percent.

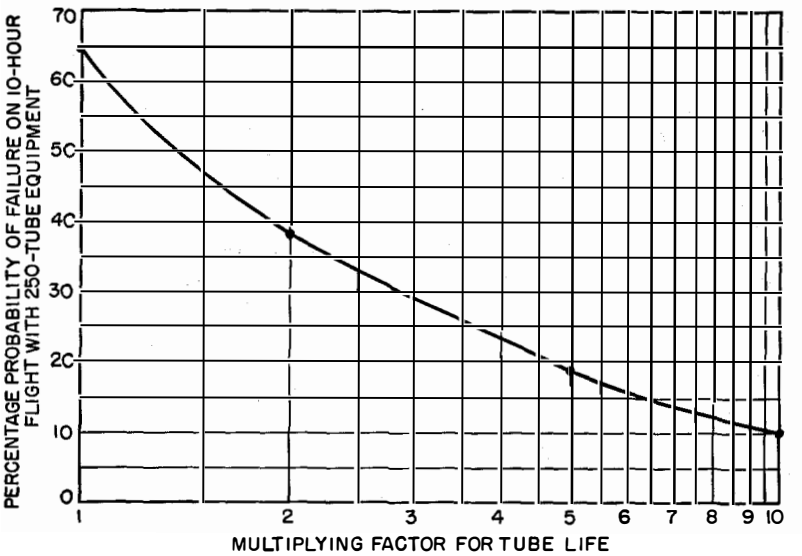

Figure 2—Probability of failure as the mean life of the vacuum tubes is increased by the multiplying factors of the abscissas.

For some time it has been considered (at least in the United States) that the airborne air-navigation and traffic-control equipment should provide the following services.

A. Distance measuring.

B. Identity and altitude (via a beacon).

C. Bearing indication.

D. Localizer indication.

E. Glide-slope indication.

F. Marker indication.

As the foregoing services are examined, it is noted that the distance-measuring service is provided by means of two radio-frequency channels, each lying in the 960–1215-megacycle-per-second band, and that a receiver provides a ground-to-air service on one channel while a transmitter provides air-to-ground service on another of these channels. Similarly, the beacon also has a transmitter and a receiver operating on two radio-frequency channels in 960–1215-megacycle band. The bearing service has been provided by a radio receiver operating on a single channel

TABLE 1

NUMBER OF TUBES AND FAILURE PROBABILITY

Service	Number of Tubes	Probability Percent of Failure
Distance Measuring	51	19.5
Beacon	40	18.0
Very-High-Frequency Omnidirectional Range	23	9.0
Localizer	15	5.5
Glide Slope	15	5.5
Marker	7	3.0
Total	151	48.0

[1] Research and Development Board Committee on Electronics, "Report on the Reliability of Electronic Equipment," volumes 1 and 2; February 18, 1952.

in the 112–118-megacycle band. The localizer service has been provided by a receiver operating in the 108–112-megacycle band. The glide-slope indication has been furnished by a receiver operating on one channel in the 325–339-megacycle band and the marker service by a receiver operating in the 75-megacycle band. It is thus seen that the conventional system utilizes no fewer than 2 transmitters and 6 receivers, each operating on a different radio-frequency channel at any one time. Of course, as stations at different locations are selected, different frequencies are employed in the respective bands mentioned, but some of the services would have to be deleted if 8 different radio-frequency channels were not available in about as many different bands.

Associated with each receiver and each transmitter are a series of circuits that may be described as translators. They are called translators because they translate the radio-frequency undulations into indications readily appreciated by the human senses or, conversely, translate information into radio-frequency undulations. The total number of tubes that might be employed with these equipments (as diagrammed in Figure 3), together with the probability of failure on a 10-hour mission, is shown in Table 1.

The foregoing information indicates that there is less than a good gambler's chance (50–50) that the complete system will be in operation when an aircraft carrying it reaches the terminal at the end of a 10-hour mission. The development of information theory since the end of the war provides a clue to one solution to the problem of increased reliability in air-navigation–traffic-control systems. The application of information theory forms the basis of the *coordinated-system concept.*

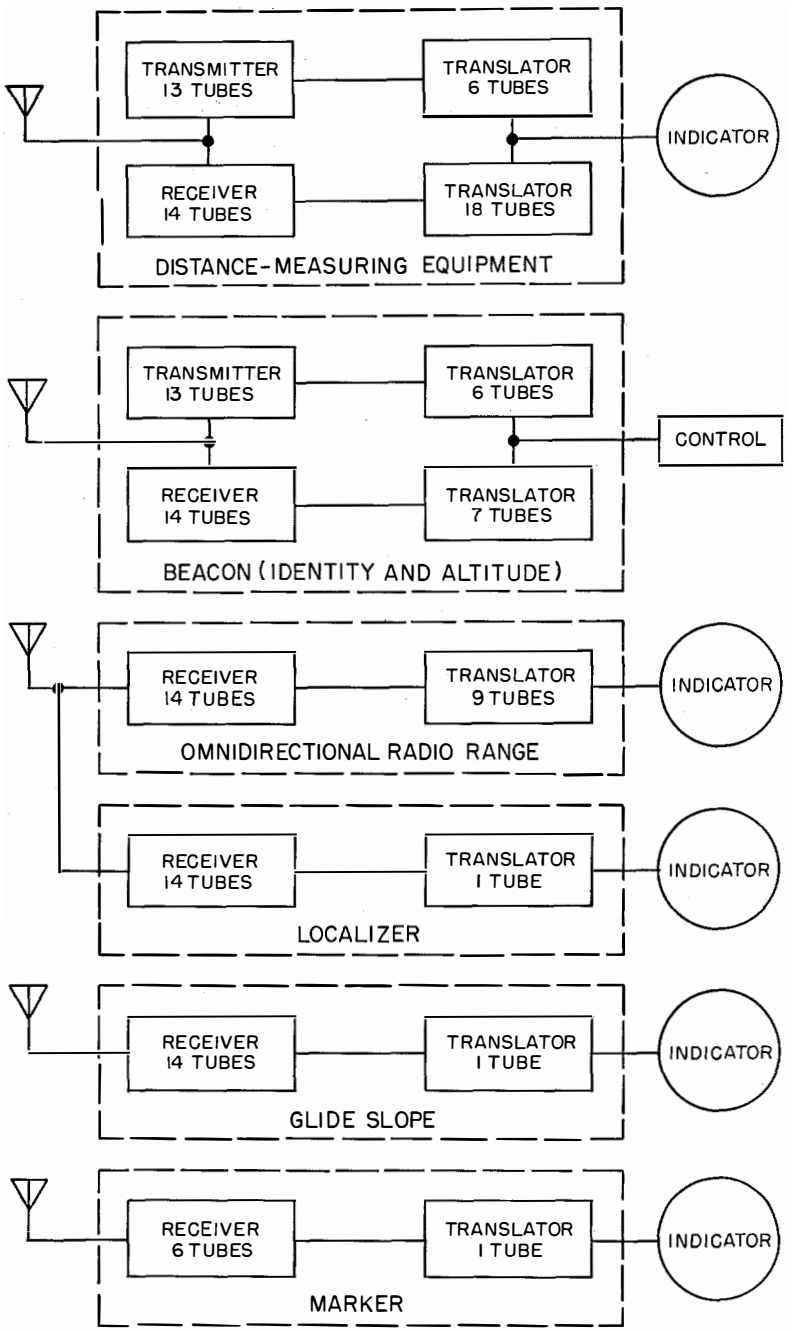

Figure 3—Conventional airborne installation utilizing 2 transmitters and 6 receivers.

It has been shown[2,3] that the total amount of information required by air-navigation–traffic-control systems is relatively small. Expressed in binary digits, the requirement for the services previously enumerated is shown in Table 2.

TABLE 2

SERVICE INFORMATION REQUIREMENTS

Service	Information Content in Binary Digits
Distance Measuring	3000
Identity and Altitude	2000
Bearing Indication	720
Localizer	306
Glide Slope	306
Marker	50
Total	6382

From the above, it is seen that 6382 binary digits of information are sufficient to take care of the requirements of the air-navigation–traffic-control system. Shannon and others[4–6] have developed the following equation for the information capacity of a radio-frequency channel.

$$C = W \log \frac{P + N}{2N}, \qquad (2)$$

where

C = information capacity in binary digits
W = channel width in cycles
N = noise power
P = signal power.

The signal and noise powers are expressed in the same units.

For a channel 1-megacycle wide and signal power twice that of the noise power, the channel capacity is 1.59×10^6 binary digits (bits). It is thus seen that the capacity of a single radio-frequency channel exceeds the total requirement for the air-navigation–traffic-control system by about 250 times. Why, then, carry radio receiving and transmitting apparatus for 8 radio-frequency channels?

In a properly designed system, there is no reason why the various translators (employing no more tubes) cannot extract the information from one radio-frequency channel as well as from several. For example, the translator in the marker receiver could separate from the radio-frequency channel signals of 400, 1300, and 3000 cycles. The localizer separates out 90 and 150 cycles. If the marker translators were connected to the output of the localizer receiver, it is evident that they could perform the same task as previously although, of course, some special arrangements would be required in the ground transmitting equipment.

A hypothetical coordinated system is shown in Figure 4. This figure shows no difference in the number of tubes used in the individual radio-frequency transmitting or the radio-frequency receiving equipment. There is no change in the number of tubes in the translators, and this condition would be substantially true *if these circuits were not required to provide a higher-grade service than previously.* The total number of tubes in the system, however, has been reduced from 151 to only 76. Therefore, the probability of system failure has been reduced from 48 percent to only 28 percent for a 10-hour mission. An aircraft with a coordinated system would, therefore, arrive at its destination with a much-greater probability that all of its equipment would be functioning than with the conventional system. However, through the use of the coordinated system, about half the number of tubes (together with their associated apparatus and space that they occupy) have been saved. Utilizing these tubes and components, two complete coordinated systems can now be had for the space, weight, and circuit complexity of the previous single conventional system. With two systems employed, the probability of failure is the product of the individual system probabilities or about 7.8 percent. Thus, the probability of failure of the complex air-navigation–traffic-control system has been reduced to substantially that of the simple marker receiver.

[2] H. Busignies and M. Dishal: "Some Relations Between Speed of Indication, Bandwidth, and Signal-to-Random-Noise Ratio in Radio Navigation and Direction Finding," *Proceedings of the IRE*, volume 37, pages 478–488; May, 1949: page 479. Also *Electrical Communication*, volume 26, pages 228–242; September, 1949: page 230.

[3] Radio Technical Commission for Aeronautics, Special Committee 40, "DME System Characteristics (Transition Period)": paper 121–48/DO–24; December 15, 1948: page 19.

[4] C. E. Shannon, "Mathematical Theory of Communications," *Bell System Technical Journal*, volume 28, pages 379–423, July, 1948.

[5] C. E. Shannon, "Recent Developments in Communications Theory," *Electronics*, volume 99, pages 80–83; April, 1950.

[6] W. G. Tuller, "Theoretical Limitations on the Rate of Transmission of Information," *Proceedings of the IRE*, volume 37, pages 468–478; May, 1949.

The advantages of the coordinated system are many, and some of these are as follows:

A. Radio frequencies, which are recognized as a national commodity and may soon be in short supply, are saved by a very large factor.

B. The inefficient carrying of many equipments for hours when they actually perform duties for only a few minutes during an entire mission is stopped. Each tube is made to perform a useful service during most of the duration of the mission.

C. The total number of equipments that it is necessary to carry to perform the air-navigation–traffic-control function may be reduced to one.

D. The number of airborne antennas required is reduced to one.

E. The types of spare parts required to be carried in stock are greatly reduced.

F. The training of service personnel is simplified since it is only necessary to train them on one equipment.

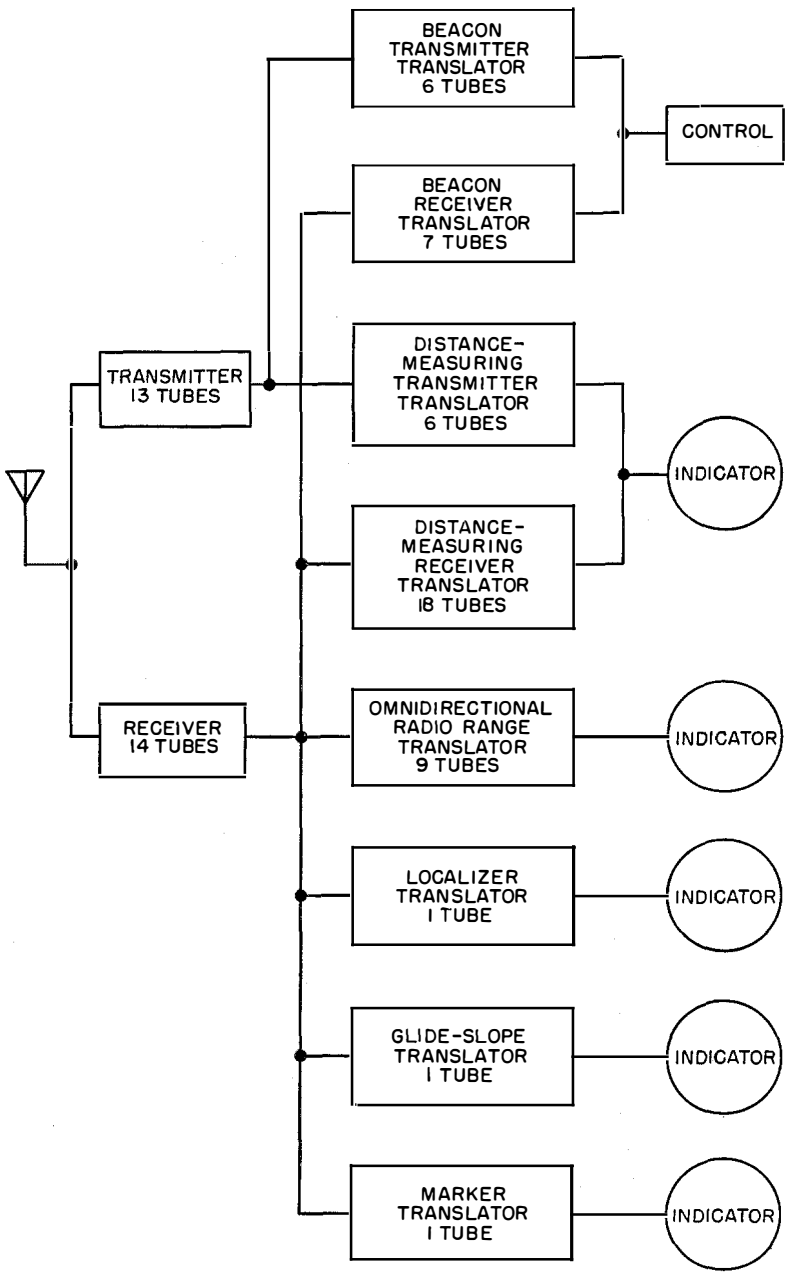

Figure 4—Coordinated airborne installation consisting of only 1 transmitter, 1 receiver, and 8 translators.

It is to the concept of the coordinated system that the tacan system was designed. It was the coordinated system that brought about the agreement in Committee *SC-31* of the Radio Technical Commission for Aeronautics. Following[7] is a quotation from page 15 of the report of that committee.

"b. The Navigation Equipment is a transmitter–receiver having multiple channels. This equipment with associated ground equipment:

"(1) Provides distance and bearing information for navigation. These data, when used in conjunction with a computer, will allow the pilot to fly any desired course.

[7] Radio Technical Commission for Aeronautics, Special Committee 31, "Air Traffic Control," paper 27–48/DO–12; May 12, 1948: page 15.

"(2) Provides precise slope, localizer, and distance information for instrument approaches.

"(3) Provides information for airport surface navigation to enable the pilot to taxi his aircraft.

"(4) Provides air–ground aural communication of a reliable and static-free type.

"(5) Provides a situation display in pictorial form which enables the pilot to monitor traffic conditions in his vicinity or receive other pertinent data such as holding areas, airlane locations, and weather maps from the ground.

"(6) Provides suitable output to allow the aircraft to be automatically flown, either enroute or during final approach and landing."

The system is further described[8] on page 34 as follows.

"The airborne navigation equipment and its directly associated ground elements are wholly contained in the 960–1215-megacycle band. The azimuth, landing, voice, situation display, and airport surface navigation functions will be multiplexed with the ground-to-air function of the DME."

From other papers, it will be seen that the tacan system in its present embodiment does not fulfill all of the functions of the coordinated system specified by *SC-31*. It has, however, been so designed that nothing precludes the later additions of these functions.

[8] Page 34 of reference 7.

Quartz-Crystal Control at 1000 Megacycles

By SVEN H. DODINGTON

Federal Telecommunication Laboratories, a division of International Telephone and Telegraph Corporation; Nutley, New Jersey

TOWARDS the end of the second world war, it became evident that the problems created by a greatly expanded air traffic would soon make necessary some entirely new pieces of navigational equipment; at the same time, it appeared that our wartime advances in electronics would give us the tools with which to create such apparatus.

The history of radio navigation for aircraft had involved the addition of another "black box" each time a new facility was needed, in time leading to the carrying in each aircraft of a large number of such boxes, many of the circuits of which duplicated each other. It was therefore the desire of all parties that in planning the postwar system an earnest attempt be made to choose the basic parameters in such a way that an integrated system could eventually be possible. Specifically, it was necessary that the new system provide a large number of channels and that each channel have a fundamentally high information-carrying capacity. It was generally agreed that the band from 960 to 1215 megacycles per second offered the best opportunities; it was large enough for the expected needs, yet it was low enough in frequency to permit the use of triodes.

Special Committee *31* of the Radio Technical Commission for Aeronautics was established to review the over-all requirements of an integrated system, but long before this committee concluded its deliberations it was apparent that distance-measuring equipment would be an important feature of such a system and that active development of this facility should therefore commence.

Distance measurement is an extension of the familiar interrogator-responsor principle, whereby an airborne meter indicates the elapsed time between transmission of an interrogating pulse and the receipt of a reply pulse from a transpondor situated at a known location.

Several companies started such developments in the summer of 1945; the approach to the problem by Federal Telecommunication Laboratories was unique in being built around the use of crystal control of frequency. This was considered to be essential because the distance-measuring equipment would form part of a proposed integrated system in which all channelling was to be done by frequency selection, while separation of functions on each channel was to be done by pulse coding. The reasons for this choice are complex and can be summarized only briefly here.

A. Channelling by frequency control is a well-established technique that is in universal use throughout the radio spectrum. There is no theoretical limit to the amount by which an unwanted channel can be rejected.

B. Channelling by pulse coding, on the other hand, is not so well established. Moreover, there are definite theoretical and practical limits to its application; chief of these are echoes, which make strong unwanted pulses take up more time than necessary, and nonsynchronous operation that results in "bunching" or the generation of false codes.

C. Pulse coding for separation of functions within one channel, however, is a clean-cut procedure. Since all pulses are the same amplitude, the echo problem vanishes. Moreover, synchronous multiplex may now be employed, thus avoiding "bunching."

This proposal aroused sufficient Air Force interest for a development contract to be awarded in April 1946 for a distance-measuring equipment embodying 51 two-way channels spaced 2.5 megacycles apart. This was the *AN/APN-34* (*XA-3* to *5*) with corresponding ground equipment *AN/GPN-4* (*XA-3* to *5*).

There were, of course, two major problems to be solved in this equipment: development of the radio-frequency system and development of the ranging system. Both these developments were subsequently to form major building blocks for tacan as shown in Table 1.

TABLE 1

CHRONOLOGICAL DEVELOPMENT OF RADIO-FREQUENCY, RANGING, AND BEARING CIRCUITS

Year	Radio Frequency	Ranging	Bearing
1945	Federal proposed crystal control		
1946	Air Force *APN-34/GPN-4*; 51 channels of 2.5-megacycle spacing	Air Force *AN/APN-34*	
1947	6-channel (*XA-3*) preliminary models delivered	Delivery of (*XA-3*) electronic voltmeter display	
1948	51-channel model (*XA-4*) delivered	2-speed (*XA-4*) electromechanical, with rate	Navy *AN/ARN-16/URN-1* 3-lobe, 30 and 90 cycles
	Navy *AN/ARN-16/URN-1* adopted same channelling system		Air Force modified *AN/APN-34/GPN-4* 9-lobe, both 30 cycles
1949	Navy *AN/ARN-21/URN-3* (*XN-1*) used same channelling system	Navy *AN/ARN-21* (*XN-1*) used same range system, omitted rate	Navy *AN/ARN-21/URN-3* (*XN-1*) used *AN/ARN-16/URN-1* bearing system
1950	During summer, *AN/APN-34* and *AN/ARN-16* combined in breadboard form to demonstrate capabilities of *AN/ARN-21*. Tacan named		
1951	*AN/ARN-21/URN-3* (*XN-1*) tested by Navy in March		
	Navy *AN/ARN-21/URN-3* (*XN-2*) reduced channel spacing to 1 megacycle, provided 126 channels	Navy *AN/ARN-21* (*XN-2*) added number display	Navy *AN/ARN-21/URN-3* (*XN-2*) 9 lobes, 15 and 135 cycles
1952	First (*XN-2*) delivered (September)		
1953	Limited production commenced, ground and air (December)		
1954	Extensive evaluation programs		
1955	Full production		

The ranging system developed for the *AN/APN-34* (*XA-4* and *5*) has been retained in tacan and is covered in a companion paper.[1] The objective of this paper is to cover the radio-frequency problems.

The 255 megacycles between 960 and 1215 megacycles were divided into two equal bands; 960 to 1087 for air-to-ground interrogation and 1087 to 1215 for ground-to-air reply, with a fixed spacing of 126 megacycles between the interrogation and reply frequencies.

At the outset of the development, it was apparent that distance measurement would require sensitive superheterodyne receivers in both the airborne interrogator and in the ground transpondor. Also, that the airborne interrogator would require a transmitter power of about 1 kilowatt and that the ground transpondor, because of lower airborne receiver sensitivity due to multichannel operation, would require a transmitter power of 5 kilowatts. It quickly was established that the necessary crystal control of the receivers was readily obtainable using miniature tubes in a 4-stage frequency multiplier that would bring the output of a 40-megacycle crystal oscillator up to a frequency suitable for injection into the mixer of the receiver. Moreover, by proper choice of multiplying factors, it was found that this multiplier could be broadbanded so that the only airborne elements to be moved mechanically were the turret mounting 51 crystals and the preselector. In the ground equipment, of course, the problem was even easier since only a fixed frequency was involved. Thus, direct crystal control of 1000-megacycle receivers became a reality in 1947 when the first 6-channel equipments were delivered. In the following year, delivery was made of equipments tuning over the full 125-megacycle range, providing 51 operating channels with 2.5 megacycle spacing.

[1] S. H. Dodington, "Airborne Tacan Equipment AN/ARN-21," *Electrical Communication*, volume 33, pages 60–64; March, 1956.

The transmitter problem was an entirely different matter, however. About one milliwatt of 1000-megacycle energy sufficed for the receiver; bringing this crystal-controlled power to one kilowatt would require an amplifier having 60 decibels of gain at 1000 megacycles. Obviously, it would require many stages, all of which would have to be ganged and tracked. Alternatively, a higher-power frequency multiplier requiring less 1000-megacycle amplification might be used. Some experiments were made along the latter lines, but the results in 1946 were quite discouraging and it was not until the summer of 1950 that success was achieved. In the meantime, we decided to proceed with the *AN/APN-34* and *AN/GPN-4* using pulsed oscillators for the transmitters. These oscillators were motor-tuned under control of the receiver local-oscillator frequency and therefore constituted automatic frequency control based on a reference crystal. This system was gradually refined and used in a number of other equipments such as the *DIA* and *DTA* apparatus for the Civil Aeronautics Administration, the *AN/APN-72* and *AN/GPN-5* for the Air Force, and the *AN/ARN-21* (*XN-1*), *AN/URN-1*, and *AN/URN-3* (*XN-1*) for the Navy. A fuller description was published[2] several years ago.

The automatic frequency control of pulsed transmitters, however, has its limitations. At best, it cannot do more than control the frequency of each pulse in accordance with frequency deviation of the previous pulse. Furthermore, it introduces additional inaccuracies that stem from errors in the frequency discriminator and the characteristics of the feedback system. It did not, therefore, appear to commend itself to systems requiring channel spacing closer than 2 megacycles at these frequencies, even though this system was successfully used in the *AN/APN-72*, which employed this spacing.

As early as 1948, there had been a demand in some quarters for more than 51 channels (largely due to improper channeling assignments), but no means of implementing this appeared at hand. However, in 1950 the means finally became available. In May of that year, the communication and navigation laboratory at Wright Field demonstrated a 4-stage pencil-triode 1000-megacycle amplifier with an output of 1 kilowatt and a gain of 30 decibels. In June, Federal demonstrated a 3-stage 1000-megacycle amplifier using *2C39* tubes and having a gain of 50 decibels with an output up to several kilowatts. Direct crystal control of airborne transmitters had at last become a possibility.

For ground equipments operating at a fixed frequency, another significant development had occurred. This was the development by the Sperry Gyroscope Company of the *SAL-39* klystron amplifier, providing in one tube a gain of some 30 decibels and a power output of many kilowatts at high duty cycle.

Thus, in the summer of 1950, we were able to start planning a system using channel spacing closer than 2 megacycles.

In 1947, Federal had proposed to the Navy and to the Air Force that existing omnidirectional-range accuracies could be greatly improved and siting problems reduced by the use of the multilobe principle. This resulted in 1948 in the award of contracts for a Navy 3-lobe system and for an Air Force 9-lobe system. Both of these used the 2.5-megacycle channelling system of the *AN/APN-34*. In 1949, the Navy decided to combine their 3-lobe system with the distance-measuring equipment of the *AN/APN-34*, thus providing a single airborne box generating both distance and bearing information. This was the *AN/ARN-21* (*XN-1*) and it continued to use the *AN/APN-34* channeling arrangement. The corresponding ground equipment was the *AN/URN-3* (*XN-1*).

With the possibility now arising of an increase in the number of channels, together with the growing recognition of the potential merits of the multilobe bearing design, it was time for a review of the whole program. This took place in October 1950 at a series of meetings attended by the Navy, Air Force, and Federal. It was decided that tacan (as the *AN/ARN-21/URN-3* now had been named) would be redesigned to provide 1-megacycle channel spacing to give 126 clear channels and that the number of lobes in the bearing system would be increased to 9, but retaining the same general principles as the Navy's 3-lobe system and the distance-measuring principles of the *AN/APN-34*. Specifications

[2] S. H. Dodington, "Crystal Control at 1000 Megacycles for Aerial Navigation," *Electrical Communication*, volume 26, pages 272–278; December, 1949.

reflecting these changes were published in the spring of 1951.

In all Federal's airborne designs, it had been the practice wherever possible to use the transmitter frequency as the receiver local-oscillator frequency; this saved considerable circuitry and was obviously desirable in the new tacan airborne equipment. The previous division of the 960-to-1215-megacycle band into a single receiving and a single transmitting band was now, however, not so desirable, since such a solution would have automatically involved use of a receiver intermediate frequency of 126 megacycles. With automatic-frequency-controlled transmitters, any convenient intermediate frequency could be used provided the automatic-frequency-control discriminator had a complementary value, the two totalling 126 megacycles. An intermediate frequency of 126 megacycles was not thought to provide sufficient frequency stability without resort to a double superheterodyne and its noise factor was some 3 decibels poorer than the best obtainable at 63 megacycles. It was therefore decided to split the 960-to-1215-megacycle band into 4 equal portions, the two ends being used for ground-to-air transmission and the two middle bands for air-to-ground transmission; this allowed a 63-megacycle intermediate frequency without complexity. The major remaining problem was then the generation in the airborne equipment of adequate transmitter power on 126 channels between 1025 and 1150 megacycles.

Federal had hitherto been discouraged by the military services from considering crystal-saving schemes in this band, the feeling being that such schemes could well wait until over-all system performance had been established. Now, however, it was obvious that 126 separate crystals would occupy too much space. Some sort of saving must be practiced; this involved using fewer crystals and mixing their frequencies so as to obtain many more frequencies. The penalty is usually the generation of spurious frequencies.

In 1951, Federal built three different crystal-saving circuits before settling on the present one. First, a scheme was devised whereby one of a bank of 13 crystals was mixed with one of a bank of 10 crystals to provide up to 130 channels. Since the mixture contained many unfilterable spurious output frequencies, another "clean" oscillator was locked by automatic frequency control to the mixture. The output of this clean oscillator was then multiplied to the desired output frequency. The scheme was rejected partly because of complexity and partly because of the stigma associated with the use of automatic frequency control, whose abandonment had made the 1-megacycle spacing possible.

The second scheme employed 13 crystals mixed with 10 crystals, as above, but with greater attention to the reduction of spurious responses. This arrangement required that the two frequencies to be mixed have the highest possible ratio and thus the problem of filtering the mixture became severe. However, the high-order harmonics of the low-frequency oscillator were weak compared with the fundamental of the high-frequency oscillator, and unfilterable beats were thus also weak. This scheme was abandoned because of difficulty in tracking the necessary high-Q filters.

The third system is now in use. It divides the 1025-to-1150-megacycle band into 3 equal parts, each 42 megacycles wide. The middle band is provided by a conventional oscillator–multiplier using 42 crystals, while the end bands are provided by beating a fixed 42-megacycle crystal against the output of the multiplying chain. This system produces only weak spurious frequencies and requires no additional filters. It also uses more crystals than the other systems but not an intolerable number. It was adopted in September 1951 and a block diagram appears in Figure 1.

It will be seen that since the output of the oscillator–multiplier chain is only 42 megacycles wide, broadbanding can be employed for this chain without undue loss of gain. This greatly simplifies the mechanical problems of ganging and tracking. The only mechanically tracked stages are the mixing stage and the three final amplifier stages, all of which operate at the same frequency.

For the final transmitter amplifiers, it was decided to retain use of the *2C39*. This tube had been used in every Federal 1000-megacycle airborne transmitter built since 1946 and had amply demonstrated its performance and reliability. No other tube, even today, features such a combination of high mutual conductance, high emission, high voltage and altitude capability combined with ruggedness, and availability from

multiple sources of supply. Five of these tubes are used in the *AN/ARN-21*. The last three are cascaded amplifiers at the final frequency. While our 1950 experiment had shown a 50-decibel gain from three such stages, this was obtained with over 4000 volts on the anodes. The airborne tacan application limits us to 2500 volts because of altitude problems and, allowing for some mistracking, we must content ourselves with about 30 decibels for these three stages.

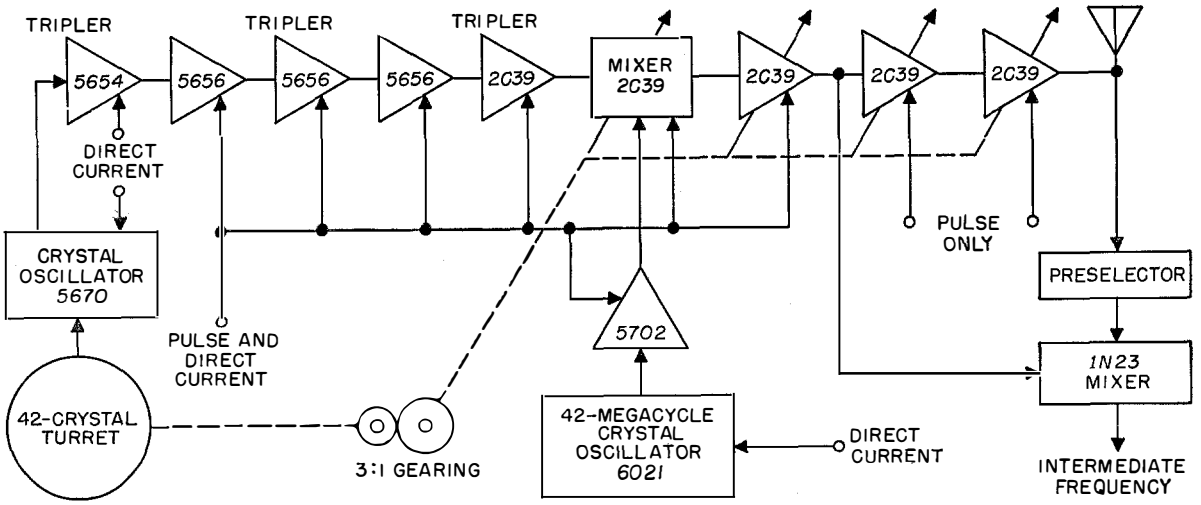

Figure 1—Arrangement for producing 126 channel frequencies with only 43 crystals.

Interference-free transmission and reception of pulses on channels spaced closer than the width of the pulse spectrum is only possible by use of the Ferris discriminator. This circuit, initially used by Federal in the *AN/APN-34* and *AN/GPN-4*, allows a wide-spectrum pulse to be received over only a narrow band. Pulses outside of this band are rejected and adjacent-channel interference is thereby wholly eliminated. The price paid, however, is that occasionally an adjacent-channel pulse will "knock out" a desired-channel pulse. This "hole punching" in the desired channel could eventually prevent full exploitation of the duty cycle available on each clear channel for future additional services. While the Ferris discriminator was retained in the tacan system, a step towards its eventual elimination was taken by changing the shape of the transmitted pulses from rectangular to a rounded shape of minimum bandwidth. This, of course, would not have been feasible with pulsed oscillators, but was made possible by the advent of direct crystal control. These rounded pulses do not rely so completely on Ferris discriminator action for their selection as do rectangular pulses.

The price of generating these pulses has so far been high, however. In the ground equipment, which uses a klystron final amplifier, the over-all efficiency of this final stage has been only some 5 percent due to the need of turning on the full beam current from start to finish of the shaped pulse. Fortunately, there are now becoming available new types of klystrons that will permit modulation of the beam current by the shaped pulse, thus permitting the full klystron efficiency of 25 to 40 percent to be realized.

Reduction in Ferris discriminator action coupled with the use of 3.5-microsecond pulses has permitted a substantial improvement in both ground and airborne receiver sensitivity. Thus, the same transmitter powers used in the *AN/APN-34* and *AN/GPN-4* allow a much-greater range to be achieved, and tacan is conservatively rated as a 200-nautical-mile (371-kilometer) system at line-of-sight altitudes.

In conclusion, it may be stated that crystal control has made available for tacan 126 clear channels, each providing distance service to 100 aircraft and bearing service to an unlimited number of aircraft. It has done this using a duty cycle per channel of only 2 percent thus leaving a vast information-handling capability for future exploitation of additional functions.

Error Reduction in Tacan Bearing-Indication Facility

By MARTIN MASONSON

Federal Telecommunication Laboratories, a division of International Telephone and Telegraph Corporation; Nutley, New Jersey

STUDIES are presented of the reduced error of estimating azimuth in the presence of interference, notably reflections, featured by the tacan omnirange 9th-harmonic function. The introduction of a 9th-harmonic variation is viewed as an encoding of the azimuthal data that, while redundant under conditions entirely free of error, provides 9 times the number of data at the receiving point compared with a 1st-harmonic system. When perturbed by reflections, the 9-cycle code is changed differently in each cycle. An average over the 9 phases defines the indicated azimuth less a multiple of 40 degrees. The 1st-harmonic code resolves which multiple to apply. The averaging technique employed is that of computing the phase angle of a 9th-harmonic variation that departs from the received data in the least-mean-square way. The motivation for this particular technique and for a harmonic encoding as well is the comparative simplicity of system instrumentation and automatic indication of azimuth.

This paper consists of three parts. In the first, the notion of encoding the azimuthal data is illustrated with two better-known systems, a pulsed and a 1st-harmonic encoding. The characteristics of the tacan system pertinent to this presentation are described. In the second part, the error-reduction character of the 9th harmonic is examined in some generality and illustrated in two specific cases. In the third, a small-reflection analysis is presented in detail. This analysis relates error in the estimation of azimuth to the geometry and reflectivity of a multiplicity of reflecting points. A numerical analysis of the case of a single reflector corroborates the applicability of the approximate analytical formulation.

• • •

1. Data Encoding

Radio-direction-giving facilities transmit electromagnetically data that identify the azimuth of propagation to the point at which the data are received. The specification of an azimuth, that is, of an angle, entails the transmission of two data: the position of the initial side of the angle and the number of degrees to the terminal side. At the very least, all facilities transmit this data "couplet." Systems differ by way of the electromagnetic representation or encoding assigned to this couplet, in the number of couplets transmitted per unit time, and in the processing of the received data.

A simple encoding of the couplet is a pair of pulses whose spacing is modulated proportionately to the azimuth of transmission. The physical embodiment here could be a nondirective pulsed reference radiation that identified the initial side of the azimuth angle plus a beam rotated uniformly through 360 degrees in the time between successive reference pulses to identify the terminal side. Were it not for the hazards of electromagnetic transmission, one such couplet received and recorded at a distant point would suffice to establish positive identification of the azimuth of propagation to that point by measurement of the pulse spacing. By transmission hazards is meant primarily noise and reflections. The measurement at the receiving point is of course committed to instrumental inaccuracy too. The error in measurement, if nondeterministic, may be regarded as noise. The repeated transmission or presentation of data to a receiver avoids the severe operational and practical problems of "capturing" a single couplet and provides many samples of the same couplet from which some kind of average estimate of the intended data can be formed.

Perhaps the most commonly employed encoding of a data couplet, certainly one of the earliest, is a pair of sine waveforms, each a cycle long, spaced or phased by an angle equal to the azimuth of transmission. The embodiment here can be a sine-wave-modulated nondirective reference radiation and a uniformly rotated cardioid. While repeated transmission of

couplets may merge the sine waveforms continuously, the intrinsic discreteness of the transmitted data, cycle for cycle, should not be overlooked. There are numerous practical reasons for this encoding. For one, it is possible that the radio-frequency assignment in combination with other factors does not afford much latitude in design of radiating structures. From the standpoint of processing the data received, this encoding might be selected because it lends itself naturally and simply to automatic measurement of data and indication of the azimuth estimated. In fact, it is not uncommon to measure spacing between pulse pairs, as in the first encoding illustrated, in terms of the phase shifts in the harmonics of the pulse-train just in the interest of simplifying the instrumentation.

In the past, the encoding of the azimuthal data has largely been influenced by system-component limitations. Transmission hazards have been met more in terms of transmitting the same signals at greater power, by more repetitions of the data per unit time, or simply by attempting to escape them by changing space, time, and frequency of operation. With regard to reflections, neither increased power nor faster time repetition offers improvement. The reflected power received varies proportionally with the transmitted power level. As to faster repetitions of the same data, in any given configuration of transmitter, reflectors, and receiver, the reflecting sources merely contribute the same reflections at the faster rate. The potential efficacy of averaging cannot be realized here. Something more than just increased power and speed of transmission is demanded. For the same increase in bandwidth required of a faster repetition rate, one possibility would be to transmit data at the slower speed but in frequency diversity. In this way, there is provided an increased number of independent samples of the real data in the presence of reflections. The added complication in terminal equipment is apparent though. Directivity, essentially a pulsed encoding of the azimuthal data (which may be viewed as a "smear" of frequencies in diversity), offers improvements only when the desired signal can be resolved from the pulsed ghosts. Even assuming well-separated signal and ghosts, such discrimination is not easy to obtain by instrument and for this reason is often left to visual observation —in opposition to the current trend toward wholly automatic indication. Increased power is usually effective against noise, except perhaps for large impulsive disturbances for which other protection must be sought. An increased rate of data repetition is usually also effective, provided that the noise introduced into the system with the additional data does not increase inordinately with the wider acceptance bands.

After a period of years of study and experimentation with systems involving such factors, Federal Telecommunication Laboratories concluded that an optimum solution for an omnidirectional-bearing facility lay in the harmonic encoding or multilobed pattern of radiation employed in the tacan system. The antenna array in Figure 1, which was successfully flight-tested in 1948, is evidence of early work on this type of system. There are of course many schemes for encoding the azimuthal data. Whether a scheme is in general *the* optimum has no single answer, unless it were to result in absolutely no error under all conditions—and even then it might be extravagant. By optimum is meant a systematic technique that uses radiated power effectively in achieving a faster

Figure 1—Experimental omnidirectional-bearing antenna tested in 1949.

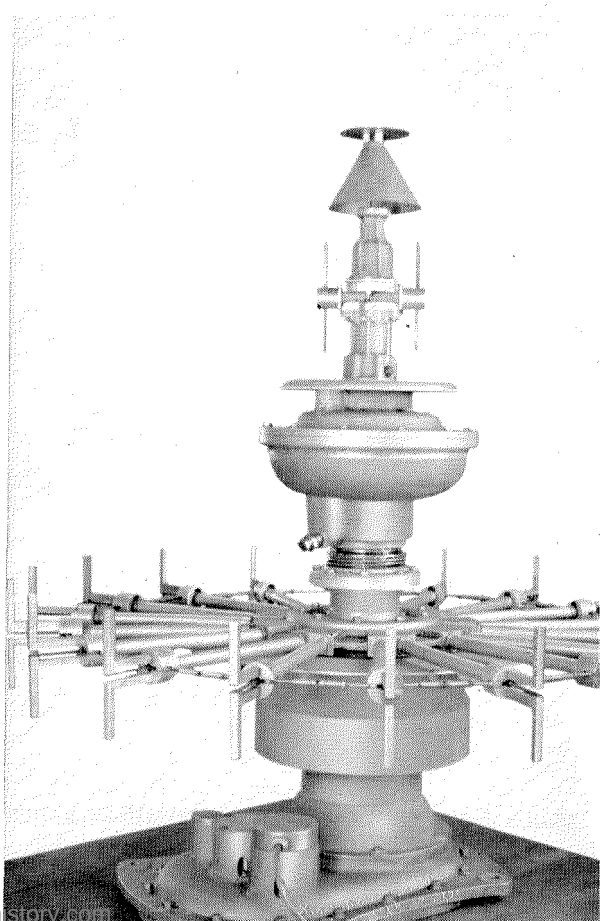

data rate to combat both noise and reflections and is compatible with practical and operational demands, particularly those for automatic indication, little bulk of airborne instrumentation, and coordination with other navigational facilities.

The electromagnetic representation of the azimuthal data in tacan has a complex structure that permits operation jointly with a distance-measuring facility; that is, an over-all structure that includes both rho and theta (polar-coordinate) data. A detailed over-all description of the composition of the radiated signals is not essential to the study of the attributes of the azimuthal data encoding. For this purpose, the encoding of the data couplet may be regarded as depicted in Figure 2.

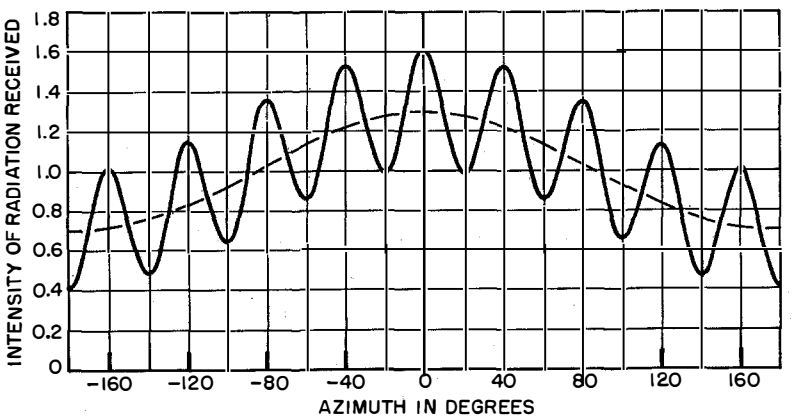

Figure 2—Rectilinear pattern of radiation from antenna conforming to (1), where $m_1 = 0.3$ and $m_9 = 0.3$. Marker pulses for azimuthal reference angles are indicated below the graph.

The continuous waveform shown in Figure 2 is the radiation pattern of a tacan transmitting array and is given by

$$p(x) = 1 + m_1 \cos x + m_9 \cos 9x \qquad (1)$$

The vertical lines at the bottom of Figure 2 represent pulses that serve as time markers fixing zero-reference azimuth. A polar plot of $p(x)$ appears in Figure 4A. It is a limaçon with a pronounced 9th-harmonic ripple added. The radiation pattern is uniformly rotated through 360 degrees of azimuth in the time between 2 larger (1st-harmonic) markers, or 10 smaller (9th-harmonic) markers. When the radiation pattern is received relative to the markers as shown, then the azimuth indicated is 0 degrees. At a receiving point somewhere along an azimuth ϕ the pattern received ideally would be $p(x - \phi)$, that is, $p(x)$ displaced a distance ϕ along the x axis with respect to the 1st-harmonic marker at $x = 0$. The azimuth indicated would then be ϕ.

The processing of the received data consists of determining the phase of the 1st harmonic in the received pattern relative to the 1st-harmonic reference markers and the phase angle of the 9th harmonic in the received pattern relative to 9th-harmonic markers. The 9th-harmonic phase so determined is divided by 9 and is, in effect, added to $s(2\pi/9)$, where s is the number of that 40-degree sector in which ϕ falls. This computation on the 9th-harmonic phase results in the indicated azimuth ϕ. It is related to the fact that the 9th-harmonic phase angle equals $(9\phi - s \cdot 2\pi)$, where 9ϕ is the *total change* in 9th-harmonic phase in response to displacement ϕ of $p(x)$.

In the absence of all sources of error, this computation on the 9th harmonic is completely redundant. The measurement of 1st-harmonic phase alone is adequate to establish ϕ. The 9th-harmonic phase measurement enters significantly when noise and reflections interfere with the radiated pattern so that the pattern received at an azimuth ϕ is no longer $p(x - \phi)$, but some distorted version of it $\tilde{p}(x)$. Here the measured phase ϕ_1 of the 1st harmonic in $\tilde{p}(x)$ is only an estimate of ϕ. The measured phase angle ϕ_9 of the 9th harmonic $\tilde{p}(x)$ now affords data from which a second estimate of ϕ can be inferred. This is to say,

phase of 1st harmonic in $\tilde{p}(x)$:

$$\phi_1 = \phi + \epsilon_1, \qquad (2)$$

phase of 9th harmonic in $\tilde{p}(x)$:

$$\phi_9 = (9\phi - s \cdot 2\pi) + 9\epsilon_9, \qquad (3)$$

where ϵ_1 and $9\epsilon_9$ denote the errors in the estimates ϕ_1 and ϕ_9, respectively. On proper identification of the sector s, the second estimate of ϕ,

which becomes the indicated azimuth, is made as follows.

$$\text{Indicated azimuth} = \phi_i = \frac{\phi_9}{9} + s\cdot\frac{2\pi}{9},$$

whereupon substituting for ϕ_9 its value in (3)

$$\phi_i = \phi + \epsilon_9. \qquad (4)$$

Accordingly ϵ_9, which is 1/9th the error in the estimate ϕ_9, is the error in the indicated azimuth.

Of real interest here is how ϕ_9, the azimuthal estimate derived from the 9th-harmonic code, compares with ϕ_1, the estimate of azimuth given by the 1st harmonic alone, or more to the point how the error ϵ_9 compares with the error ϵ_1. For the difference in these errors measures the success of the encoding $p(x)$ in (1), relative to a cardioid or 1st-harmonic encoding. It is the purpose of this paper to make this comparison and to discuss what may be termed the underlying error-reduction character of the 9th harmonic, or of any high-order harmonic.

2. *Error-Reduction Character*

The estimate ϕ_i of the true ϕ is viewed here as a problem in curve-fitting or data-smoothing. The data to be smoothed are represented by a curve $\tilde{p}(x)$, which is the envelope or resultant modulation of all signals appearing at the receiving point. It is known that $\tilde{p}(x)$ is in reality a symmetrical curve $p(x)$ that has been shifted by an amount ϕ, the azimuth of the receiving point, that is

$$\tilde{p}(x) = p(x - \phi) + \delta(x), \qquad (5)$$

where $\delta(x)$ represents a perturbation of $p(x - \phi)$. It is required to estimate ϕ from $\tilde{p}(x)$.

The principle of the data encoding and processing in the tacan omnirange is demonstrated by two cases for $\tilde{p}(x)$ illustrated in Figure 3. Curve A shows the erroneous pattern $\tilde{p}(x)$ as received at azimuth $\phi = 0$ degrees in the presence of a single reflection. The reflection chosen for this illustration is 0.4 times the magnitude of the true pattern radiated directly to the receiving point. The radio-frequency phases of reflected and direct signals received were taken to differ by 135 degrees; their modulation phases on 1st and 9th harmonics were taken to differ by 90 degrees. The erroneous pattern shown in curve B results for a radio-frequency phase difference of 45 degrees while the other factors were kept the same as for curve A. It is of course not known to a receiver that the azimuth of reception is 0 degrees. A receiver can only infer from the available data some estimate of the azimuth sought.

If the estimate were attempted by eye, the procedure would be one of fitting or adjusting a mental image of the unperturbed pattern (Figure 2) to the observed data. To begin with, one would search for some over-all central trend to the position of $\tilde{p}(x)$. This trend, indicated by the dashed outline tangent to the lowermost points in curve A, could be associated with the 1st harmonic in $\tilde{p}(x)$. (In the absence of a radiated 9th harmonic, this dashed outline shifted upwards to pass through the middle of the faster fluctuations essentially represents the data that would be received in a pure 1st-harmonic encoding.) Based on the 1st-harmonic trend alone in curve A, a visual estimate of azimuth would be about $-$ 10 degrees (and thus would be in error by $-$ 10 degrees).

On the other hand, it would generally be agreed that the more salient features of the data received are the faster fluctuations. These correspond essentially to the perturbation of the radiated 9th-harmonic cycles. The peaks of the

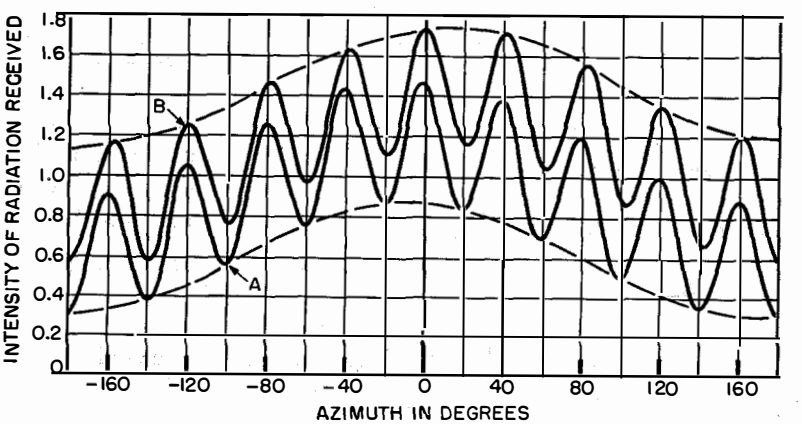

Figure 3—Two erroneous patterns as received in the presence of single reflections. Curve A is for reflection factor $a_1 = 0.4$, reflection modulation phase $x_1 = 90$ degrees, and reflection radio-frequency phase $\gamma_1 = 135$ degrees. For curve B, the corresponding values are 0.4, 90, and 45.

fluctuations in curve A all line up fairly closely with 40-degree markers. In fact, comparing the perturbed pattern *over-all* with the unperturbed pattern, there appears to have been little displacement of $p(x)$, despite the apparent 1st-harmonic trend of -10 degree in $\tilde{p}(x)$. A receiver might visually estimate the displacement at about -1 or -2 degrees and assert this to be the azimuth of reception.

Thus, if the faster fluctuations in the perturbed pattern were disregarded or were nonexistent, the estimate of azimuth in the case illustrated results in an error of some 10 degrees. However, when the evidence of the 9 harmonic cycles is weighed, it appears much more likely that $p(x)$ has been displaced no more than 1 or 2 degrees from the marker at zero, resulting in an azimuthal error of not more than 1 or 2 degrees. This reduction in error is characteristic of the 9th-harmonic encoding. The finer structure of the 9th-harmonic variation in the radiated pattern, although distorted under perturbation, will generally show through and hence define a more-accurate estimate of the pattern displacement than will a pure 1st-harmonic encoding.

A tacan receiver is instrumented to duplicate approximately the estimation procedure outlined above. In effect, the unperturbed pattern may be considered as available to the receiver on a transparent overlay. The overlay is placed on the pattern as received. It is then brought into a position in which the 1st-harmonic trends are reasonably matched. But matching the slower trends could leave considerable discrepancy between the 9th harmonic on the overlay and the fluctuations observed. The position of the overlay would then be adjusted to bring the 9th-harmonic cycles and received fluctuations into sharper focus. The final position of the overlay is taken as the estimate of azimuth. For the distorted patterns illustrated in Figure 3, the azimuths as derived from a 9th-harmonic estimate and indicated by a tacan receiver are, respectively, -1.0 and $+2.2$ degrees, whereas the 1st-harmonic azimuthal estimates are, respectively, -9.2 and $+20.1$ degrees.

Now the success of the 9th-harmonic encoding is seen to depend on a structural resistance of the finer variations in a pattern to being masked by interference and on the ability to form an estimate of 9th-harmonic movement in $p(x)$ as some over-all impression of the fluctuations received. This resistance to masking of patterns, or of representations in general, provided by great detail in the composition of a pattern has long been known in configuration or *gestalt* psychology. In recent years, this characteristic has come to the attention of communication engineers through the development of the theory of information with particular regard to the error-free reception of a signal transmitted in the presence of interference. While the recognizability of patterns has psychological implications, it emerges in the theory of information primarily as a statistical phenomenon. In the present application, the 9th-harmonic detail is equivalent to a redundant encoding of the azimuthal data. An average over the 9 cycles per cycle of 1st harmonic affords a 9-times-sharper estimate in a statistical sense of the displacement of $p(x)$ than does the 1st harmonic. The averaging instrumented in a tacan receiver, as discussed before in connection with the overlay procedure, consists of an over-all impression or match of 9 sinusoidal cycles as a *whole* to the observed fluctuations. While this over-all matching does not conform strictly to the more-common understanding of an average, wherein the individual phases of the 9 cycles would be measured and 1/9th of their sum taken as the estimate of 9th-harmonic phase, it can be shown that there is little practical distinction between the two when the perturbation of the radiated pattern is moderate as is usually the case. In the following, the reduction in error of estimation of azimuth achieved with the 9th harmonic is reviewed in a general analytic way when the radiated pattern is subject to arbitrary distortion. First, though, the receiver function, that is, the way the received data are processed, is specified analytically.

In essence, the instrumentation electromechanically fits a curve composed of a 1st and a 9th harmonic to the observed data, much the same as described before. As to the phases assigned these harmonics, the two are chosen so that the fitted curve differs from the received pattern in the least-mean-square sense. That is, for example, of the possible phases that may be assigned the 9th harmonic that one is chosen that produces the smallest squared difference

between the fluctuations and the nine 9th-harmonic cycles. As is well known, the phases so chosen are the phase angles ϕ_1 and ϕ_9 of 1st and 9th harmonics in $\tilde{p}(x)$. That is

$$\phi_1 = \arg \frac{1}{2\pi} \int_{-\pi}^{+\pi} \tilde{p}(x) \exp(jx)\, dx, \qquad (6)$$

$$\phi_9 = \arg \frac{1}{2\pi} \int_{-\pi}^{+\pi} \tilde{p}(x) \exp(j9x)\, dx. \qquad (7)$$

The integrations are instrumented as selective 1st- and 9th-harmonic filters; the operations "argument of" are instrumented as phase comparators. The division of ϕ_9 by 9 is accomplished by a 9-to-1 geared reduction in the mechanical rotation of the 9th-harmonic phase comparator.

The phase averaging performed on the received data is of course implicit in these integrals. To bring out the averaging in play, these integrals have been represented pictorially in Figure 4. Here, as throughout the paper, the azimuth of reception ϕ is taken equal to zero. The azimuthal estimates ϕ_1 and $\phi_9/9$ are then themselves the errors ϵ_1 and ϵ_9 ((2) and (3)). Further, $\tilde{p}(x)$ is separated into the unperturbed pattern at zero azimuth $p(x)$, and the net distortion in the pattern as received $\delta(x)$; that is,

$$\tilde{p}(x) = p(x) + \delta(x). \qquad (8)$$

Referring to the polar diagrams in Figure 4A, the integrals on $p(x)$ and $\delta(x)$ are readily interpreted as the resultants of the continuous distributions of phasors $p(x) \exp(jx)$ and $\delta(x) \exp(jx)$. Due to the symmetry of $p(x)$ the resultant m_1 (the amplitude or percent modulation of the 1st harmonic) points along 0 degrees, the correct azimuth. $\delta(x)$ is in general not symmetrical with respect to $x = 0$ degrees. Thus the resultant 1st-harmonic-distortion phasor d is shown pointing away from the correct azimuth. The phase of the sum of m_1 and d establishes the 1st-harmonic estimate ϕ_1, which is as well the error ϵ_1. The same kind of interpretation may be placed on the integral (7) determining the estimate ϕ_9. With regard to Figure 4B, this integral is first transformed by the change of variable $u = 9x$, in effect, expanding each 40-degree segment of $\tilde{p}(x)$, corresponding to each 9th-harmonic cycle, into 360 degrees in u. In this way, the perturbations of the 9 cycles may be considered to be magnified comparable to the 1st harmonic. On integration of $p(u/9)$, which is the correct part of the received data, there results m_9 at $u = 0$ degrees. The integral on $\delta(u/9)$ is not treated as a whole but rather in piecewise fashion over nine 40-degree intervals

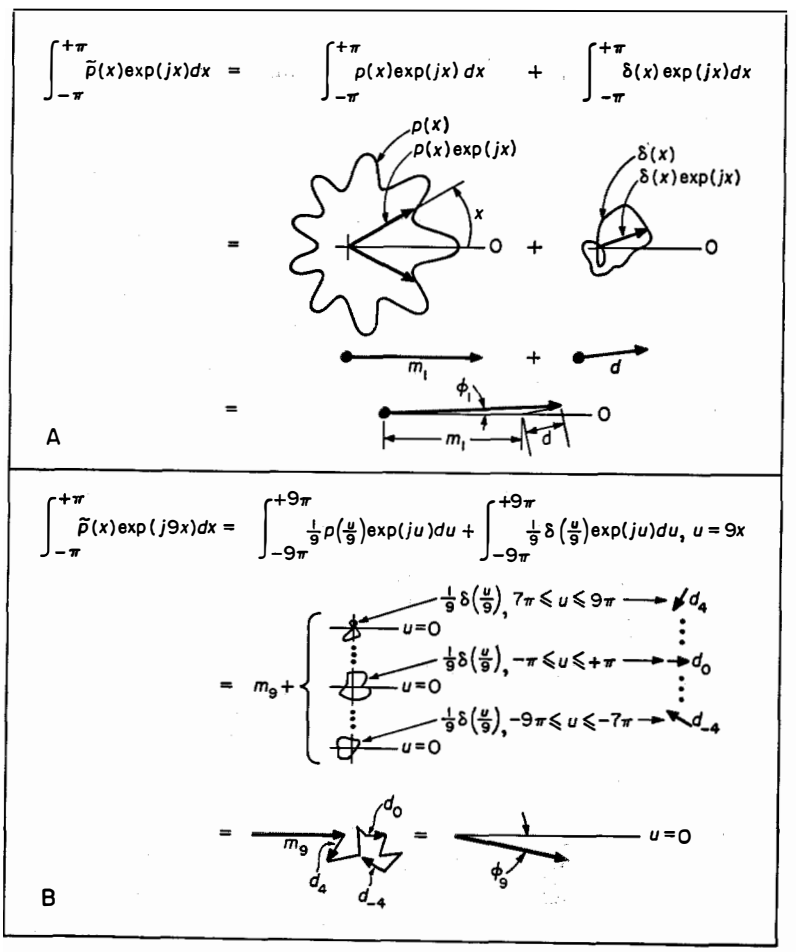

Figure 4—Graphic representation of integrals determining 1st- and 9th-harmonic estimates of azimuth. (See sections 6 and 7.)

in x, or nine 360-degree "sheets" in the angle u. On each sheet $\delta(u/9)$ is weighted continuously by 1/9 times the unit phasors $\exp(ju)$. This accounts for the smaller distortion figures on the u-plane sheets and consequently the smaller 9th-harmonic-distortion phasors $d_{-4} \ldots d_0 \ldots d_{+4}$. The resultant 9th-harmonic-distortion phasor, that which adds to m_9 to produce the error ϕ_9 in estimating the 9th-harmonic phase angle, is the sum of the 9 smaller phasors $d_{-4} \ldots d_{+4}$. The error in the azimuth indicated by the tacan receiver is $(1/9)\phi_9$, that is, the error angle ϵ_9.

The graphic interpretation of the integrals, (6) and (7), given in Figure 4 highlights the averaging performed when some arbitrary distortion of the correct data is present. While it would be possible to follow the procedure indicated in computing the azimuthal error incurred when any particular distortion $\delta(x)$ is assigned, the intention here is more to illustrate the factors affecting the errors in the azimuthal estimates and how the 9th harmonic leads to reduced error. Since the 9th-harmonic azimuthal estimate is $\phi_9/9$, consider first ϕ_1 and ϕ_9. Referring to Figures 4A and 4B, the relative sizes of m_1 and m_9, the amounts of 1st and 9th harmonic in the radiated pattern, must in general be considered in determining whether ϕ_1 or ϕ_9 deviates the lesser from zero. The "shorter" that m_1 or m_9 is, the more likely is a distortion phasor to produce larger deviations from zero in the angle of the resultant. Then, the 1st- and 9th-harmonic-distortion phasors themselves, implying size and angle, resulting from a given distortion function $\delta(x)$ must be considered.

Now the 9th-harmonic resultant distortion phasor is the sum of 9 smaller phasors, $d_{-4} \ldots d_{+4}$, each of which might be associated with the distortion in the individual cycles of the 9th harmonic. Letting $m_1 = m_9$, a comparison between ϕ_1 and ϕ_9 and in turn ϵ_1 and ϵ_9 depends then on how the smaller $d_{-4} \ldots d_{+4}$ add up compared to the larger single distortion phasor d. The possibilities are infinitely varied. However, a comparison can be drawn definitely in any number of special cases and also in a certain general sense as well.

A rather-obvious case is one in which a perturbation produces a distortion function $\delta(x)$ that is symmetrical with respect to the correct azimuth, 0 degrees. The phasor resultants of $\delta(x)$ on 1st and 9th-harmonic estimates lie along 0 degrees and so ϵ_1 and ϵ_9 are both zero here. This symmetry condition practically arises, as an instance, when the reflection discussed in Figure 3 differs in radio-frequency phase from the direct signal by an angle of 114 degrees. The pattern received is distorted but essentially symmetrical, correctly indicating zero phase angles ϕ_1 and ϕ_9. In operation, this instance of symmetry is apt to be momentary since small changes in the azimuth of reception may well change the radio-frequency phase difference to 135 or 45 degrees, for example, resulting in the patterns illustrated in Figure 3. As an important special case to be discussed fully in section 3, when a single reflection distorts the radiated pattern as in Figure 3, it will be found that ϕ_9 is never larger than ϕ_1; in fact ϕ_9 is often zero when ϕ_1 is large. Thus ϵ_9 $(= \phi_9/9)$ will never exceed ϵ_1 and at worst is only 1/9th the error possible on the 1st-harmonic estimate.

With no further specification of the perturbing influence, it is still possible to realize a comparison of ϵ_1 and ϵ_9 as they result on the average in an ensemble of possible assignments of $\delta(x)$. That is, considering reasonable possibilities for $\delta(x)$, the spreads of errors most likely to be encountered on 1st- and 9th-harmonic estimates can be evaluated and compared. By reasonable possibilities for $\delta(x)$ is meant here simply that smaller differences between observed and correct patterns are more probable than larger ones, such as occurs when noise, for example, is the perturbing influence. This problem has already been considered by the writer in a previous paper.[1] The result is that the root-mean-square spread in the error of azimuthal estimation in the presence of random perturbation varies inversely as the product of the amplitude and the number of the harmonic on which the estimate is based. In the tacan system, the harmonic amplitudes m_1 and m_9 are essentially equal for elevation angles up to about 30 degrees. Thus, in this range

$$\epsilon_{9\text{rms}} = \frac{1}{9}\,\epsilon_{1\text{rms}}. \qquad (9)$$

The result (9) expresses what was referred to previously as the sharper estimate of the pattern

[1] M. Masonson, "Radio Direction Finding from the Standpoint of Sampling and Interpolation," *Convention Record of the IRE 1955 National Convention*, Part 5, Aeronautical and Navigational Electronics; page 88.

displacement obtainable from the 9th harmonic. In statistical parlance, it can be said that an interval of given confidence in the estimation of azimuth, that is, an interval around the correct azimuth in which the estimate has a preassigned probability of falling, is only 1/9th as wide for a 9th-harmonic estimate as it is for a 1st-harmonic estimate. In other words, the 9th-harmonic estimate is much more probable to meet a specified allowable departure from the correct azimuth than a 1st-harmonic estimate.

Now the result (9) might perhaps appear at first to be somewhat less than appropriate when examining the reduction of error in the presence of reflections. For the assignment of distortions $\delta(x)$ directly to the radiated pattern is more properly the approach when effects of noise-type perturbations are considered. When reflections are the perturbing influence, it appears to be more realistic to form $\delta(x)$ of assignments from an ensemble of ghosts of the radiated pattern $p(x)$. It would be still more desirable to have a determinate, as opposed to average, analytic description of the errors ϵ_1 and ϵ_9 as functions of the reflectivity and positions of many reflectors acting simultaneously. These latter problems are treated in section 3. With respect to the result (9), study of reflections from a statistical standpoint shows that the root-mean-square spread of error on 9th-harmonic estimates is again 1/9th the root-mean-square spread of error on 1st-harmonic estimates, as occurs with noise perturbations. There is a certain practical distinction, though, that should be observed between noise and reflections. In the presence of reflections, it is found that the error reduction is largely independent of harmonic amplitude; it is mainly a function of the harmonic number. Thus the root-mean-square-error relation (9) will not be very sensitive to changes in m_1 and m_9 with elevation angle if reflections are the source of perturbation. This is discussed again in section 3.

Now a 9th-harmonic estimate of the displacement of the radiated pattern does not indicate movement relative to any particular 40-degree marker, as discussed at the outset in section 1. The 1st-harmonic estimate is required to localize a marker from which the 9th-harmonic movement is to be indicated. In (4), the selection of a marker was expressed as the identification of the sector number s, which determines the multiple of 40 degrees to be added to the 9th-harmonic movement $\phi_9/9$. Actually, sector identification as described is not employed in the tacan receiver. If this were so, a minute error in ϕ_1 when ϕ is near a boundary of a sector could make s be mistaken as 1 too large or too small. The computation of ϕ_i by (4) would be in error by $\epsilon_9 \pm 40$ degrees.

In the tacan receiver, the indicated azimuth is reached essentially in these two steps. First the estimate ϕ_1 is indicated. Then, disengaging the indicator from the 1st-harmonic drive, the initial indication is shifted to a second position ϕ_i by a 9-to-1 geared drive from the 9th-harmonic channel. The second position will necessarily be within 20 degrees of the first, that is, $|\phi_i - \phi_1| < 20$ degrees because the instrumentation automatically rejects any other equilibrium condition. For example, in curve A of Figure 3 the indicated azimuth is -1.0 degree since $|-1.0 + 9.2|$ degrees is less than 20 degrees. Similarly, for the case of curve B in Figure 3, the indicated azimuth is $+2.2$ degrees since $|2.2 - 20.1|$ degrees is also less than 20 degrees. From these illustrations, it can be seen that only errors ϵ_1 and ϵ_9 whose difference is more than 20 degrees can produce error in ϕ_i greater than ϵ_9. Thus, while the instrumented computation differs mechanically from that in (4), the results are equivalent to the extent that

$$\phi_i = \phi + \epsilon_9, \quad |\epsilon_1 - \epsilon_9| < 20 \text{ degrees.} \quad (10)$$

It is of course conceivable that certain combinations of ϵ_1 and ϵ_9 will differ by more than 20 degrees. Such circumstances are rare as may be appreciated from Figure 5, which shows the

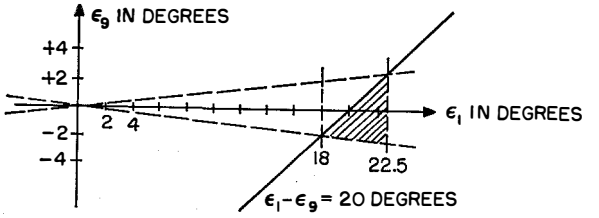

Figure 5—The dashed lines are for $|\epsilon_9| = |\epsilon_1|/9$.

ϵ_1, ϵ_9 plane. Every point is a certain combination of ϵ_1 and ϵ_9. Those points above the line $\epsilon_1 - \epsilon_9 = 20$ degrees (and under the line $\epsilon_1 - \epsilon_9 = -20$ degrees, which does not appear on the part of the plane shown) are those for which (10)

is valid. Of all the points in the plane, those in the region within $|\epsilon_9| = |\epsilon_1|/9$ are the most likely to occur. Of the latter, some fall below the critical line. These are points for which (10) is not valid. Thus on the rare occasions when the 1st-harmonic estimate is in error by some 18 to 22 degrees, and then only about half the time, the indicated azimuth will be in error by more than ϵ_9.

There are two reasons for ignoring such possibilities. First, the choice of a 9th-harmonic system rather than some higher harmonic was dictated in part by the fact that 1st-harmonic errors of 12 degrees or less have been found in practice to be most common. This provides some 8-degree leeway to the critical area. Second, if errors of 20 degrees should occur, it would be exceedingly unlikely for them to be prolonged since a receiving point is usually in motion. That is, changes in position of a fraction of a wavelength, which is one foot (30 centimeters) at the tacan frequency, could shift the radio-frequency picture, bringing the errors within the required limits.

The changing radio-frequency-phase conditions in the presence of reflections is noteworthy for it brings with it a second averaging in system operation—an averaging over the positions of the point along the course of travel. In the receiver, this corresponds to a time average of estimates made at the various positions, sometimes referred to as "Doppler averaging." Smoothing of this kind is a function of the course, speed of travel, and the speed of response of the measuring and indicating components. The short wavelength of the tacan system thus implies an advantage in this regard. This Doppler averaging is not however of primary concern to this paper. Of main interest here is the intrinsic reduction in error brought about by the 9th-harmonic encoding at a fixed point in space.

3. *Small-Reflection Analysis of* ϵ_1 *and* ϵ_9

In this section, an analysis is made of the errors in estimation of azimuth based on the 1st and 9th harmonics when a number of reflectors act together in perturbing the radiated pattern. The analysis is restricted to a total reflection that is small compared to the direct signal. This limitation does not constitute a serious practical objection because reflection magnitudes that are beyond the scope of the analysis occur infrequently, and in any event ordinarily induce errors in 1st-harmonic estimates that are too large to be tolerable operationally.

The mathematical situation underlying the evaluation of ϵ_1 and ϵ_9, the errors in 1st- and 9th-harmonic estimates of azimuth, is readily stated with reference to Figure 6. It is a matter of

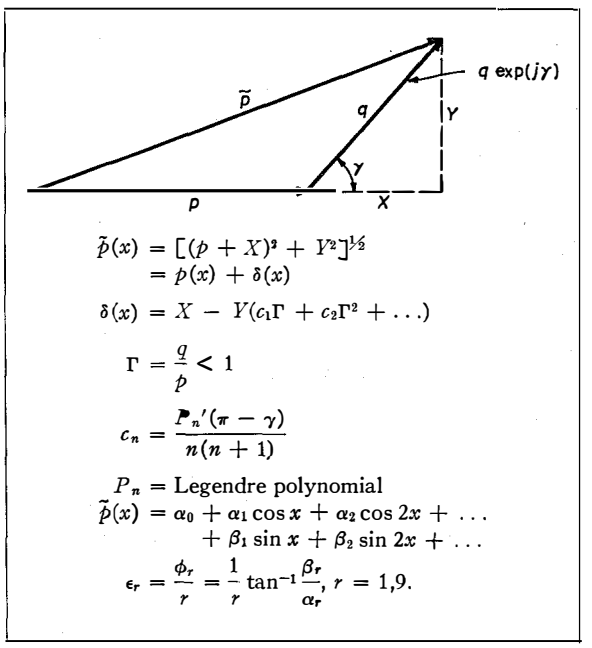

$$\tilde{p}(x) = [(p + X)^2 + Y^2]^{1/2}$$
$$= p(x) + \delta(x)$$
$$\delta(x) = X - Y(c_1\Gamma + c_2\Gamma^2 + \ldots)$$
$$\Gamma = \frac{q}{p} < 1$$
$$c_n = \frac{P_n'(\pi - \gamma)}{n(n+1)}$$
P_n = Legendre polynomial
$$\tilde{p}(x) = \alpha_0 + \alpha_1 \cos x + \alpha_2 \cos 2x + \ldots + \beta_1 \sin x + \beta_2 \sin 2x + \ldots$$
$$\epsilon_r = \frac{\phi_r}{r} = \frac{1}{r}\tan^{-1}\frac{\beta_r}{\alpha_r},\ r = 1,9.$$

Figure 6—Evolution of $\tilde{p}$, the pattern received in the presence of reflections. p = radiated pattern, q exp $(j\gamma)$ = the magnitude q and phase γ of the sum of the reflections, X and Y are the in-phase and quadrature components of q exp $(j\gamma)$.

computing the erroneous field pattern observed at a receiving point when the transmitting array is rotated in the presence of a distribution of fixed sources of reflections. p is a phasor denoting the radio-frequency signal received along the direct path from transmitter to receiver. p is the unperturbed pattern and is a function of the normalized time x. To p must be added q exp $(j\gamma)$, the phasor sum of all contributing reflections of which q is the magnitude and γ is the phase. In general, q and γ are also functions of x. The resultant $\tilde{p}$, which is the distorted pattern or envelope of the composite radio-frequency signal received, must then be analyzed for its 1st and 9th harmonics. These harmonics subsequently determine the phase

angles ϕ_r $(r = 1, 9)$ and finally the errors $\epsilon_r = \phi_r/r$.

The explicit evaluation of ϵ_r in complete generality along the lines indicated in Figure 6, even when only a single reflector is present, imposes severe mathematical hardship and would not lend itself to ready interpretation. The expansion[2] of $p(x)$ in powers of Γ, the ratio of the total reflection magnitude to direct-signal magnitude at all points of the modulation cycle, formally identifies the distortion term $\delta(x)$ in (8) with the series $X - Y\{\ldots\}$ in Figure 6. From this series, it may be noted that X, which is the in-phase component of all reflections taken together, constitutes the dominant distortion when Γ is small except, of course, when X is itself zero. In the treatment of ϵ_1 and ϵ_9 that follows, the approximation $\delta(x) = X$ will be made. This is tantamount to approximating the hypothenuse of the right triangle in Figure 6 by the long side throughout the cycle of modulation. The approximate analytical results so derived will then be least valid when $X = 0$ or γ is 90 degrees. γ, though, is by no means a constant throughout the modulation cycle, except in the case of a single reflector, so that the error in analysis is not so great as might be anticipated.

To gauge this error, the case of a single reflector was analyzed numerically by a 36-point schedule and compared with the results of the analytic approximation (to be derived later). The results of the numerical analysis are shown in Figure 7. In both parts of the figure, the phase of the modulation of the reflection is 90 degrees (for 1st and 9th harmonics), which is very nearly the modulation phase inducing maximum error in the estimate of azimuth for any radio-frequency phase. The reflection factor or ratio of carriers was taken at 0.2 in Figure 7A and at 0.4 in B. In Figure 7A, the maximum difference between ϵ_1 as approximated analytically and as

[2] C. B. Aiken, "Theory of the Detection of Two Modulated Waves by a Linear Rectifier," *Proceedings of the IRE*, volume 21, pages 601–629; April, 1933. This expansion was derived in connection with amplitude distortion and intermodulation products generated in the simultaneous linear rectification of two single-tone-modulated carriers.

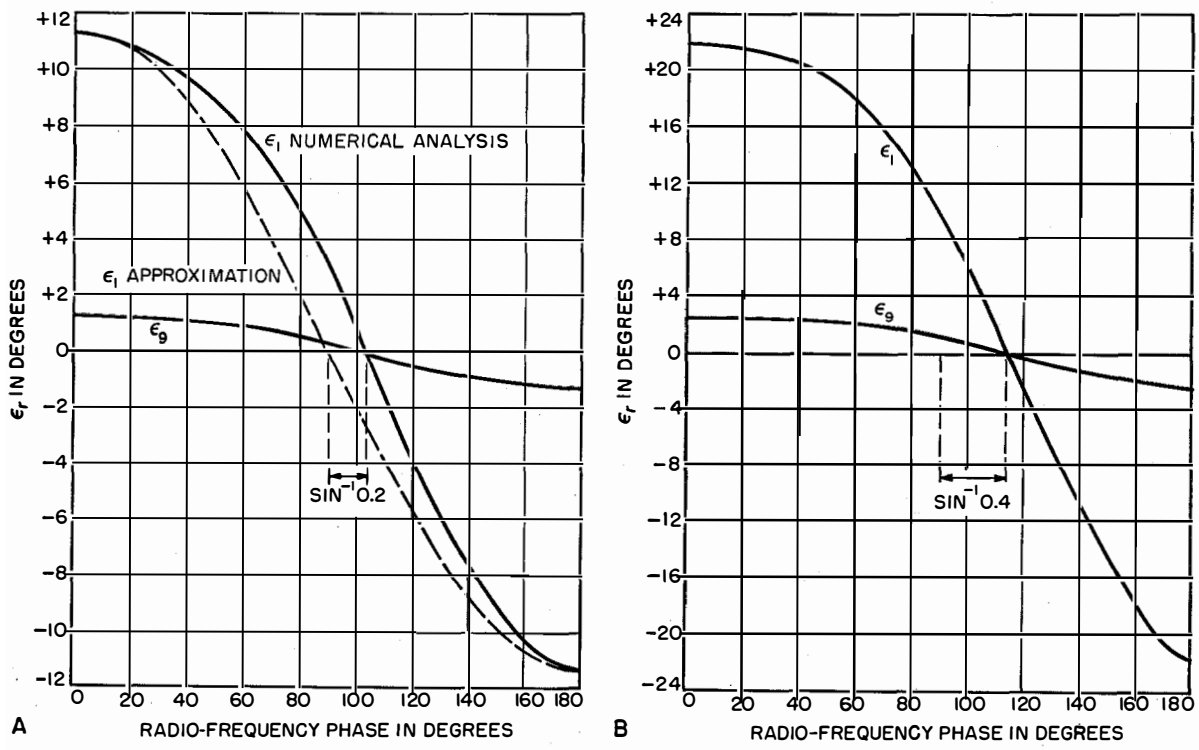

Figure 7—Numerical evaluation of error ϵ_r plotted against radio-frequency phase γ_1 for a single reflection with a modulation phase of 90 degrees. In A, the reflection amplitude $a_1 = 0.2$ and in B it is 0.4. The broken-line curve for ϵ_1 in A is an analytic approximation to the numerical result, $\epsilon_1 = (0.2 \cos \gamma_1) \cdot 57.3$ degrees.

computed numerically is 3.1 degrees; the maximum difference in the values obtained for ϵ_9 is 0.27 degree. The maximum differences in ϵ_1 and ϵ_9 obtained in Figure 7B are 10.0 and 1.1 degrees, respectively. The analytic approximation to the error ϵ_9 in the 9th-harmonic estimate of azimuth is quite good even at the larger reflection factor. The analytic approximation to ϵ_1, the error in the 1st-harmonic estimate, is not so good at the larger reflection factor; but it should be recalled that the conditions chosen here of a single reflector, and radio-frequency and modulation phases of 90 degrees are about the worst possible for the approximation made.

Having thus justified the approximation of $\tilde{p}(x)$ by $p(x) + X(x)$, the evaluation of ϵ_r is now undertaken in the general case defined in Figure 8A. (s_k, x_k) are polar coordinates of one of a number of sources of reflection. The signal arriving at the receiver along the direct path $\phi = 0$ is $p(x)$ (that is, the phase of the carrier of the unperturbed pattern is taken as zero). The reflection received from (s_k, x_k) is $p_k(x) \cdot \exp(-j\gamma_k)$, where γ_k is the lag in reflection carrier phase caused by the longer path of travel between the transmitter and receiver. $p_k(x)$ is an attenuated and delayed ghost of

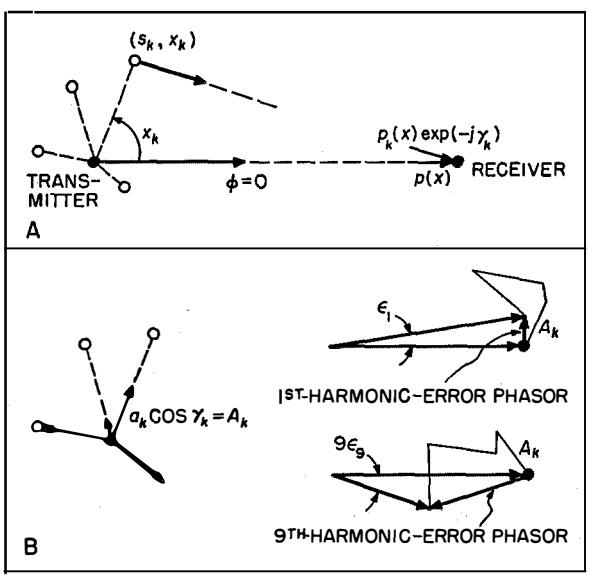

Figure 8—Graphic evaluation of ϵ_r in (13). The transmitting and receiving points and sources of reflection, one of which is (s_k, x_k), are shown.

$p(x)$. Ignoring the small shift in envelope introduced by path-length differences, $p_k(x) = a_k p(x - x_k)$. That is, x_k, the space angle to the kth reflector measured from the direct path, predominantly determines the modulation shift in the reflection. a_k is the reflection magnitude as received relative to the direct signal. X, the in-phase component of the summed reflections, is the sum of the in-phase components of the individual reflections. Thus

$$\tilde{p}(x) \approx p(x) + \sum_k a_k \cos\gamma_k p(x - x_k). \quad (11)$$

Using $p(x) = 1 + m_1 \cos x + m_9 \cos 9x$, the 1st- and 9th-harmonic terms in $\tilde{p}(x)$ can be readily separated and collected since these are the only harmonics (other than direct current) that appear in the approximation made. That is, dropping the quadrature component Y in the series for $\delta(x)$ has left $\tilde{p}(x)$ in (11) as a simple linear sum of the $p_k(x)$. (Thus nonlinear distortion and intermodulation of pattern harmonics do not appear in this analysis. The virtual freedom of $\tilde{p}(x)$ from such distortion can be observed in the patterns of Figure 3.) The resulting approximations to the phase angles $\phi_r (r = 1, 9)$ are then

$$\phi_r = r \cdot \epsilon_r = \tan^{-1} \frac{\sum_k a_k \cos\gamma_k \sin rx_k}{1 + \sum_k a_k \cos\gamma_k \cos rx_k}, \quad r = 1, 9. \quad (12)$$

The same result may be recast in a way that is more easily envisioned relative to the geometric distribution of reflecting points. Using $\epsilon_r = (1/r)\phi_r$, this is,

$$\epsilon_r = \frac{1}{r} \arg\left[1 + \sum_k a_k \cos\gamma_k \exp(jrx_k)\right]. \quad (13)$$

Equation (13) is the general expression relating azimuthal error to magnitudes, radio-frequency phases, and modulation phases of a number of reflections. Consider first the meaning that can be attached to ϵ_1 from (13). As shown in Figure 8B, every reflecting point may be associated with an error phasor $a_k \cos\gamma_k \exp(jx_k)$, that is, a phasor of magnitude $A_k = \pm a_k \cos\gamma_k$ (depending on the sign of $\cos\gamma_k$) along a line from the transmitter to (s_k, x_k). The resultant of all the error phasors so assigned added to unity defines

the error angle ϵ_1. Similarly, the same magnitudes A_k directed this time at angles of $9x_k$ produce a resultant that added to unity yields 9 times the error angle ϵ_9.

Interpreting (13) from pictures such as 8B, various specific situations can be discussed. For example, with only one reflecting point (s_1, x_1) present, it is readily seen that the maximum possible ϵ_1 equals arc sine A_1 radians, that the maximum ϵ_9 can only be 1/9th as great, and that at no angle x_1 is ϵ_9 ever greater than ϵ_1. (The maximum value of ϵ_r from (13) for $A_1 = 0.2$ $\cos \gamma_1$ and $x_1 = 90$ degrees is plotted as a function of γ_1 as the dashed curve in Figure 7A. The approximation to maximum ϵ_r is zero when γ_1 equals 90 degrees whereas maximum ϵ_r is actually zero when $\gamma_1 = 90$ degrees + arc sine a_1.

When more than one reflector is present, it is still possible though now cumbersome to employ such error-phasor diagrams in specific distributions of reflecting points and amplitude factors A_k. Certain rather-special comparisons of ϵ_1 and ϵ_9 may be made easily with the aid of the diagrams. Consider, for example, any distribution of reflectors that is geometrically symmetrical with respect to the direct path between transmitter and receiver, all reflectors having the identical A_k. The resultants of the 1st- and 9th-harmonic-error phasors point along the direct path to the receiver, making $\epsilon_r = 0$. Consider next a set of N reflection phasors of the same magnitude spaced $2\pi/N$ apart though not symmetrically about the transmitter–receiver path. Here again $\epsilon_1 = 0$, since the resultant 1st-harmonic-error phasor is zero, but ϵ_9 in general is not. Geometric symmetry and identical A_k are not at all necessary for ϵ_1 to be zero, for any combination resulting in *electric* symmetry about $x = 0$ will suffice. Obviously, any phasor conditions hypothesized as a 1st-harmonic distribution can always be hypothesized as a distribution on the 9th as well. Then ϵ_9 will become zero whereas ϵ_1 in general will not. It is thus clear that *singular* situations can be concocted that make ϵ_1 and ϵ_9 anything desired, such situations being more of academic than practical import. It would appear that what is required here in the absence of definite real situations—and from a practical standpoint the real situations are largely nondeterministic, especially allowing for random variations in the terrain such as windblown obstacles and water waves—is the statistical behavior of ϵ_1 and ϵ_9 as a function of azimuth in an ensemble of terrains.

In view of this, two types of distributions of reflecting points will be considered. In one, the reflectors are assumed to be uniformly distributed around 360 degrees in the statistical sense, that is, one is as likely to find a reflector at any one azimuth as another. In the second, the reflecting points are assumed to agglomerate along a given direction relative to the shortest path from transmitter to receiver. Preparatory to the statistical analysis, a simplification of (12) is made. In this equation, $\sum a_k \cos \gamma_k$ is small compared to unity since, in the first place, the analysis is based on small total reflection. Moreover, let it be noted that when many reflectors are present this sum will inherently tend to be small on the average. Hence,

$$\epsilon_r \approx \sum_k \epsilon_{r,k}, \tag{14}$$

where

$$\epsilon_{r,k} \equiv (1/r)(a_k \cos \gamma_k) \sin rx_k.$$

Also, assuming parallel rays to emanate from the transmitter and (s_k, x_k) to the receiver

$$\left.\begin{aligned} \gamma_k &= b_k s_k, \\ b_k &\equiv (2\pi/\lambda)(1 - \cos x_k). \end{aligned}\right\} \tag{15}$$

The quantity $\epsilon_{r,k}$ may be thought of as a partial error term, so to speak, namely the part of the total ϵ_r introduced by the kth reflecting point. For a single reflector $\epsilon_r = \epsilon_{r,1}$. The approximation $\epsilon_{r,1}$ is sketched in Figure 9A as a function of x_1, assuming a_1 is constant, that is, the reflector is nondirective. The cosine factor is similar to a frequency-modulated carrier and the sine factors to amplitude modulation of it. $\epsilon_{1,1}$ and $\epsilon_{9,1}$ differ in modulation peak amplitude and frequency by a factor of 9. If the reflector is directive, then a_1 is a function of x_1, which brings in another modulation factor *common* to both ϵ_1 and ϵ_9.

The statistical study of the total error ϵ_r is reduced through (14) to the case of the average behavior of the kth reflector with respect to position (s_k, x_k) and reflectivity a_k summed over all reflectors. The averages to be considered are $E(\epsilon_{r,k})$ and $E(\epsilon^2_{r,k})$ and the relation between

them given by

$$\text{var } \epsilon_{r,k} = E(\epsilon^2_{r,k}) - E^2(\epsilon_{r,k}), \qquad (16)$$

where $E(z)$ denotes the average value or expectation of z and var z denotes the mean-square variation of z around $E(z)$. Then

$$E(\epsilon_r) = \sum_k E(\epsilon_{r,k})$$

$b = (2\pi/\lambda)(1 - \cos x)$. Here

$$E(\epsilon_{r,k}) = \frac{\sin rx}{r} E(a_k) \cdot E(\cos bs_k)$$

$$\text{var } \epsilon_{r,k} = \frac{\sin^2 rx}{r^2} [E(a_k^2) \cdot E(\cos^2 bs_k) - E^2(a_k) \cdot E^2(\cos bs_k)].$$

If a_k were nonstatistical, which is to say that the kth reflection amplitude were kept the same in

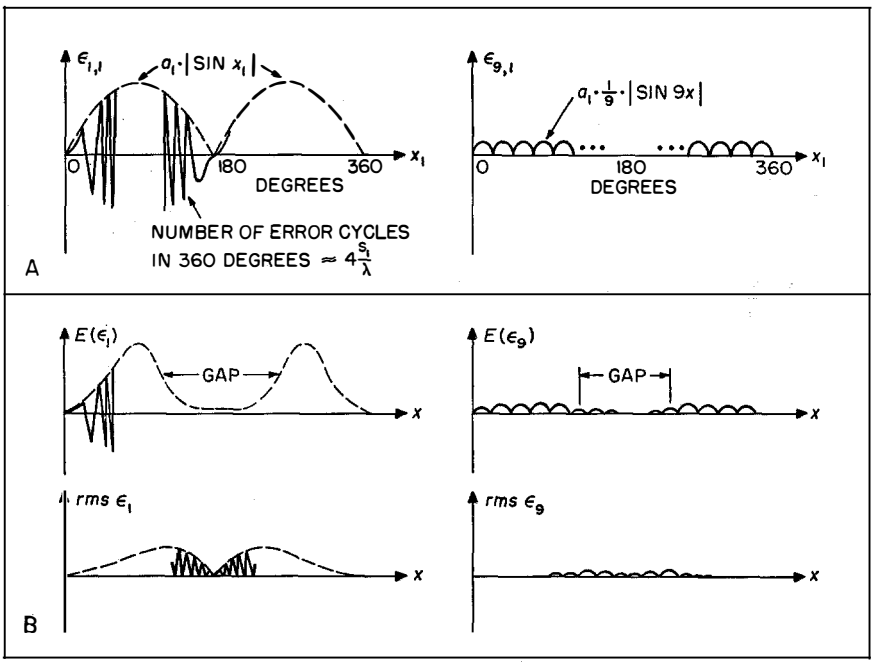

Figure 9—Approximation $\epsilon_{r,1}$ as a function of x_1 is given in A.
$\epsilon_{r,1} = a_1 \cdot [(\sin rx_1)/r] \cdot \cos[2\pi(s_1/\lambda)(1 - \cos x_1)]$, $r = 1,9$.
B is a sketch of (17) for average and root-mean-square values of ϵ_r for reflectors along a radius x degrees off the direct path to the receiver.

and

$$\text{var } \epsilon_r = \sum_k \text{var } \epsilon_{r,k}. \qquad (17)$$

The last expression is based on the fact that the partial errors contributed are mutually independent.

Consider now a string of reflectors distributed at random along a radius at angle x relative to the transmitter-to-receiver path, that is, all $x_k = x$ but s_k is randomly variable. Then cos γ_k is a random variable since $\gamma_k = bs_k$, where every assignment of reflecting points, then $E(a_k^2) = E^2(a_k)$ and

$$\text{var } \epsilon_{r,k} = E(a_k^2) \frac{\sin^2 rx}{r^2} \text{var cos } bs_k. \qquad (18)$$

Equation (18) is still applicable approximately when a_k is variable and $E(a_k^2) \approx E^2(a_k)$. This occurs, for example, when a_k has a Rayleigh density of probability; in which case $E^2(a_k) = 0.79E(a_k^2)$. The issue here is not of basic significance and is rather a matter of obtaining compactness in the mathematical expressions.

In any event, the result (18) will be seen to be quite proper when the radial spread of reflectors is considered, for then $E(\cos bs_k)$ will be found to be close to zero. Letting the positions s_k vary normally about an average position s_0 with standard deviation in radial position of s, then

$$E(\cos bs_k) = \exp\left[-\tfrac{1}{2}(bs)^2\right] \cos bs_0$$

and

$$\text{var} \cos bs_k = \tfrac{1}{2}\{1 - \exp\left[-\tfrac{1}{2}(bs)^2\right]\} \cdot \{1 - \exp\left[-\tfrac{1}{2}(bs)^2\right] \cos 2bs_0\}.^* \quad (19)$$

In turn from (17),

$$\left.\begin{aligned} E(\epsilon_r) &= \frac{1}{r} P' \sin rx\, E(\cos bs_k) \\ \text{var } \epsilon_r &= \frac{1}{r^2} P \sin^2 rx \text{ var } (\cos bs_k), \end{aligned}\right\} (20)$$

where

$$\left.\begin{aligned} P' &\equiv \sum_k E(a_k) \\ P &\equiv \sum_k E(a_k^2). \end{aligned}\right\} (21)$$

$E(\epsilon_r)$ and $(\text{var } \epsilon_r)^{1/2}$ in (20) are sketched in Figure 9B as a function of x, which is the angle between the line of reflectors and the line from transmitter to receiver.

The curves of Figure 9B are essentially the averages of the purely determinate error curves $\epsilon_{1,1}$ and $\epsilon_{9,1}$ of Figure 9A and of the root-mean-square departure from average with respect to changes in a_1 and s_1. The maximums of $E(\epsilon_r)$ and $(\text{var } \epsilon_r)^{1/2}$ for $r = 1$ and 9 are in the ratio 9 to 1 as before. The amplitude modulation on $E(\epsilon_r)$ and $(\text{var } \epsilon_r)^{1/2}$ are in 1-to-9 frequency ratio but there is another modulation factor, too. This factor, $\exp\left[-\tfrac{1}{2}(bs)^2\right]$, produces the gap shown. The width of the modulation gap, as a result of the averaging, depends on the root-mean-square spread s of reflectors measured in wavelengths. In the condition shown, $s \approx 1\lambda$. With s increased to about 10λ, then $E(\epsilon_r)$ is much less than $0.05[(1/r)P']$ throughout 360 degress in x. With little further increase in s, $E(\epsilon_r)$ may be approximated as zero. The variation in $(\text{var } \epsilon_r)^{1/2}$ as shown is out-of-phase with $E(\epsilon_r)$. With increasing s, it approaches $(\tfrac{1}{2}P)^{1/2}(|\sin rx|/r)$. The values of $E(\epsilon_r)$ and $\text{var}(\epsilon_r)$ for $s/\lambda \gg 1$ are those that would result if γ_k were uniformly distributed through 360 degrees and independent of x. That is, for large s/λ, the reflection radio-frequency phases are in effect equally likely to be anywhere in 360 degrees with no regard to x (except for the special angles $x = 0$, 180 degrees).

This effective uniformity and independence of γ_k allows P of (21), in effect the average total power reflected away from the reflecting points, to be associated with the average total power as received in the summation of reflections. This may be seen as follows

$$q^2 = (\sum p_k \cos \gamma_k)^2 + (\sum p_k \sin \gamma_k)^2 = \sum p_k^2 + \sum p_i p_j \cos(\gamma_i - \gamma_j),\ i \neq j.$$

The average of q^2 with respect to γ_k and time is then

$$Eq^2 = E \sum p_k^2 = \left(1 + \frac{m_1^2}{2} + \frac{m_9^2}{2}\right) \cdot \sum E(a_k^2).$$

Thus, $\sum E(a_k^2) = P$ is the ratio of the average reflection power as received to the average power in the direct signal.

In terms of P and for large s/λ, (21) becomes

$$\left.\begin{aligned} E(\epsilon_r) &\approx 0 \\ \epsilon_{r,\,rms} &= (\text{var } \epsilon_r)^{1/2} \\ &\approx \left(\frac{P}{2}\right)^{1/2} \frac{|\sin rx|}{r} \text{ radians.} \end{aligned}\right\} (22)$$

Consider next the case of reflecting points that cluster statistically in a narrow *angle* about an azimuth x with respect to the transmitter–receiver line. Let x_k be normally distributed around x with standard deviation x'. If the radial spread of reflectors in wavelengths is large, then γ_k and x_k are effectively independent as discussed before. $E(\epsilon_{r,k})$ is then the product of the expectations of the trigonometric factors contained in $\epsilon_{r,k}$ of (14). Since $E(\cos \gamma_k) \approx 0$ then

$$\left.\begin{aligned} E(\epsilon_{r,k}) &= 0 \\ \text{var } \epsilon_{r,k} &= \frac{1}{2r^2} E(a_k^2) E(\sin^2 rx_k). \end{aligned}\right.$$

* This is obtained by noting that if $G(g)$ is the probability density of a variable g, and if the density is symmetrical about g_0, then

$$E(\cos \omega g) = \text{real } \mathfrak{F}G(g) = \cos \omega g_0 \cdot \mathfrak{F}G(g + g_0).$$

Using Campbell and Foster transform pair 710.0, the results above follow.

Summing these over all reflectors, then

$$E(\epsilon_r) = 0$$
$$\text{var } \epsilon_r = \left(\frac{P}{2}\right)\frac{1}{2r^2}\{1 - \exp[-2(rx')^2]\cdot\cos 2rx\}. \quad (23)$$

For small angular spread x', (23) reduces to the results of the preceding case of a string of reflectors, (22). As the root-mean-square angular spread x' is increased, the case of reflectors uniformly distributed in azimuth is approached. The result here is that

$$\left.\begin{aligned} E(\epsilon_r) &= 0, \\ \epsilon_{r,\,rms} &= \frac{P^{1/2}}{2r} \text{ radians.} \end{aligned}\right\} (24)$$

For intermediate values of x', it may be seen from (23) that $\epsilon_{r,rms}$ is smallest when the reflectors cluster about the line between transmitting and receiving points and that $\epsilon_{r,rms}$ is a maximum of $P^{1/2}/2r$ radians when the reflectors are off to 90 degrees of this line.

In summary of the statistical results obtained for ϵ_r, (20), (23), and (24) all show a dependence of $\epsilon_{r,rms}$ on P, the average total reflection power received, and on the factor $1/r$. When reflectors are uniformly distributed over all angles, (24), there is a flat 9-to-1 reduction in the root-mean-square spreads of the errors on 1st- and 9th-harmonic estimates of azimuth. In the other cases, where the reflectors were assumed to be along (20) and near (23), a certain azimuth, there are variations of $\epsilon_{9,rms}$ and $\epsilon_{1,rms}$ with azimuthal angle. In these cases, $\epsilon_{9,rms}$ and $\epsilon_{1,rms}$ vary with azimuth very nearly as the envelopes of $\epsilon_{9,1}$ and $\epsilon_{1,1}$ in Figure 9A. Thus, there is a 9-to-1 reduction in the maximum root-mean-square spreads, and nowhere is $\epsilon_{9,rms}$ larger than $\epsilon_{1,rms}$.

The reduction in error on a harmonic estimate of azimuth in the presence of reflections, as indicated by (12) and (13), varies inversely as r the number of the harmonic employed and does not depend on m_r the amplitude of that harmonic. This would imply for example that the 9th-harmonic amplitude can be made arbitrarily small and, in the absence of any overriding noise, the errors caused by reflections are still reduced by the 1/9 factor. This is almost the case, though of course not without qualification. For one thing, if there were a large harmonic amplitude unbalance, say more than 10 to 1, then nonlinear distortion of the larger harmonic in the presence of reflections and further harmonic interactions could produce "tones" that significantly interfere with the phase determination of the harmonic of interest. Such unbalance of harmonic amplitudes does not exist in practice. Furthermore, distortion effects of this type are not likely to be felt since the reflecting signals are ordinarily small in magnitude. As was mentioned in connection with (10), when the reflections are small, the distorted pattern, that is, the envelope formed of all radio-frequency energy received, is practically a linear sum of the reflection modulations so that no new tones or beats appear.

Still another reason why harmonic amplitude does not have a major effect on errors in the presence of reflections is that the percentage modulation of the harmonics in the ghosts of the radiated pattern are usually the same as in the radiated pattern. (This was tacitly assumed in the analysis given.) That is, the perturbation of a harmonic tends to be proportional to the size of that harmonic. Noise differs distinctly from reflections in this respect, for in the presence of a given noise power, that is, data variance, all harmonics in the radiated pattern are subjected to perturbations of the same size on the average. Thus, the factor of harmonic amplitude necessarily enters there.

4. Conclusions

The study presented here demonstrates that the 9th-harmonic encoding is superior to a 1st-harmonic encoding in affording the better estimate of azimuth. It is not possible to assess the improvement by a single factor.

In section 2, it was demonstrated that in the presence of one reflection of rather large magnitude a visual estimate of azimuth derived from the 9th harmonic results in essentially 1/9th the error that is incurred by observation of the 1st harmonic alone. The error due to a single reflection was discussed in detail in section 3 as a special case of (12) and (13). These are quite-general results for the error in 1st- and 9th-harmonic azimuthal estimates when a number of reflectors are present. For the case of one reflector,

it was shown that the error possible on a 1st-harmonic estimate can be as much as arc sine a_1 radians, where a_1 is the ratio of direct and reflected carriers, and that the 9th-harmonic error can be only 1/9th as great. Further, at no azimuth does the 9th-harmonic error ever exceed the error on the 1st harmonic.

In section 3 it was shown how it is possible in the presence of many reflections to devise instances where the error on the 9th harmonic could exceed by any factor that on the 1st harmonic. However for every such case, it is equally possible to devise another in which the results are just the reverse. Such situations are of little significance in practical aerial navigation.

In sections 2 and 3, the errors most likely to be made on 1st- and 9th-harmonic estimates of azimuth are examined from a statistical standpoint. In section 2, errors due to arbitrary distortion in the radiated pattern are considered. In section 3, distortion composed of the ghosts of the radiated pattern is considered and related to the distribution of reflector positions and reflection factors. In all cases, it was shown that the root-mean-square spread of errors to be encountered on 9th-harmonic estimates of azimuth is 1/9th that on 1st-harmonic estimates.

The conclusions of this study have been substantiated in numerous field tests of the tacan system. Figure 10 is a photograph of a particularly unfavorable site at which an experimental installation of a tacan antenna was made intentionally. In this installation, the tacan antenna was located in a gravel pit.

5. Acknowledgments

The writer is indebted to his associates at these Laboratories; to Mr. F. Biagi for having performed the numerical study in section 3, and Messrs. R. I. Colin, L. A. deRosa, and F. J. Lundburg for their stimulating and constructive criticisms.

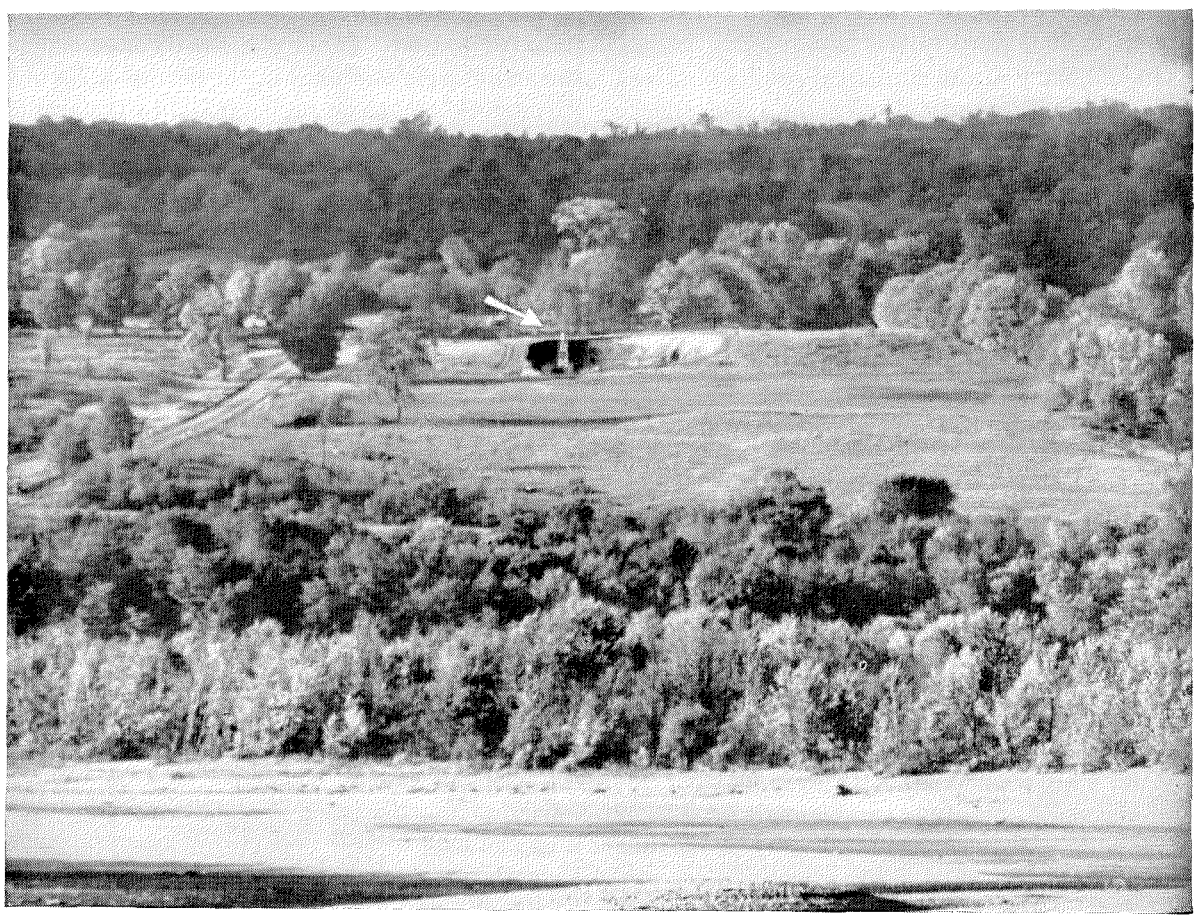

Figure 10—Tacan installation in a gravel pit intentionally selected as being a highly unfavorable site.

United States Patents Issued to International Telephone and Telegraph System August–October, 1955

UNITED STATES patents numbering 24 were issued between August 1 and October 31, 1955 to companies in the International System. The inventors, titles, and numbers of these patents are given below.

J. I. Bellamy and L. Hemminger, Remote Supervisory and Control System, 2 715 719.

R. P. Boyer, Jr., Auxiliary-Service Telephone System, 2 718 557.

G. Buchmann, Wideband Loudspeaker, 2 717 047.

A. G. Clavier, Long-Range Navigational System, 2 718 002.

J. L. Culbertson, Line-Clearing Apparatus for a Telephone System, 2 717 284.

L. A. deRosa, M. J. DiToro, and L. G. Fischer, Signal-Correlation Radio Receiver, 2 718 638.

H. Drubig, J. Eisele, G. J. Strattner, and G. Parow, Rectifier Stack, 2 714 694.

C. W. Earp, Radio Navigation, 2 717 379.

F. P. Gohorel, Telephone Systems, 2 717 924.

K. Gossler, Indirectly Heated Cathode for Cathode-Ray Tubes, 2 717 325.

D. D. Grieg and H. F. Engelmann, Microwave Cable, 2 721 312.

R. Haberkorn and A. Ziegler, Carrier Guidance in Elbows and Switches of Pneumatic Tube Systems, 2 719 681.

A. J. Henquet and A. Gaugain, Automatic Telephone Systems, 2 719 882.

K. Klinkhammer and A. Mehlis, Circuit Arrangement for All-Relay Connector Switch Composed of Tens and Units Relays, 2 719 880.

G. F. Klepp, Electric Discharge Devices, 2 719 933.

I. A. Krause, Remote Synchronization-Hold Circuit, 2 720 555.

J. J. Nail and W. M. Spanos, Wedge Antenna System for Sector Operation, 2 720 590.

S. B. Pickles, Omnidirectional Radio Range System, 2 715 727.

H. Seidel, Directional Couplers for Microwave Transmission Systems, 2 721 309.

F. H. Taylor, Radio-Beam Antenna Arrangements, 2 717 312.

E. Touraton, C. Dumousseau, and R. Zwobada, Velocity-Modulation Devices, 2 717 327.

C. G. Treadwell and D. B. Munday, Electric Multichannel Pulse Communication Systems, 2 719 877.

N. Weintraub, Transient Surge Detector, 2 717 992.

E. A. White, Controllable Sweep Generator, 2 718 594.

Long-Range Navigational System

A. G. Clavier

2 718 002—September 13, 1955

A long-range radio beacon system using amplitude modulation of long-wave energy. This patent covers a method in which separate carrier waves are modulated with respective low-frequency waves and in which the relative phase of the low-frequency waves is cyclically varied, the carrier waves being transmitted from a plurality of spaced points. A synchronizing signal is transmitted at a time of predetermined phase relationship of the modulated waves.

The signals from the beacons are simultaneously received on a craft and are demodulated to obtain a beat frequency between the phase-varied low frequencies; the beat frequency is then compared with the synchronizing signals to determine the navigational path.

In Memoriam

© Baron Studios

EDWARD STANLEY BYNG

EDWARD Stanley Byng, vice chairman of Standard Telephones and Cables, Limited, died at his home in Purley, Surrey, England, on January 13, 1956 in his 73rd year.

He was born in Derby in 1883. After graduation from Sheffield University, he joined the National Telephone Company in 1904. Later, he was transferred to London and, when that system was absorbed by the General Post Office in 1911, he became chief inspector, dealing with plant studies and estimates. His interest in uniting the staffs of the Post Office and National Telephone Company into a single coherent organization brought him in contact with certain administrative problems to which he later gave a great deal of attention.

In 1913, he accepted the post of engineer in charge of telephone-cable contracts with the Western Electric Company. During the first world war, while on loan to the British Admiralty, he visited the Shetland Islands, Malta, and Corfu as a technical advisor on submarine detection.

In 1921, he was transferred to the construction and maintenance section of the European engineering department of the International Western Electric Company, which in 1925 became the International Standard Electric Corporation. Returning to London in 1928, he was appointed managing director of Standard Telephones and Cables, Limited, becoming vice chairman in 1933.

Mr. Byng was a member of the Institution of Electrical Engineers and served also as treasurer and council member. Among the many papers he contributed to its journal, that on "Telephone Line Work in the United States" received the Fahie Premium. He was a Fellow of the American Institute of Electrical Engineers.

His experience with administrative problems, for which no formal training was then available, stimulated his activities in the development of such organizations as the Institute of Industrial Administration, Industrial Management Research Association, National Institute of Industrial Psychology, and the British Association for Commercial and Industrial Education. He was a pioneer in the demand for the broadest possible education for engineers at a time when this need was not generally recognized.

Evidence of his exceptionally wide range of interests is his service on numerous committees established by the British Government, Federation of British Industries, London Chamber of Commerce, and the London Regional Advisory Council for Youth Employment.

Contributors to This Issue

ANTHONY M. CASABONA

ANTHONY M. CASABONA was born in New York City on June 16, 1920. He received the B.S. degree in electrical engineering in 1941 from the College of the City of New York.

On graduation, he joined the International Telephone Development Corporation, which is now Federal Telecommunication Laboratories. He has been active in the aeronautical radio field, specializing in short-range navigational and instrument low-approach systems.

Mr. Casabona is a member of the Institute of Radio Engineers, Tau Beta Pi, and Eta Kappa Nu.

• • •

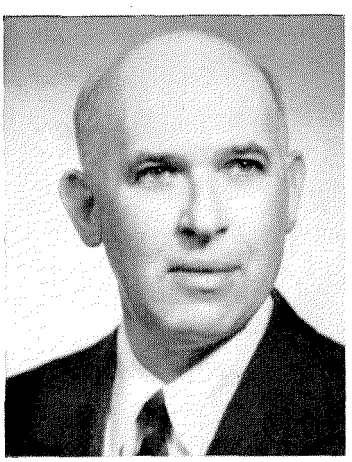

ROBERT I. COLIN

ROBERT I. COLIN was born in Brooklyn, New York on February 16, 1907. He studied engineering and physics at Cornell University and received an A.B. degree in 1928. The next year, under an exchange fellowship, he attended the University of Frankfurt (Germany). From 1929 to 1933, he served as a graduate assistant in physics at New York University and received an M.S. degree.

From 1934 to 1939, he was a member of the teaching staff of Hebrew Technical Institute. From 1941 to 1944, he was an instructor, then head, of the aircraft electrical systems branch of the Army Air Forces Technical School.

Entering Federal Telecommunication Laboratories in 1944 as an engineer and technical writer, he is now assistant to the technical director of the laboratories.

• • •

ETTIENNE DEFAYMOREAU was born on June 9, 1912, in Paris, France. He received an engineering degree from Ecole Centrale de TSF in Paris in 1930.

On completing school, he became an engineer in the radio department of Phillips Gloeilampenfabrieken. From 1933 to 1934, he served in the engineering corps of the French army.

In 1934, he joined the laboratory of Le Matériel Téléphonique. After working on television transmitters and radar, he came to Federal Telecommunication Laboratories in 1946. There he was assigned to projects on aerial navigational systems. He has been associated with the tacan program from its start and was responsible for the development of most of the airborne *AN/ARN–21* equipment and the associated test gear. He is now associate director of the radio navigation laboratory and has charge of the tacan evaluation program.

• • •

SVEN H. DODINGTON was born on May 22, 1912, in Vancouver, British Columbia, Canada. After early schooling in Denmark, England, and the United States, he received the A.B. degree from Stanford University in 1934.

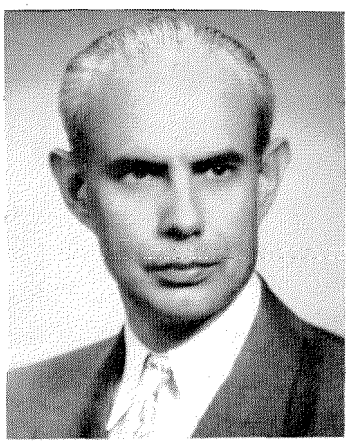

ETTIENNE DEFAYMOREAU

In 1935, he went to Scophony, Limited, in London and was transferred to New York City in 1940. The next year, he joined the laboratories division of International Telephone and Radio Manufacturing Corporation. Mr. Dodington is currently the director of the radio navigation laboratory at Federal Telecommunication Laboratories.

• • •

MARTIN MASONSON was born on April 6, 1926 in New York City. He received a bachelor's degree in

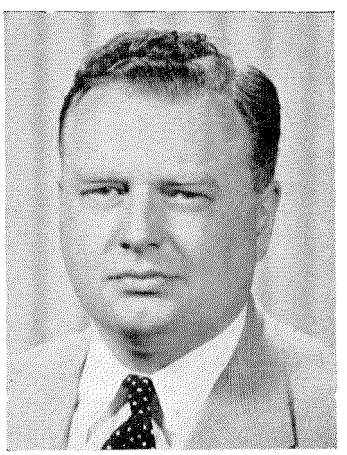

SVEN H. DODINGTON

MARTIN MASONSON

electrical engineering in 1949 from the College of the City of New York and a master's degree in electrical engineering from Polytechnical Institute of Brooklyn in 1955.

From 1949 to 1951, he was employed in the television-receiver division of DuMont Laboratories. Since then, Mr. Masonson has been with Federal Telecommunication Laboratories, where he has been associated with various projects in communications, countermeasures, and direction-finding.

• • •

PETER C. SANDRETTO was born on April 14, 1907, in Pont Canavese, Italy. He received from Purdue University the B.S. degree in electrical engineering in 1930 and the degree of electrical engineer in 1938. He also attended Northwestern University and was graduated from the Command and Staff School of the United States Army.

From 1930 to 1932, he designed aircraft radio equipment at Bell Telephone Laboratories. As superintendent of the communication laboratories of United Air Lines from 1932 to 1942, he pioneered in radio aeronautical problems such as precipitation static, direction finding, instrument approach, and altimetry. During the second world war, he served with the United States Air Force in the American, European, and Asiatic theatres. He is now a brigadier general in the Air Force reserve.

In 1946, he joined Federal Telecommunication Laboratories and is now vice president and technical director for military research and development projects.

General Sandretto is a Fellow of the Institute of Radio Engineers, a Member of the Institute of Navigation, and an Associate Member of the Institution of Electrical Engineers.

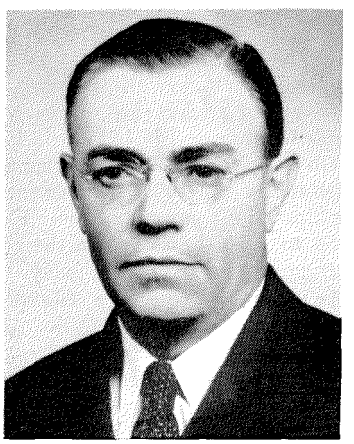

PETER C. SANDRETTO

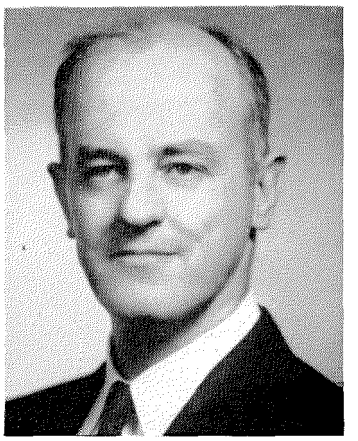

HENRY B. SCARBOROUGH

He has served on committees of the Radio Technical Commission for Aeronautics since its inception in 1935. He is the author of "Principles of Aeronautical Radio Engineering."

• • •

HENRY B. SCARBOROUGH is a native of North Carolina. He received the A.B. degree in 1937 and the M.A. degree in 1939 from Duke University. He then became an assistant professor at West Georgia College, moving to Georgia Institute of Technology two years later and to Duke University in 1942.

Since joining Federal Telecommunication Laboratories in 1943, Mr. Scarborough has been engaged in the development of fixed-station and airborne radio direction finders and of radio beacons for aerial navigation. He is an executive engineer in the aerial-navigation laboratory.

INTERNATIONAL TELEPHONE AND TELEGRAPH CORPORATION

MANUFACTURE AND SALES

North America

UNITED STATES OF AMERICA —

Divisions of International Telephone and Telegraph Corporation

Capehart–Farnsworth Company; Fort Wayne, Indiana

Farnsworth Electronics Company; Fort Wayne, Indiana

Federal Telephone and Radio Company; Clifton, New Jersey

Kellogg Switchboard and Supply Company; Chicago, Illinois

Federal Electric Corporation; Clifton, New Jersey

International Standard Electric Corporation; New York, New York

International Standard Trading Corporation; New York, New York

Kellogg Credit Corporation; Chicago, Illinois

Kuthe Laboratories, Inc.; Newark, New Jersey

CANADA — (*See British Commonwealth of Nations*)

British Commonwealth of Nations

ENGLAND —

Standard Telephones and Cables, Limited; London

Creed and Company, Limited; Croydon

International Marine Radio Company Limited; Croydon

Kolster-Brandes Limited; Sidcup

CANADA — Standard Telephones & Cables Mfg. Co. (Canada), Ltd.; Montreal

AUSTRALIA —

Standard Telephones and Cables Pty. Limited; Sydney

Silovac Electrical Products Pty. Limited; Sydney

Austral Standard Cables Pty. Limited; Melbourne

NEW ZEALAND — New Zealand Electric Totalisators Limited; Wellington

Latin America and West Indies

ARGENTINA —

Compañía Standard Electric Argentina, S.A.I.C.; Buenos Aires

Capehart Argentina; Buenos Aires

BRAZIL — Standard Electrica, S.A.; Rio de Janeiro

CHILE — Compañía Standard Electric, S.A.C.; Santiago

CUBA — International Standard Products Corporation; Havana

MEXICO — Standard Electrica de Mexico, S.A.; Mexico City

PUERTO RICO — Standard Electric Corporation of Puerto Rico; San Juan

Europe

AUSTRIA — Vereinigte Telephon- und Telegraphenfabriks A. G., Czeija, Nissl & Co.; Vienna

BELGIUM — Bell Telephone Manufacturing Company; Antwerp

DENMARK — Standard Electric Aktieselskab; Copenhagen

FINLAND — Oy Suomen Standard Electric AB; Helsinki

FRANCE —

Compagnie Générale de Constructions Téléphoniques; Paris

Le Matériel Téléphonique; Paris

Les Téléimprimeurs; Paris

GERMANY —

Standard Elektrik A.G.; Stuttgart

Divisions

Mix & Genest; Stuttgart and Berlin

Süddeutsche Apparatefabrik; Nürnberg

C. Lorenz, A.G.; Stuttgart and Berlin

Schaub Apparatebau; Pforzheim

ITALY — Fabbrica Apparecchiature per Comunicazioni Elettriche Standard S.p.A.; Milan

NETHERLANDS — Nederlandsche Standard Electric Maatschappij N.V.; The Hague

NORWAY — Standard Telefon og Kabelfabrik A/S; Oslo

PORTUGAL — Standard Eléctrica, S.A.R.L.; Lisbon

SPAIN —

Compañía Radio Aérea Marítima Española; Madrid

Standard E éctrica, S.A.; Madrid

SWEDEN — Aktiebolaget Standard Radiofabrik; Stockholm

SWITZERLAND — Standard Téléphone et Radio S.A.; Zurich

TELEPHONE OPERATIONS

BRAZIL — Companhia Telefônica Nacional; Rio de Janeiro

CHILE — Compañía de Teléfonos de Chile; Santiago

CUBA — Cuban American Telephone and Telegraph Company; Havana

CUBA — Cuban Telephone Company; Havana

PERU — Compañía Peruana de Teléfonos Limitada; Lima

PUERTO RICO — Porto Rico Telephone Company; San Juan

CABLE AND RADIO OPERATIONS

UNITED STATES OF AMERICA —

American Cable & Radio Corporation; New York, New York

All America Cables and Radio, Inc.; New York, New York

The Commercial Cable Company; New York, New York

Mackay Radio and Telegraph Company; New York, New York

ARGENTINA —

Compañía Internacional de Radio; Buenos Aires

Sociedad Anónima Radio Argentina; Buenos Aires (*Subsidiary of American Cable & Radio Corporation*)

BOLIVIA — Compañía Internacional de Radio Boliviana; La Paz

BRAZIL — Companhia Radio Internacional do Brasil; Rio de Janeiro

CHILE — Compañía Internacional de Radio, S.A.; Santiago

CUBA — Radio Corporation of Cuba; Havana

PUERTO RICO — Radio Corporation of Porto Rico; San Juan

RESEARCH

UNITED STATES OF AMERICA —

Division of International Telephone and Telegraph Corporation

Federal Telecommunication Laboratories; Nutley, New Jersey

International Telecommunication Laboratories, Inc.; New York, New York

ENGLAND — Standard Telecommunication Laboratories, Limited; London

FRANCE — Laboratoire Central de Télécommunications; Paris

GERMANY—Standard Central Laboratories; Stuttgart

ASSOCIATE LICENSEES FOR MANUFACTURE AND SALES IN JAPAN

Nippon Electric Company, Limited; Tokyo

Sumitomo Electric Industries, Limited; Osaka